# ANNUAL REPORT

MODERN PATHS TO INNOVATIONS

2021

# Message from Director

Photo by E. Blaževič

## The Year of 2022: Transformation into a Public Entity

We expected the **Year of 2021** to be totally different than the previous year. We hoped the pandemic situation would relax and we would return to normal working conditions, usual travelling to the conferences, project meetings and seminars. However, these hopes were in vain - 2021 was still a pandemic year. The Center experienced the delays in installation of a new equipment and the difficulties in fulfilment of project schedules due to restricted operation of laboratories. Seminars and meeting have been mainly organized in a mixed format combining remote facilities with very limited real contacts.

Nonetheless, **the Year 2021 marked a significant milestone** – on November 4 we have changed our institution **status from the budget organization to the public entity.** It is an important step which provides more freedom in cooperation with existing high-tech industries and, in particular, in generation of new spin-offs and start-ups related to FTMC activities and technologies developed in the Center. It will also add some flexibility in arranging and managing our resources.

**Scientifically the Year 2021 was prosperous** – our scientists were keeping high activity in publishing (more than 230 articles in highly-ranked scientific journals) and in preparing national and international patents. Fifteen PhD theses were defended successfully and the number of PhDs in the Center increased up to 114. We believe that in usual conditions of work, the scientific evolution of FTMC would be even more effective, fruitful and encouraging.

**From the point of view of innovations and industry related activities,** the Year 2021 was not exceptional – we maintained high level of cooperation, the number of clients were around 400, and the number of contracts for technological and scientific services accounted to around 1700.

**The patronage,** which had been kindly displayed during the Jubilee Event in 2020 as a donation of a unique numismatic collection and a special equipment for studies of face masks filtration efficiency, was successfully continued in the **Year 2021** by supporting the Optical Coherence Tomography Laboratory in the Department of Optoelectronics.

It is my pleasure to present **Annual Report 2021** – the highlights of the main scientific achievements, essential technological progress and most important events. Welcome into the age of a public entity.

**Gintaras Valušis**

Director of Center for Physical Sciences and Technology

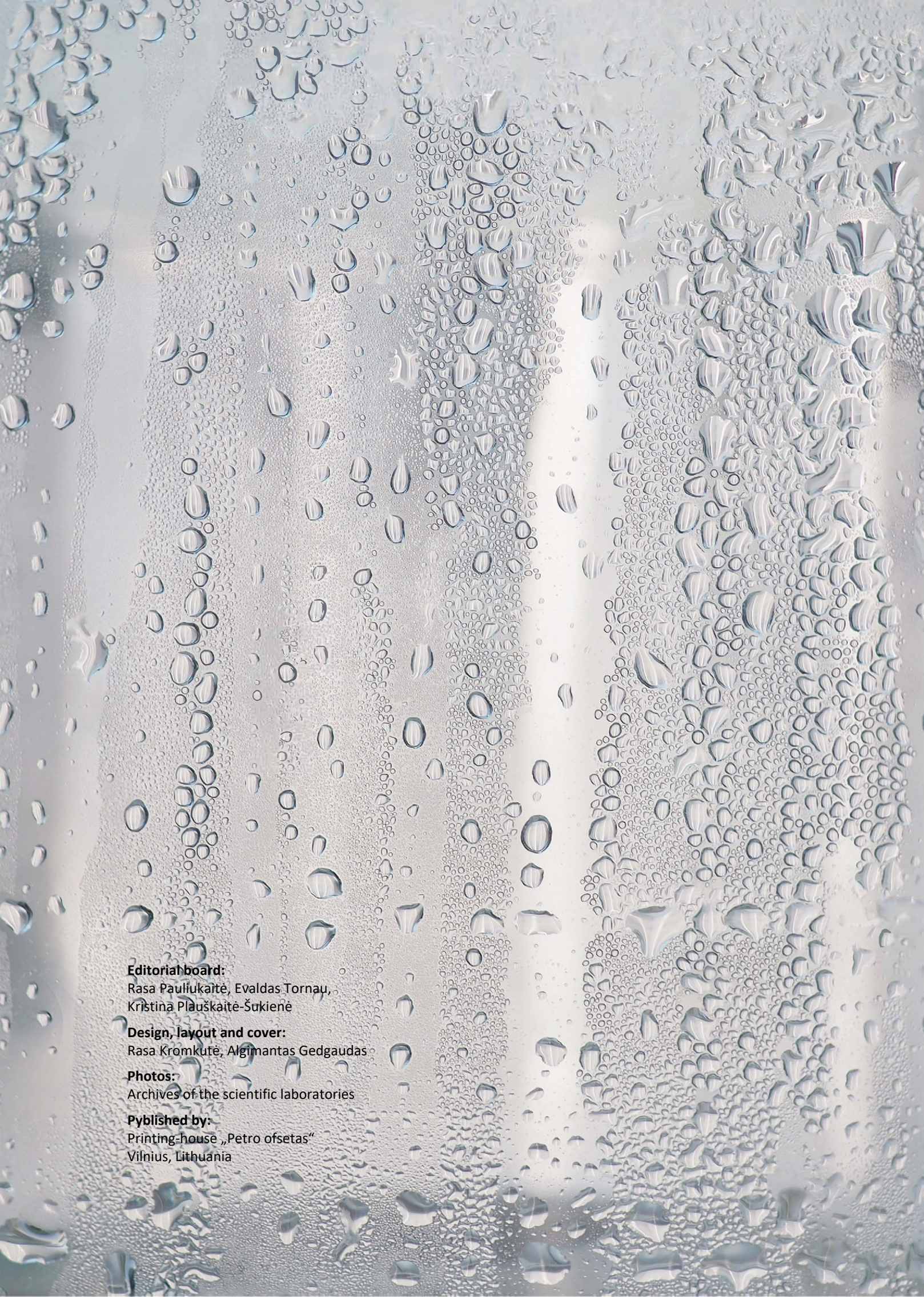

**Editorial board:**
Rasa Pauliukaitė, Evaldas Tornau,
Kristina Plauškaitė-Šukienė

**Design, layout and cover:**
Rasa Kromkutė, Algimantas Gedgaudas

**Photos:**
Archives of the scientific laboratories

**Pyblished by:**
Printing-house „Petro ofsetas“
Vilnius, Lithuania

# Contents

# Laser technologies

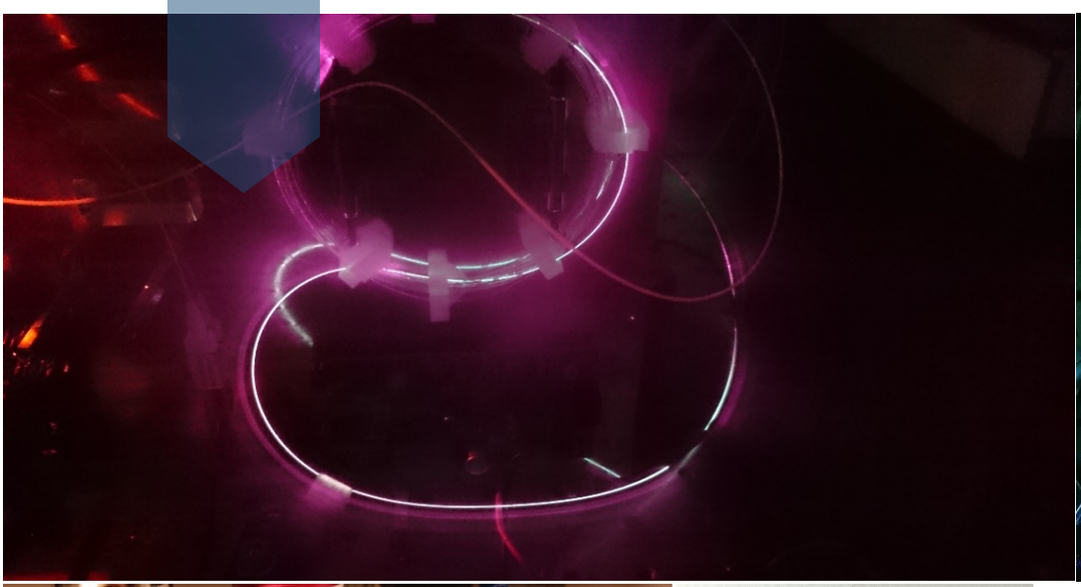

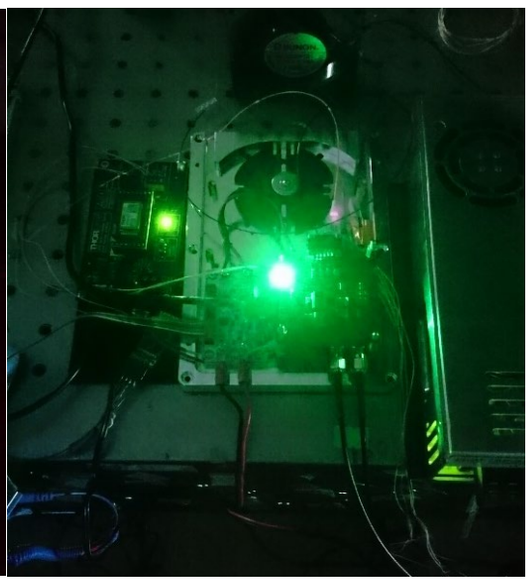

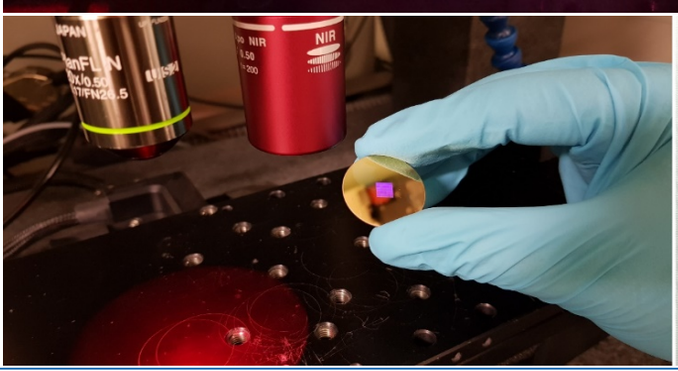

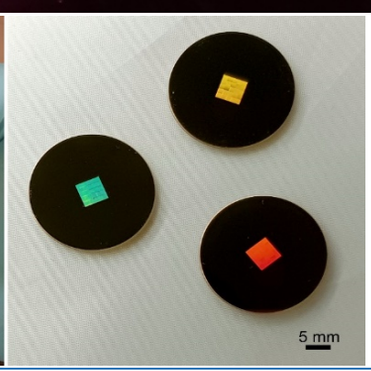


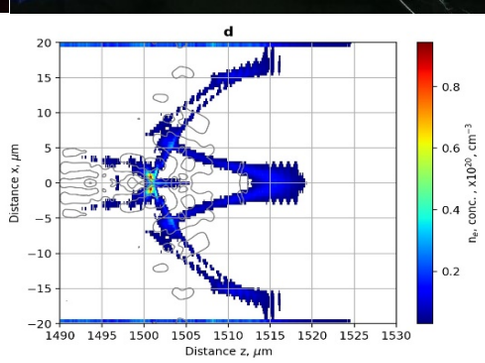


## Optical coatings, solid-state and fibre lasers, laser material processing, plasmonics and nanophotonics

The Department of Laser Technologies, with its seven laboratories, covers a significant part of the photonics related activities, ranging from newly discovered optical effects to laser machines and stepping through all technology readiness levels. The smart optical coatings developed in the Laboratory of Optical Coatings and the Laboratory of Advanced Microoptics convert the pieces of glass into valuable products able to control spectral and temporal properties of the light. New laser sources, under development in the Fiber Laser and Solid-State Laser Laboratories, based on tiny fibres, or active bulk crystals provide not only new wavelengths of coherent radiation but high peak power, ultra-short pulses and controlled wavefront as well. The combining of the coherent beams makes the lasers even more powerful. The Laboratory of Plasmonics and Nanophotonics gains its activity in nanofunctionalisation of surfaces for sensing applications. Efficient surface texturing utilising laser beam interference for metasurface formation, glass processing and 3D milling using smart pulsed lasers and distorted Bessel beams, nano-texturing for super-hydrophobic surface properties, 3D metal sculpturing by subtractive and additive technologies, laser-induced transformations in graphene-like materials and laser structuring for optoelectronic devices make up the primary working topics of the Laboratories of Laser Microfabrication Technologies. We progressed significantly in glass processing technologies with lasers. The scope in the material processing using ultrashort pulse lasers includes the investigations of the laser-matter interaction as well as hardware development in the Laboratory of 3D Technologies and Robotics. Significant progress was made in validating novel processes for electroless plating of laser-modified polymers and glasses. The Department collaborates with colleagues from other departments of FTMC, photonics companies in Lithuania and abroad, gaining new ideas for joint projects and applications. For example, 2021 was highly fruitful for the Department of Laser Technologies with new Horizon 2020 projects PhotonHUB, i.FAST, 3D Multiscan offering broad opportunities to collaborate with scientific and industrial partners in Europe and prepare scientific publications in high-ranked peer-review journals.

## Femtosecond laser ablation by biburst in the MHz and GHz pulse repetition rates

Ultrafast lasers are high-tech products with a high price for know-how and cutting-edge technology. Therefore, each laser-generated photon is expensive. Therefore, it is essential to use laser energy most efficiently. In pursuing higher processing efficiency, laser sources with burst mode capability were created. We report the in-depth experimental study of high ultrafast laser ablation efficiency for processing copper and steel with single pulses, MHz-, GHz- and burst in the burst (biburst) regimes. The comparison of burst, biburst and single-pulse ablation efficiencies was performed for beam-size-optimised regimes, showing the real advantages and disadvantages of milling and drilling processing approaches. As a result, highly-efficient ultrashort pulse laser processing was achieved

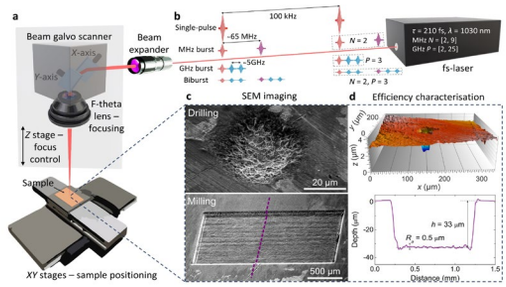


Fig. 1. Investigation of ultrafast laser burst-mode processing influence on ablation efficiency. (a) Principal scheme of laser processing setup. (b) Illustration of four possible laser working regimes: single-pulse, MHz burst, GHz burst, and biburst. (c) SEM images illustrate laser drilling and milling of copper samples and (d) corresponding graphs for efficiency evaluation.

for 1030 nm wavelength: 8.8 µm³/µJ for copper drilling, 5.6 µm³/µJ for copper milling, and 6.9 µm³/µJ for steel milling.

andrius.zemaitis@ftmc.lt

## Formation of large-scale gold microbumps arrays generating surface lattice resonances

Despite the technological progress in the fabrication of complex plasmonic systems, creating structures with extremely small dimensions of the periodic surface irregularities remains complicated, time-consuming, and expensive. The most popular fabrication method of such structures is lithography-based techniques, which are limited in producing large areas of the arrays. On the other hand, the size of the periodic arrays supported plasmonic lattice surface resonance is critical as detecting the optical response requires the illumination of a sufficient number of periodic elements with spatially coherent light over a large surface area. Here, the fabrication of large-scale gold microbumps arrays in a gold film using a cost-effective direct laser writing technique is presented. This work shows significant technological progress in forming large-scale metallic gratings via laser-based technique as the previous works based on this

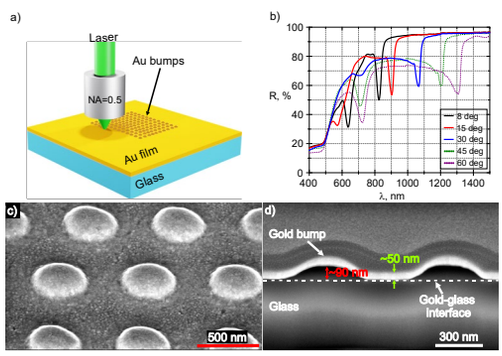


Fig. 2. (a) Illustration of Au bumps formation in a thin gold film using direct laser writing technique; (b) reflectance spectra of microbumps array with period 700 nm in 50 nm thick gold film at a different angle of incidence for *p*-polarized light; (c) SEM micrograph of fabricated gold bumps array in a thin gold film (50 nm); (d) cross-section of gold bumps.

technique demonstrated the surface plasmon resonances (SPR) of gratings in a spectral range at 2–6 µm.

evaldas.stankevicius@ftmc.lt

## Investigation of multipass Yb-doped fibre amplifiers

For satellite or airborne optical communication applications, high-efficient and compact fibre amplifiers are required to boost transmitter output power and extend the operational range of the system. One of the ways to achieve high pump-to-signal efficiency of the amplifier, together with the simple single-stage design of the system, is multi-pass amplification. We investigated 2-pass and 4-pass fibre amplifier configurations and compared their performance with conventional design of the single-pass fibre amplifier. Numerical calculations predicted the highest efficiency in 4-pass amplifier configuration, but experimentally the highest efficiency of 77% was achieved in 2-pass configuration and only 49% in 4-pass configuration. The efficiency reduction in the 4-pass configuration was caused by excess losses of components used in the setup. Therefore, the practical implementation of such a design is limited by component capabilities. On the other hand, the 4-pass fibre amplifier configuration also showed clear advantages compared to other configurations. This includes lower active fibre length required to achieve the same gain and

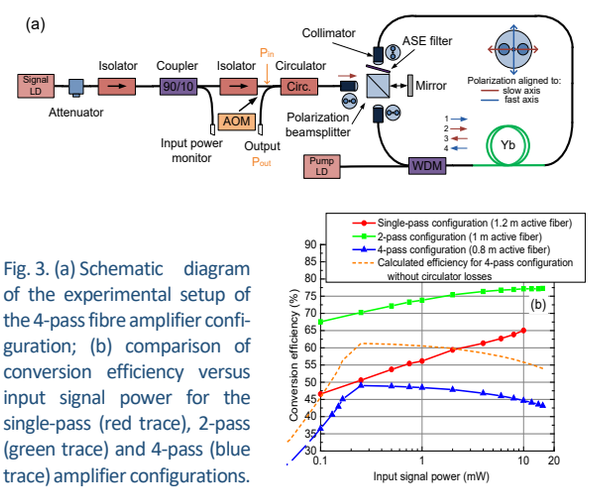


Fig. 3. (a) Schematic diagram of the experimental setup of the 4-pass fibre amplifier configuration; (b) comparison of conversion efficiency versus input signal power for the single-pass (red trace), 2-pass (green trace) and 4-pass (blue trace) amplifier configurations.

lower noise figure. However, to utilise all advantages of the 4-pass fibre amplifier configuration and achieve maximum efficiency, coupling losses of the amplifier components need to be minimised.

julijanas.zeludevicius@ftmc.lt

## *In-situ* and *ex-situ* investigation of ultrathin metal film growth

Systematically prepared ultrathin metal films were analysed for their composition, structural, optical and electrical properties. The initial growth of film thickness from several to hundreds of nanometers was studied. For silver, the four stages of the film growth, separate islands, coalescence, percolation and continuous film, were well distinguished *in-situ*. The novel description of film growth stages was introduced. For chromium films, a new set of optical constants was presented. The values of obtained optical constants were closer to the values for bulk polycrystalline specimens. Our results represent a set of data important for many scientific and practical applications.

alexandr.belosludtsev@ftmc.lt

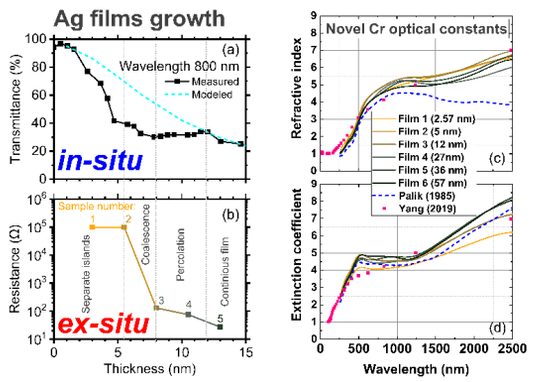


Fig. 4. (a) Transmittance and (b) resistivity versus thickness of silver films. (c) Refractive index and (d) extinction coefficient of ultrathin chromium films.

## Investigation of materials for supercontinuum generation for subsequent nonlinear parametrical and Raman amplification at 1 MHz repetition rate

Tunable femtosecond sources in visible (VIS) and near-infrared (NIR) regions are required in such applications as time-resolved spectroscopy, multiphoton microscopy and frequency metrology. Laser sources generating femtosecond pulses in infrared (IR) spectral range of 0.7-1.7 µm fits well for multiphoton fluorescence excitation and harmonics generation microscopy. One of the most established techniques to produce broadband femtosecond radiation, covering ultraviolet, visible and near-infrared spectral range, is supercontinuum (SC) generation. Our search of the crystals for efficient SC generation using MHz repetition rate femtosecond lasers revealed that Raman active crystals feature the lowest generation thresholds and SC wavelength shifted to the mid-IR wing of the spectrum. The VIS part of SC (650-960 nm) was efficiently amplified using parametric amplification in BBO crystals with mean power up to 300 mW. Pulses shorter than 50 fs were obtained. The IR SC radiation was efficiently amplified to ~100 mW power via Raman amplification in the synthetic diamond crystal.

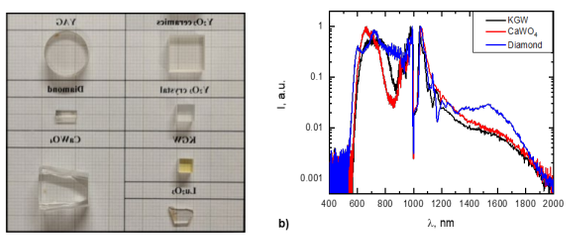


Fig. 5. (a) Materials tested for SC generation. (b) SC spectra of Raman active crystals.

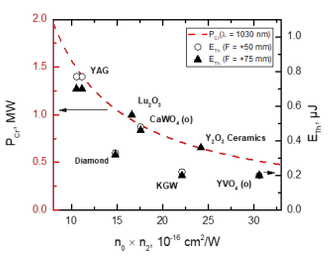


Fig. 6. Raman active crystals manifest much lower SC thresholds in comparison with theoretical predictions.

Proposed techniques pave the way to simple femtosecond laser sources generating near 1200 nm wavelength for multiphoton and nonlinear microscopy applications.

andrejus.michailovas@ftmc.lt

## Hybrid high spectral resolution broadband mid-infrared SFG spectrometer

A femtosecond middle infrared tunable radiation source for a hybrid concept of compact broadband high-resolution sum-frequency generation (SFG) spectroscopy was developed. A two-channel picosecond fibre laser was used as a seed for narrowband (~1.5 $cm^{-1}$) and broadband ultrafast radiation sources required for realisation of a new concept. Broadband femtosecond source optimisation was performed to achieve >500 $cm^{-1}$ linewidth widely tunable microjoule level pulses in mid-IR spectral region (2-10 µm). Modeling and experiments indicated that indirect (via intermediate visible SC OPA) generation of mid-IR femtosecond pulses is a more efficient way to generate tunable (from 2 to 10 µm) femtosecond pulses. Using a new hybrid laser system, the SFG spectrometer was assembled and tested. It demonstrated perfect spectral resolution (< 3 $cm^{-1}$) defined by narrowband visible

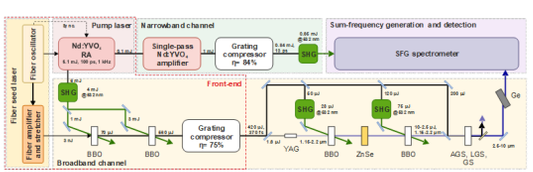


Fig. 7. The layout of the assembled SFG spectrometer setup.

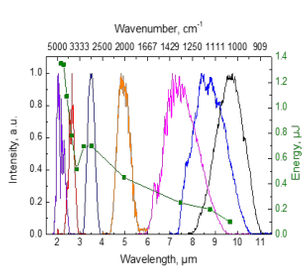


Fig. 8. The LGS OPA idler wave output spectra and pulse energies in the wavelength tuning range of 2 - 9.6 µm.

channel and fast data acquisition speed (0.1 - 30.0 seconds full spectrum) assured by broadband mid-IR femtosecond channel.

andrejus.michailovas@ftmc.lt

## Efficient milling and cutting of borosilicate glass through thin flowing water film with a picosecond laser

In recent years the demand for the miniaturisation of optical glass components significantly increased. Conventional (mechanical) glass cutting requires post-processing, increasing the manufacturing time and costs. Therefore, the lasers attracted much attention for high precision processing of glasses. However, direct laser ablation suffers from relatively low processing speeds. We introduced a thin water film into an ablation zone to improve the processing efficiency of borosilicate glasses. Under optimised parameters, the water-assisted cutting speed of 420 µm glass plates increased tenfold. The ratio of ablation efficiency in water and air strongly depends on the groove width and depth. For 500 µm deep and 130 µm wide grooves, glass ablation in water was 19 times more efficient. Laser-based glass cutting in water notably increased the quality of cuts.

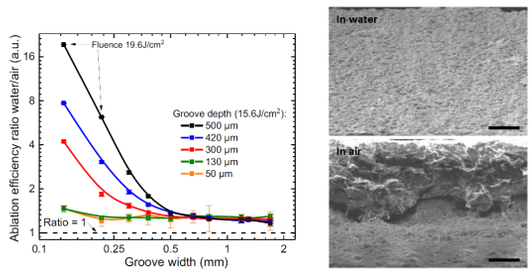


Fig. 9. (Left) The ratio of ablation efficiency through thin water film to ablation efficiency in air versus groove depth. SEM images of cut walls ablated in 420 µm thick borosilicate glass plates at 600 kHz pulse repetition rate: in (upper right) water and (lower right) ambient air.

edgaras.markauskas@ftmc.lt

## The experimental evidence of a strong coupling regime in the hybrid Tamm plasmon - surface plasmon polariton (TPP – SPP) mode

Nanostructures that are able to support energy exchanges in strong coupling regimes are promising systems for a new generation of nanolasers, ultra-sensitive optical biosensors, influencing chemical reaction rates, and in quantum information processing. We proposed a simple optical methodology using optical filters (Fig.10), which gives unambiguous experimental evidence of the strong coupling regime in the hybrid TPP-SPP mode. Present experimental studies have shown that, if the investigated system is in the strong coupling regime, this is always enough to excite only one component of the hybrid excitation. Thus, only a part of the incoming light and its dispersion relation will be the same as when the excitation is done with a whole spectrum. Application of a strong coupling of hybrid TPP-SPP excitations could be valuable due to the reduction of energy losses in the metals and tunability desired for the spectral range. Furthermore, if one component is excited at a resonant wavelength, the other is also present and can be controlled by strong coupling between TPP and SPP (Fig.11). The energy conversion between TPP and SPP shows potential applications of hybrid TPP-SPP modes for integrated photonic devices.

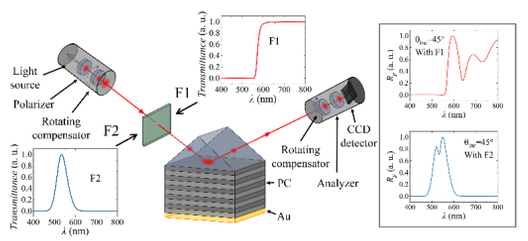


Fig. 10. Filters F1 (red line) and F2 (blue line). The optical response of the hybrid TPP-SPP mode is shown in graphs on the right side (top), h-SPP and h-TPP (bottom).

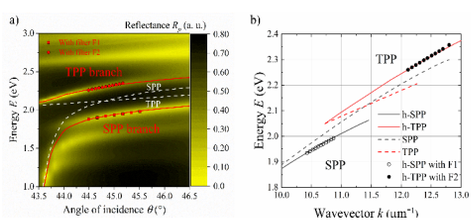


Fig. 11. (a) Dispersion of the hybrid TPP-SPP mode (red lines) with the calculated non-coupled single modes (yellow lines) and measured with filters (squares TPP branch and circles SPP branch). (b) Energy vs wavevector optical dispersion for the same sample.

zigmas.balevicius@ftmc.lt

## Broadband chirped mirrors with a porous top layer for smooth group delay dispersion

The effectiveness of ultrashort pulse compression depends on the group delay dispersion (GDD) characteristics of the chirped mirror (CM) in CM-based optical pulse compression systems. Theoretically, CMs with a porous top layer may feature smooth GDD over broader than half optical octave bandwidth. However, experimentally such bandwidth has never been achieved before. Broadband CMs with a porous top layer were deposited using ion beam sputtering technology (for dense layers) and the glancing angle deposition (GLAD) method (for porous layer). Measurements evaluated the stability of CM spectral performance at environments with different humidity. Variation in porous layer refractive index was estimated to be approximately 1 % due to the changes in humidity. In addition, GDD oscillations of the coatings exhibited low sensitivity to deposition errors of porous layer and humidity in the surrounding environment. Presented results are essential for applications in femtosecond lasers, where GDD oscillations are limiting their performance.

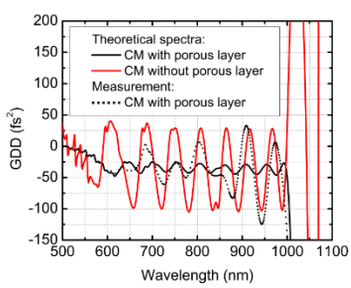


Fig. 12. Theoretical GDD spectra of two CM designs: with (black line) and without (red line) porous top layer. GDD measurement of deposited CM with porous layer is also depicted (black dots).

simas.melnikas@ftmc.lt

## Nanostructured multi-layer coatings for spatial filtering

Spatial filtering is an important mechanism to improve the spatial quality of laser beams. However, in microlasers, conventional filtering is impossible due to the lack of space in microresonators to access the far-field. In this study, a conceptually novel mechanism of spatial filtering in the near-field domain is proposed and demonstrated by a nanostructured multi-layer coating - a 2D photonic crystal structure with a periodic index modulation along the longitudinal and transverse directions to the beam propagation. The physical vapour deposition on the structured substrate was used to provide self-repeating modulation in two directions. A 5 µm thick photonic multi-layer structure composed of alternating high- and low-index materials providing spatial filtering in the near-infrared frequencies with a 2° low angle passband is experimentally demonstrated.

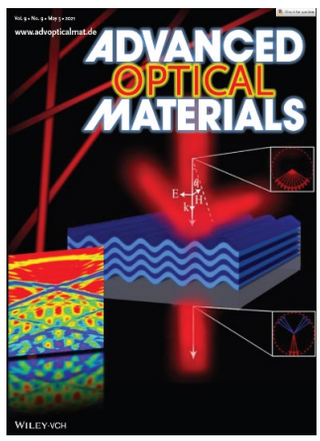


Fig. 13. Cover image of the article. The schematic representation of photonic structure consisting of a self-replicating curved multi-layer coating on a periodically modulated substrate. The map of transmission dependence on the incidence angle, and the wavelength is on the left.

The proposed photonic structure can be considered ideal for intracavity spatial filtering in microlasers.

lina.grineviciute@ftmc.lt

## Impact of deposition conditions on nanostructured anisotropic silica thin films in multi-layer interference coatings

Although sculptured thin films have been explored for decades, no optical and structural investigations have been performed for anisotropic nanostructured multi-layer coatings with different deposition conditions of the dense layer. This paper presents an extensive morphological analysis of silica nanostructured anisotropic films. Porous anisotropic thin films have been coated with surface filling ranging from 84% to 57% and reaching the maximal phase retardance value of 0.032˚/nm. The covering of such structures with the dense layer at different conditions was investigated. Furthermore, we compared measurements with Molecular Dynamics simulations of growing silica layer using experimental conditions in the Virtual Coater framework. Both analyses

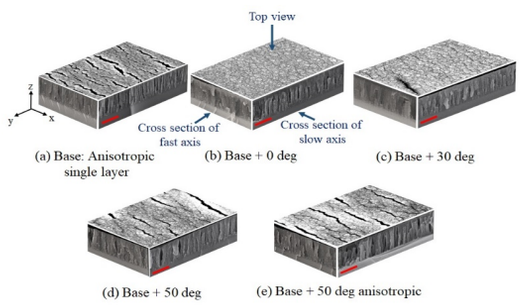


Fig. 14. The 3D representation of SEM images combination of (a) single layer with 250 nm thickness, deposited at an angle of 70◦ and 2- layers structures with the second layer deposited at (b) 0, (c) 30°, (d) 50° and (e) 50° -anisotropic case. The red bar is set at 250 nm.

indicate the minimal impact on the anisotropy of the porous layer at the deposition of a dense layer at 30˚ angle during constant substrate rotation.

lina.grineviciute@ftmc.lt

## Highly resistant all-silica polarising coatings for normal incidence applications

Several fundamental restrictions are limiting the implementation of microlasers in high power systems: low resistivity of coatings and compactness of elements, especially if control of polarisation is necessary. Therefore, a thin film-based coating with extremely high optical resistivity and polarising properties for normal incidence is preferable. Within this research, a novel multi-layer approach to form all-silica polarising coatings for normal incidence angle applications is proposed. Anisotropic silica layers, with perpendicularly aligned optical axes, allowing independently control the reflectance value for two perpendicular light polarisations. This allows adapting the coatings spectral performance to different optical systems. Laser-induced damage threshold (LIDT test 1-on-1) in the ns regime at the wavelength of 355 nm were evaluated as 39 J/cm$^2$ and 48.5 J/cm$^2$ for the R (reflected) and T (transmitted) polarisations, respectively. Such elements can significantly improve tolerated radiation power and allow the production of more compact laser systems.

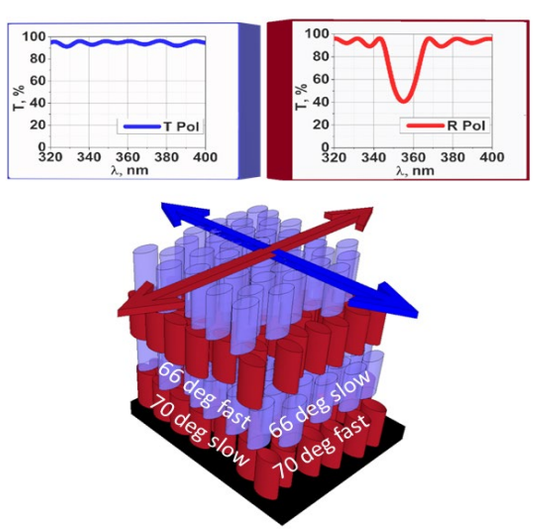


Fig. 15. The principal scheme of cross-sections of polariser for normal incidence angle, based on multi-layer coating consisting of anisotropic layers with perpendicularly aligned optical axes.

lina.grineviciute@ftmc.lt

## Chemical etching of fused silica after modification with two-pulse bursts of femtosecond laser

Two-pulse bursts of femtosecond laser were used to record internal modifications inside fused silica for selective chemical etching. Due to the enhanced absorption of the second pulse in the case of the 2:1 energy ratio regime and more efficient energy coupling, the regular nanogratings are formed, which leads to a more pronounced and enhanced etching of the inscribed modifications. Compared to a single pulse regime, a significant improvement in processing speed and etching rate (ER) was obtained. The stable etching was observed at 100 ppμ pulse density, while for single pulses, the pulse density ~ 5-10 times higher should be applied, corresponding to ~ 5-10 times longer processing time. The 38% ER enhancement for 1D horizontal channels and 35% for 2D vertical planes was found. For etching in KOH etchant, the largest ever reported etching selectivity of 1:2000 was achieved. This new processing strategy allows us to predict the etching conditions more precisely and optimise the processing time.

valdemar.stankevic@ftmc.lt

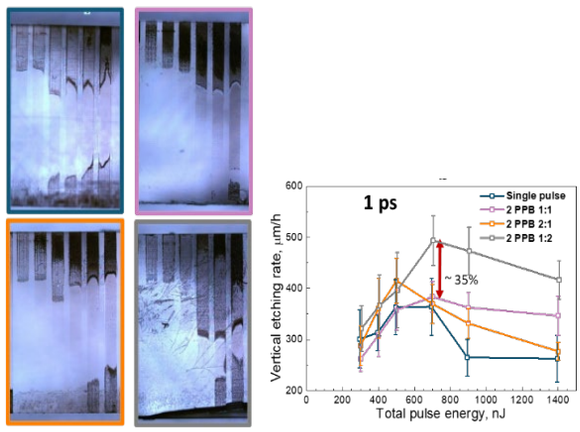


Fig. 16. The ER dependence on the pulse energy for vertical structures etched from the top surface in 10M KOH for 2 hours. The modifications were inscribed through the whole sample thickness. Dark areas from the top and bottom show the etched material. Laser pulse duration is 1 ps. The z-step distance was set to 5 μm. The colour border of the microscope pictures corresponds to the curve colour on the graphs. The error bar shows the standard deviation from the averaged value.

## Numerical study of powder flow nozzle for laser-assisted metal deposition

Metal additive manufacturing has received much attention in the past few decades. It offers a variety of technologies for three-dimensional object production. One of such large-sized object production technologies is laser-assisted metal deposition, size-limited by the capabilities of the positioning system. The already-existing nozzles have either a relatively low build rate or poor spatial resolution. A new nozzle, with a centred particle beam at high velocity, was developed for laser-assisted metal additive manufacturing technologies. Scientific challenges were addressed regarding the fluid dynamics, the particle-substrate contact and the tracking of the thermodynamic state during contact. Two nozzles were designed based on the de Laval geometry with Witoszynski and Bicubic curves of the convergence zone. The results showed that the average flow velocity is around 615 and 435 m/s in a Bicubic and Witoszynski outlet curve nozzles, respectively. Investigation of the particle beam formation for the Bicubic curve geometry revealed that small particles have the highest velocity and the lowest total force at the nozzle outlet. Fine particles have a shorter response time and, therefore, a smaller dispersion area. The elasto-plastic particle-surface contact showed that particles with a diameter up to 3 μm could reach the critical velocity without additional heating. For particle sizes above 10 μm, additional heating is needed for deposition. The maximum coefficient of restitution (COR) is achieved with a particle size of 30 μm. Smaller particles are characterised by the lower values of COR due to a relatively high velocity. Particles larger than 30 μm are scalable, characterised by a small change in velocity and a rise in temperature as their mass increases.

genrik.mord@ftmc.lt

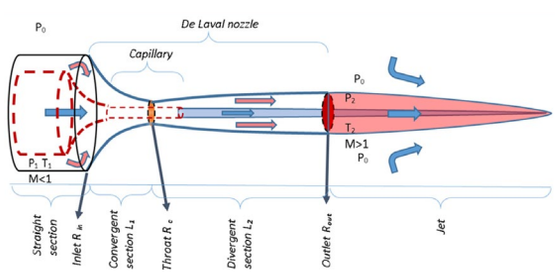


Fig. 17. De Laval nozzle geometry components.

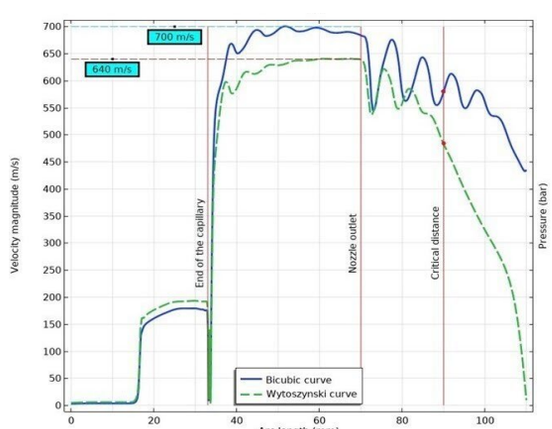


Fig. 18. Comparison of the velocity of Bicubic and Witoszynski curve nozzles.

# Optoelectronics


(Top, left) Targets for IR camera for minimal resolvable temperature difference (MRTD) tests. (Top, right) During investigation of ultrafast photocurrents in a magnetic field. (Bottom left) Inspection of InGaAs THz detectors processing. (Bottom, right) Commercially available THz emitting antenna from spin-off company Teravil.

## Focus on terahertz and infrared technologies: materials by design, optoelectronic and optical investigation, novel experimental techniques and devices

Department of Optoelectronics keeps a tradition to focus on terahertz (THz) and infrared technologies (IR) aiming to elaborate further complete and entire chain of scientific activities starting from materials design, comprehensive scientific research and development of prototypes of optoelectronic devices. The Department structure experienced no changes within the last year. It consists of five scientific laboratories: Ultrafast Optoelectronics, Optoelectronics Technology, Semiconductor Optics, Terahertz Photonics, and Optoelectronics Systems Characterization. The staff amounts to 41 researchers – 28 doctors of sciences, 7 PhD students, and 6 engineers. The Department activities cover both fundamental and applied research dedicated to semiconducting materials physics and semiconductor technology, THz physics and spectroscopy, THz imaging and holography, development of novel optoelectronic devices for THz and IR ranges as well

as their applications. Dominating scientific topics cover the design and investigation of quantum wells of GaAs/AlGasBi and GaInAsBi compounds and the development of infrared LEDs and lasers based on these structures; a special attention is paid to studies of GeSn alloys as infrared detectors and to improvement of their photo-sensitivity in the mid-infrared region. The year 2021 was quite successful for (i) further development of antenna-coupled titanium-based microbolometers and their application to control the spatial profile of weak THz sources, (ii) innovations in THz imaging systems for discrimination of packaged low-absorbing objects and (iii) investigation of plasmons and polaritons in GaN-based heterostructures. In vivo imaging of the human cornea and retina with ultrahigh-speed optical coherence tomography exhibited itself as a new promising direction. Obstacles caused by pandemic limitations had no essential effect on further evolution of THz photonics and technology Cluster, interlaboratory unit of the Department, concentrating and coordinating all modern THz experimental facilities for development of THz technology and THz photonics-related components. The scientific equipment including various THz techniques, femtosecond lasers-based THz spectrometers as well as different continuous wave-based THz set-ups for imaging, were enriched by a set of standard optical characterization techniques (photoluminescence, modulation spectroscopy, Fourier spectroscopy, optical and THz ellipsometry) equipped with low-temperature facilities and possibilities to apply short-pulse electric fields. It makes the Cluster an attractive place to perform versatile experimental THz and optical investigation both for foreign scientists and other Lithuanian research groups and high-tech companies.

## Holography and spatial filtering in terahertz frequencies

Terahertz (THz) imaging and holography experiences an exciting burst of scientific activities, both in regard to fundamental research and their versatile applications. Recently, we extended boundaries of THz imaging via development of THz spatial filtering techniques, both the dark field and the phase contrast. The techniques were demonstrated in two different THz imaging setups using focused and collimated beams. The proposed techniques exhibit enhancement in images contrast up to 30 dB, and an order of magnitude increased the signal-to-noise ratio, opening thus promising route for their further functional applications. Additional method, a two- and four-step phase shifting technique, leading to broader THz imaging capabilities in THz digital holography is proposed. It relies on the Mach–Zehnder interferometer-based setup. The phase shifting can successfully be implemented in transparent objects discrimination, and, by a proper selection of phase variation, can lead to a well-resolved increase of the quality of the reconstructed holograms.

linas.minkevicius@ftmc.lt

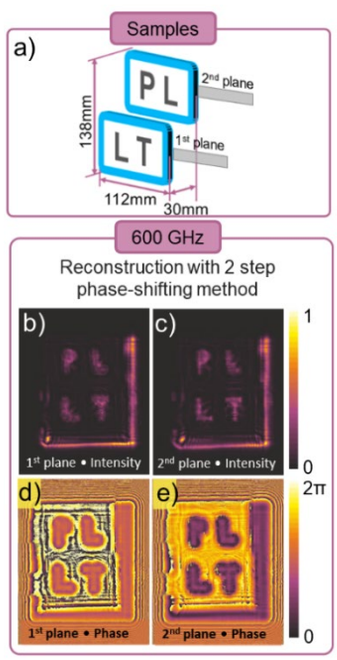


Fig. 1. Two 2D objects reconstruction at 600 GHz frequency using the phase shifting technique and Angular Spectrum of Plane Waves propagation method.

## High precision parabolic quantum wells grown using pulsed analogue alloy grading technique: photoluminescence probing and fractional-dimensional space approach

The newly implemented molecular beam epitaxy (MBE) growth technique, so called pulsed analogue alloy grading (PAAG), for parabolic AlGaAs barriers demonstrates the ground breaking achievements in the development of near- and far-infrared optoelectronic devices. In our paper we report a firm evidence of precisely accomplished 52-nm-wide GaAs/AlGaAs parabolic quantum well (PQW). The direct observation of up to 5 excited states confined within PQW in photoluminescence (PL) spectrum is supported by the fractional-dimensional space (FDS) approach calculations. The study presents the beautiful quantum mechanics in action and proves the validity of Kohn theorem.

mindaugas.karaliunas@ftmc.lt

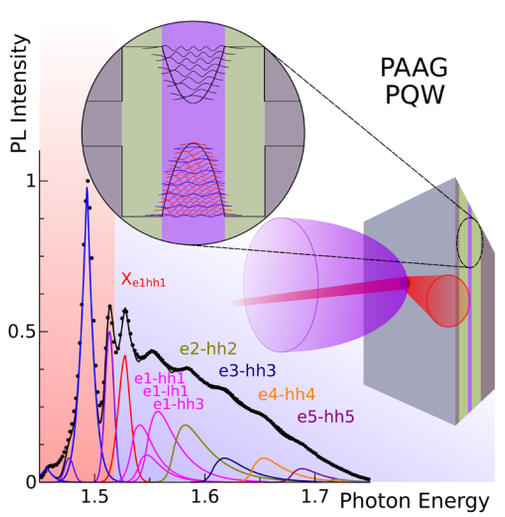


Fig. 2. (Right) the sample structure in the back-scattering geometry of PL experiment. (Top) the energy band diagram of the 52-nm-wide PQW grown using MBE PAAG technique. (Bottom) The PL spectrum at 3 K temperature and 691 kW/cm$^2$ excitation power density supplemented by FDS calculations.

## From the atomic-structure to optical properties

Bismides present a new class of III–V semiconductor alloys and are being developed for the infrared optoelectronics applications, including lasers, sensors, and multi-junction solar cells. In a series of our articles, the atomic-ordering induced optical anisotropy of GaAsBi alloys was demonstrated and analyzed from the atomic-scale up. This anisotropy is of primary importance for engineering of bismide-based optoelectronic devices. In contrast to the conventional valence band splitting, arising from the compressive strain in [001] grown GaAsBi, the CuPt-ordering axis has projection on the growth surface, and thus makes the optical anisotropy effects evident in standardly processed devices. The anisotropy effects could be used in polarization selective or sensitive infrared lasers, light-emitting diodes, sensors, and polarization rotators.

tadas.paulauskas@ftmc.lt

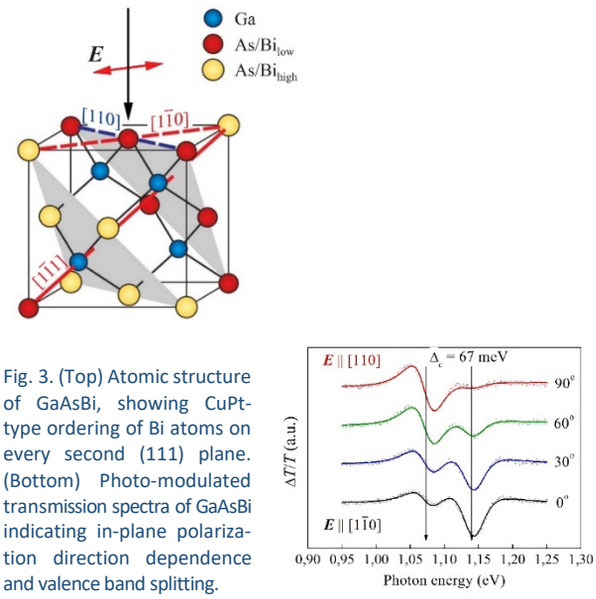


Fig. 3. (Top) Atomic structure of GaAsBi, showing CuPt-type ordering of Bi atoms on every second (111) plane. (Bottom) Photo-modulated transmission spectra of GaAsBi indicating in-plane polarization direction dependence and valence band splitting.

## Ballistic electron refraction at the semiconductor heterostructures

Terahertz emission from semiconductor surfaces illuminated by femtosecond laser pulses is, to a great part, caused by the ballistic photoelectron movement towards the bulk, which results in their separation in space with the holes and the creation of the fast changing electrical dipole. When the photoexcited carriers are created in the vicinity of the heterostructure, the situation is different. We have compared THz excitation spectra of GaInAs/InP and GaInAsBi/InP heterostructures when the femtosecond laser beam enters the structure from (i) the InP side and (ii) the narrower bandgap compound semiconductor side (Fig. 4). In the (i) case, the THz pulse polarity changes its sign at laser photon energies comparable to the energy at which the electrons excited in the compound layer can surmount the barrier separating conduction bands of both semiconductors in the structure. Thus, this effect can be used for the determination of energy band offsets in the heterostructures. Fig. 5 illustrates the origin of the THz pulse polarity inversion. At lower photon energies, when the excess energy of the electrons excited in GaInAsBi layer is too low to surmount the heterobarrier, the photoelectrons moving towards the barrier are reflected from it and remain in the layer. At higher photon energies, the photoelectrons are entering the wider bandgap InP, but move there in the opposite direction than the electrons remaining in the narrow bandgap layer. Since the electrons enter the material with lower density of states, their trajectories will be shifted towards the interface and the electron waves will be refracted.

ricardas.norkus@ftmc.lt

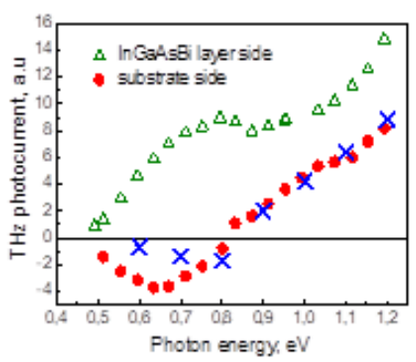


Fig. 4. The THz excitation spectra measured after InAsGaBi/InP structure excitation by femtosecond optical pulses from the layer and from the substrate side. Blue crosses are the results of the Monte Carlo simulation.

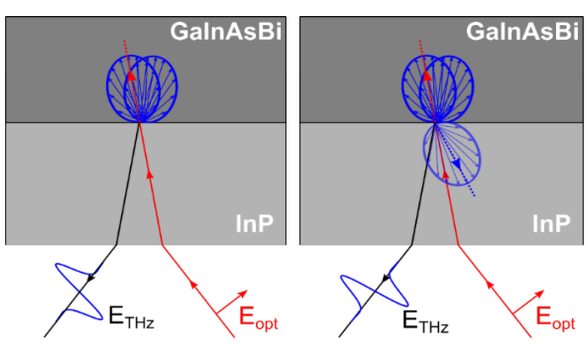


Fig. 5. The momenta of electrons excited from the heavy hole subband in the narrow bandgap part of heterostructure by linearly polarized femtosecond light pulse. (Left) The electron excess energy lower than the conduction band offset; (right) higher than the offset.

## Terahertz emission from ultrathin bismuth layers

Thin bismuth films demonstrate a rich variety of physical properties. Due to its small electron and hole effective masses, Bi has an extremely long Fermi wavelength ($\lambda_F$ ~30 nm), therefore quantum confinement effects can easily appear in the direction perpendicular to the surface of the layers. Several Bi samples were grown using solid source Veeco GEN Xplor MBE system on (111) oriented Si substrates. The growth process starts with ML thick wetting layer, proceeds with polycrystalline, rhombohedral (pseudocubic) sublayer, and finally – hexagonal sublayer. Their thicknesses were estimated by Refractive High Energy Electron Diffraction (RHEED) measurements (Fig. 6). The total thicknesses of the Bi layers determined by in-plane X-ray diffraction (XRD) were of the order of 8 nm. The THz excitation spectra were measured in the reflection and transmission geometries in the photon energy range from 0.4 to 1.9 eV. The THz emission sets on when the photon energy becomes larger than ~0.45 eV, which suggests that the energy band gap of these layers is of a similar order of magnitude. Fig. 7 shows the dependences of emitted THz pulse amplitude on the azimuthal angle ϕ between the optical field direction and the crystalline axes for two samples. There are two different contributions to the azimuthal angle dependences of THz signals radiated by thin Bi films: the component ϕ independent and proportional to cos(3ϕ). The isotropic parts of these dependences are explained by effect of photoexcited

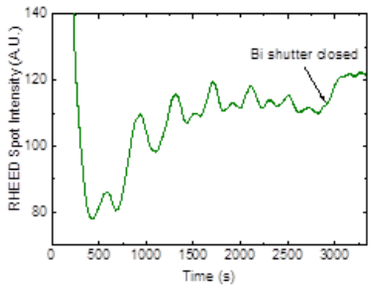


Fig. 6. RHEED pattern of Bi sample VS003.

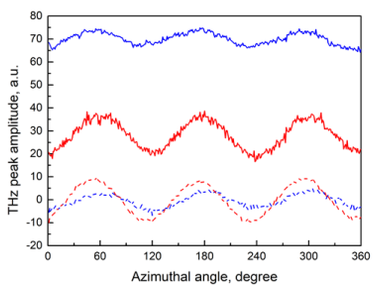


Fig. 7. Azimuthal angle dependences of THz emission from two samples: VS001 (blue) and VS002 (red). The spectra were measured in the transmission geometry: θ=30° (full lines) and θ=0° (dashed lines).

lateral currents. The azimuthal angle dependent component of the radiated THz signal could be explained in terms of the linear photogalvanic effect (shift current).

jan.devenson@ftmc.lt
ignas.nevinskas@ftmc.lt

## Devices of AlGaN/GaN heterostructures grown on SiC

Since 2014 we have been working on various AlGaN/GaN heterostructures developing custom-designed photonic and electronic devices suitable for high-power and high-frequency applications. Recent research was devoted to studies of AlGaN/GaN High-Electron Mobility Transistor (HEMT) structures affected by laser micromachining of deep channels on the substrate backside followed by mechanical cleavage along the ablated trench, so called laser assisted chip dicing. Our intention was to introduce the method into semiconductor industry of wide bandgap materials, such as sapphire (Al2O3), silicon carbide (SiC), gallium nitride (GaN), etc. Parameter optimization for laser ablation process allowed us to develop a novel laser microfabrication method which does not change the performance of the Schottky barrier diodes (SBD) and HEMTs. Note, that the trench lines were also made directly on active devices demonstrating as stable device performance as it was before the laser micromachining. In addition, we developed a technique, based on THz time-domain spectroscopy and Fourier-transform infrared (IR) spectroscopy, for the investigation of high-frequency characteristics of two-dimensional electron gas (2DEG) and GaN buffer layers in III-nitride heterostructures. We observed the renormalization effect of electron effective mass in the commercial AlGaN/AlN/GaN HEMT structures. Our results pave the way for the development of various optoelectronic devices of wide-bandgap heterostructures using laser micromachining and for remote monitoring of their performance. This, in turn, allows a smart control over the materials designed for operation in the IR band and THz frequency range.

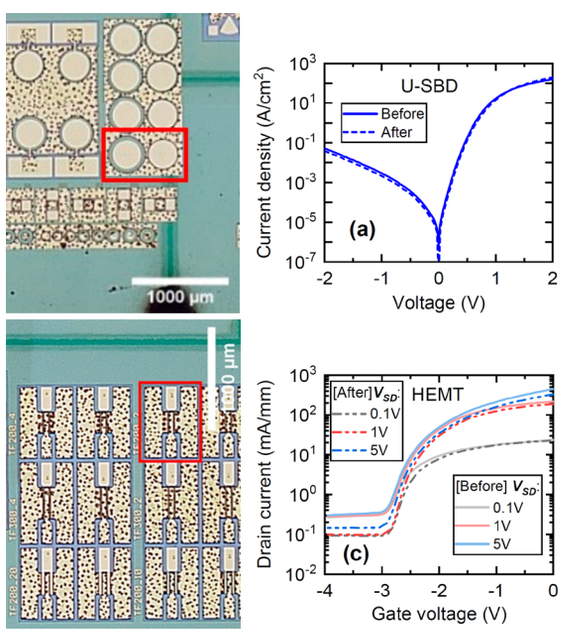


Fig. 8. Microscope images of the transparent SiC wafer with AlGaN/GaN heterostructures and electronic devices being in a focus and laser ablated trenches being on the back side. Red colour rectangles indicate selected devices for investigations: Schottky barrier diodes (top left) and HEMTs (bottom left) and their corresponding current-voltage (I-V) characteristics on the right hand side. The same devices were characterized before (solid lines) and after (dashed lines) laser processing of trenches on the SiC wafer side in a depth up to 270 µm.

irmantas.kasalynas@ftmc.lt

## High spatial coherence of hybrid polaritons in shallow *n*-GaN gratings

Hybrid surface plasmon-phonon-polaritons (SPPhPs) on the air/polar semiconductor interface were investigated by means of shallow surface relief grating using emission spectroscopy methods. For this a set of gratings with optimal 1 μm depth and periods from 8 to 22 μm were developed on a surface of the heavily-doped GaN crystal. The SPPhPs were excited by thermal heating or electrical biasing of conductive material which radiated directive polarized light in an extremely narrowband spectrum range. Detailed analysis of damping factors and propagation losses revealed maximum values of quality factor and spatial coherence length of hybrid polariton modes. Highest quality factor was found to be practically independent on the period of the shallow grating, as it was always detected near the frequency of transverse optical phonon, demonstrating values as high as 88 (200) in experiment (theory). Meanwhile, the largest value of coherence length strongly depended on the grating as the propagation losses of hybrid polariton modes showed a tendency to accumulate with the increase of wavevector (or observation angle, see figure). The SRG3 sample demonstrated the best performance among others with its highest coherence length at an angle of 12 deg reaching values up to 2.4 mm and 1.5 mm in theory and experiment, respectively. The highest coherence length value of 130 λ (87 λ), found in this work for modelled (measured) performance of SPPhPs in GaN, exceeded the maximum values of 60 λ and 104 λ reported in literature by other groups for SiC and w-GaN crystals, respectively. The results open a path for development of narrowband, directive thermal sources of coherent radiation in IR and THz ranges [87].

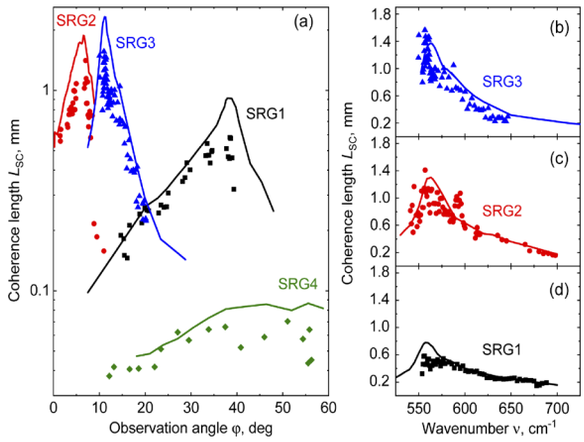


Fig. 9. (a) Coherence length dependence on the observation angle of the of SPPhPs emission from four different n-GaN gratings SRG1, SRG2, SRG3, SRG4 with the period of 11, 16, 22, and 8 μm, respectively. Symbols denote the experiment and solid lines represent the RCWA calculations taking into account that angular field of view (AFO) is 0 deg. (b)–(d) Coherence length dependence on frequency of SPPhPs emission from indicated samples. Symbols denote the experiment and solid lines represent the RCWA calculations taking into account that AFO=0.6 deg. Note that maximum of the coherence length is found in the vicinity of TO phonon frequency for all SRG samples.

vytautas.janonis@ftmc.lt

## GeSn IR photodiodes for near-IR spectrum

Photo-detection in the near-infrared is commonly performed by Ge or InGaAs-based photodetectors. Further extension of the detection range to the mid-infrared region can be performed by germanium-tin (GeSn) material which shows promising characteristics and is fully compatible with silicon electronics as can be directly grown on silicon substrates. In this work, we investigated optoelectronic properties of the photodiodes prepared of 200 nm thick Ge0.95Sn0.05 epitaxial layers on Ge/n-Si substrate with aluminum contacts. Set of test diodes were irradiated by pulsed Nd:YAG laser with the intensity ranging from 60 to 260 MW/cm2. The laser-irradiated diode was found more sensitive in the long wavelength range due to laser induced Sn atoms redistribution providing formation of graded bandgap structure. Sub-millisecond photocurrent relaxation in the diodes revealed their suitability for image sensors. Authors findings open the perspective for development of the GeSn alloys with laser irradiation improved photo-sensitivity in the mid-infrared region [215, 216].

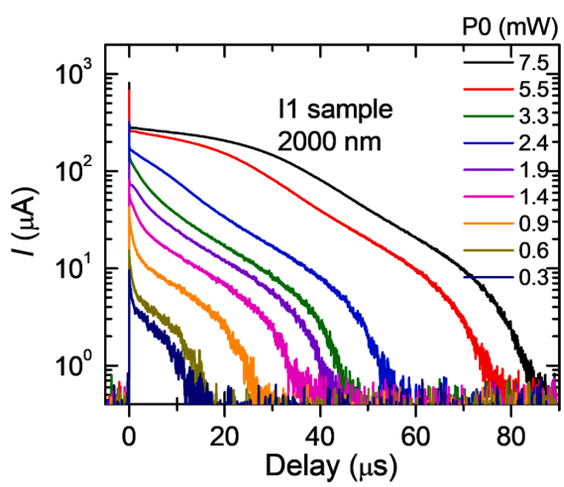


Fig. 10. Temporal response (photocurrent relaxation curves) of GeSn IR photodiodes (I1 sample) under 0.5 V reverse bias using different laser power at wavelength of 2000 nm. With the excitation increase, the response of the photodiode becomes slower due to the screening of charge separation potential by injected carriers.

liudvikas.subacius@ftmc.lt

## Optical anisotropy of CuPt-ordered GaAsBi alloys

The spontaneous CuPt-type atomic ordering in investigated MBE-grown $GaAs_{1-x}Bi_x$ epitaxial layers (of ~ 1 μm thickness and $x \sim 0.04$ composition) induces a pronounced optical anisotropy, which was revealed by numerous optical spectroscopy techniques. The photoluminescence of the bismides is polarized predominantly along the [110] direction, which is perpendicular to a projection of the $CuPt_B$-ordering axes onto a sample surface. The modulation spectroscopy reveals two distinct, polarization dependent, optical features in the vicinity of the fundamental bandgap, indicating a splitting of the valence band $\Delta_{vb}$ of about 60 meV. The polarized optical transmittance spectra, measured at the $[110]$ and $[1\bar{1}0]$ polarizations, are shifted with respect to each other by the spectral difference close to the determined $\Delta_{vb}$. In a spectral region of split-fundamental-gap, investigated samples manifest linear birefringence and dichroism with respect to the same, atomic-ordering related, $[110]$ and $[1\bar{1}0]$ axes. Both the valence band splitting and optical anisotropy in dilute, $x \sim 0.04$, bismides quantitatively are of the same order of magnitude as in conventional III-V semiconductor alloys despite the fact that the ordering parameters in bismides (due to their small $x$ values) are an order of magnitude lower [103].

vytautas.karpus@ftmc.lt

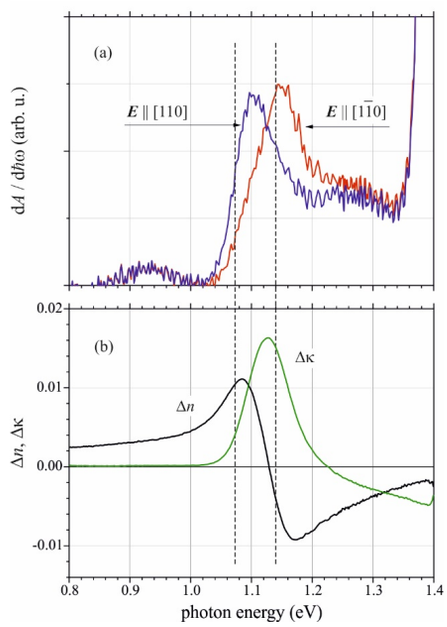


Fig. 11. (a) Optical density differential spectra and (b) the spectra of birefringence $\Delta n = n_{[110]} - n_{[1\bar{1}0]}$ and linear dichroism $\Delta\kappa = \kappa_{[110]} - \kappa_{[1\bar{1}0]}$ for the $GaAs_{1-x}Bi_x$ ($x$=0.042) sample. Vertical dashed lines indicate spectral positions of the optical features observed in photo-modulated transmittance / reflectance spectra.

## In vivo imaging of the human cornea and retina with ultrahigh-speed optical coherence tomography

Imaging of the human cornea and retina *in vivo* is important for diagnosing and following a range of eye diseases, such as macular degeneration, glaucoma and diabetic retinopathy. Optical coherence tomography (OCT) can rapidly acquire 3D (volumetric) images of various parts of the eye. However, spatial resolution, imaging speed and depth is still a major issue in OCT. Better resolution would enable resolving various retinal features, such as photoreceptors, high-speed imaging would help to combat imaging artefacts caused by involuntary eye motion and deep-tissue imaging would allow seeing choroidal layers with better contrast providing wealth of information. Recently, to speed up OCT imaging, Fourier-domain Full-Field OCT (FF-FD-OCT) has been introduced that uses a multipixel (2D) detector (camera) to parallelize signal acquisition. We have shown that to image the human cornea *in vivo* with this technology, a multimode fiber can be used with a small core that breaks down the spatial coherence of a laser [11]. The spatially coherent laser otherwise focuses to a tiny spot on the retina, when imaging cornea, causing damage risk. Simply solving this safety issue enabled us to acquire high-resolution images of various layers in the cornea, as shown in Fig. 12. This demonstrates potential of FD-FF-OCT as a non-contact method in clinical use. Coherence noise suppression by the same multimode fiber in FD-FF-OCT enabled acquisition of retinal and choroidal layers with high contrast, as shown in Fig. 13. There, multiple volumes were stitched together to generate large field-of-view lateral and axial images. It shows that this technology is suitable for retinal and choroidal imaging, and especially of hard-to-image layers, such as choriocapillaris. We have also used a pupil splitting approach in both optical layouts of the systems in order to incorporate a real-time imaging module that provided corneal/retinal axial images for visual guidance [12].

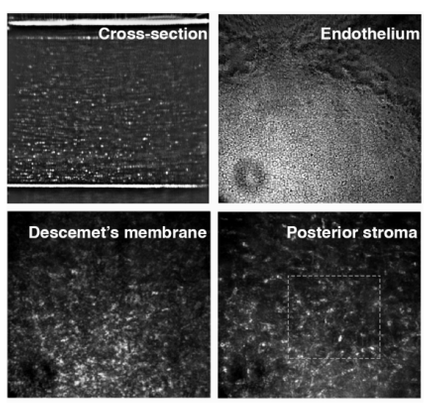


Fig. 12. Human cornea recorded in vivo with ultra-high-speed OCT. Volumetric (3D) data were recorded over 0.6 mm x 0.6 mm area and ~1 mm axial range in just 0.2 sec., and with lateral resolution of 2.5 μm.

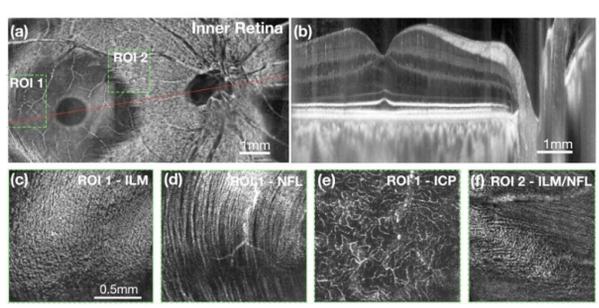


Fig. 13. Montaged retinal images (9 mm x 4.6 mm) of macula and optic nerve head recorded in vivo with ultrahigh-speed OCT. (a) thin en face projection of the inner retinal layers featuring the optic nerve discs, retinal nerve fiber layer (NFL), and retinal ganglion cell layer (GCL). (b) Cross-sectional image along the papillomacular axis of the human retina indicated by red line in panel (a); (c-f) details of the inner limiting membrane (ILM), NFL and intermediate capillary plexus (ICP).

egidijus.auksorius@ftmc.lt

# Molecular physics

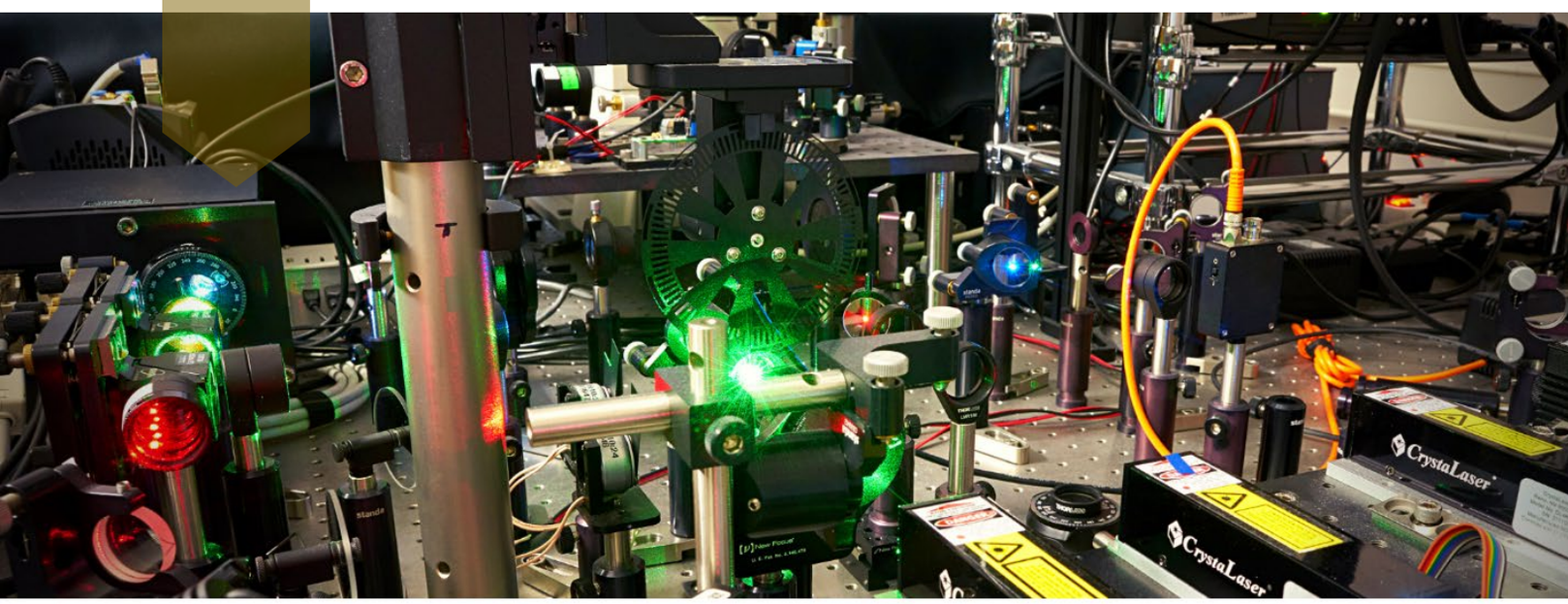


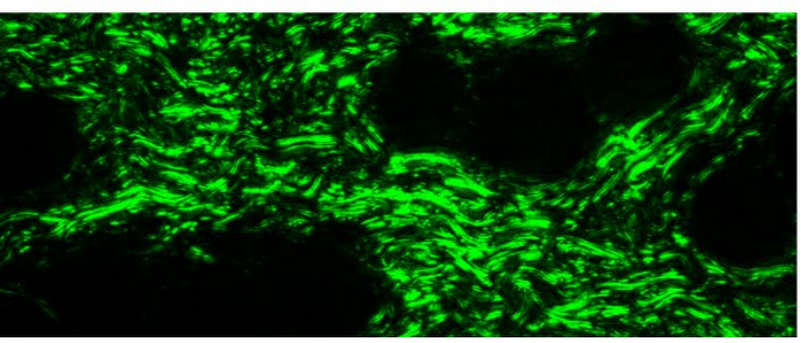

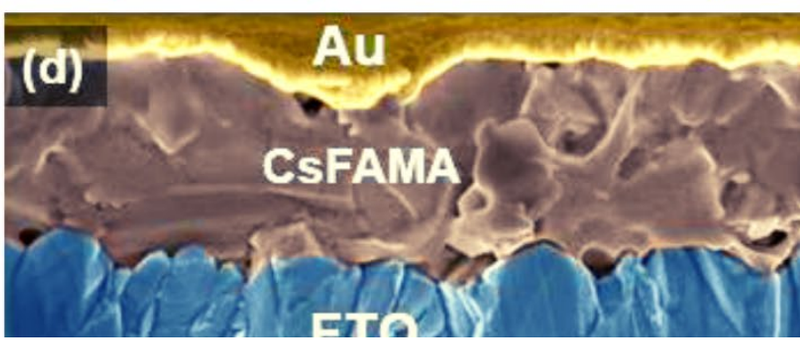


## The Department of Molecular Compounds Physics

performs research related to molecular photonics, ranging from investigations of natural and artificial molecular systems utilizing optical techniques to the development of molecular and hybrid devices. We seek a better understanding of photoinduced processes in biological and artificial molecular systems, optimization of the material properties and photoinitiated processes in photonic devices. Organic materials increasingly penetrate into electronics—the field that used to be totally dominated by the inorganic semiconductors in the past. Unlimited variety of organic molecules, as well as a broad range of technological fabrication abilities promise a wide spectrum of device characteristics and their application fields. On the other hand, that raises requirements for a detailed understanding of molecular properties responsible for processes that take place in the molecular-based materials. Molecular systems are characterized by particularly high degree of complexity. Various intramolecular and intermolecular interactions create complex hierarchical structures determining properties of molecular systems and their functional peculiarities. In addition to electrons and holes, excitons and ions play crucial roles in organic semiconductors, while relatively week intermolecular interactions determine morphology of molecular materials and complex structures of biological systems. All this complexity has to be taken into consideration in order to enhance the efficiency of the molecular devices and to understand functions of molecular systems in nature. We use advanced experimental techniques, such as ultrafast spectroscopy, nonlinear and single molecule microscopy and optoelectrical methods, together with theoretical calculations to address questions related to complex excited-state dynamics and the sequence of electronic events in optically excited molecular and hybrid systems. The objects of our investigations are numerous – from biological photosynthetic and protein-DNA complexes, molecular viscosity sensors to organic and perovskite solar cells.

## Carrier mobility dynamics under actual working conditions of organic solar cells

Though organic photovoltaics has made significant progress since its appearance decades ago, the underlying physics of charge transport in working cells is still under debate. Carrier mobility, determining their extraction and recombination is one of the most important parameters, but it is too complex to be well understood. Low energy charge carrier states acting as traps play a particularly important role in carrier transport. Occupation of these states in real operation conditions of solar cells induces additional complexity. We used several transient methods and numerical modelling to address carrier transport in actual working conditions of bulk-heterojunction organic solar cells based on fullerene and non-fullerene acceptors. We show that occupation of low-energy states strongly depends on the blend materials and the effective electric field. We define the conditions when such an occupation increases carrier mobility, making it less time-dependent on µs time scale, and when its influence is only marginal.

rokas.jasiunas@ftmc.lt

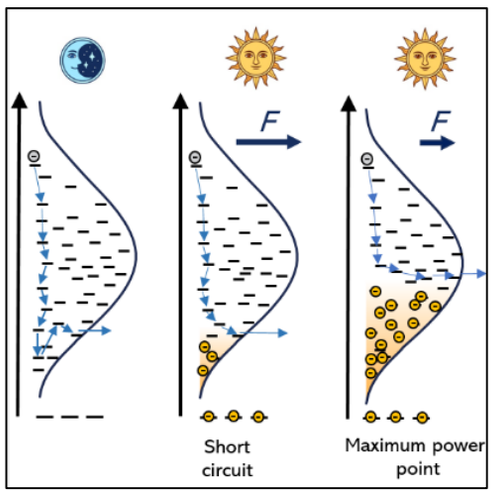


Fig. 1. Population of distributed density of states (DOS) and carrier relaxation within DOS at different solar cell operation conditions. The carrier mobility dynamics is determined by their relaxation within high energy part of the distributed density of states. The mobility strongly decreases with time independently of population of low-energy states.

## Confronting FCP structure with ultrafast spectroscopy data: evidence for structural variations

Diatoms are a major group of algae, responsible for a quarter of the global primary production on our planet. Their adaptation to marine environment is ensured by their light-harvesting antenna – the fucoxanthin-chlorophyll protein (FCP) complex, which absorbs strongly in the blue–green spectral region. Only in 2019, 3D structures of several FCP complexes – an FCP dimer from the pennate diatom *Phaeodactylum tricornutum* and the PSII-FCP supercomplex from the centric diatom *Chaetoceros gracilis* – were revealed. Surprisingly, we find that the published FCP structures cannot explain several observations obtained from ultrafast spectroscopy, describing the excitation energy transfer in the FCP from another centric diatom *Cyclotella meneghiniana*. Using the available structures and results from electron microscopy, we construct a trimer-based FCP model for *C. meneghiniana*, consistent with ultrafast experimental data. Our observations suggest that the structures from the proteins belonging to the FCP family display larger variations than the equivalent LHC proteins in plants, which may reflect species-specific adaptations or original strategies for adapting to rapidly changing marine environments.

leonas.valkunas@ftmc.lt

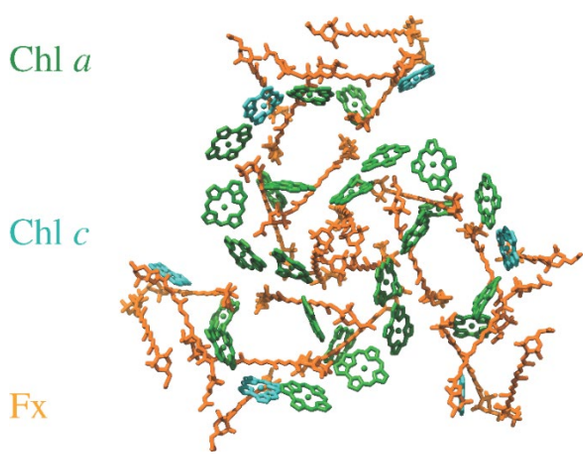


Fig. 2. Proposed pigment arrangement in the trimeric FCP of *Cyclotella meneghiniana* consistent with ultrafast spectroscopic data. Here Chl *a/c* is chlorophyll *a/c* and Fx is fucoxanthin. For clarity, Chls are only shown as porphyrins.

## Surface-enhanced Raman spectroscopy of organic molecules and living cells with gold-plated black silicon

Black silicon (bSi) refers to an etched silicon surface comprising arrays of microcones that effectively suppress reflection from UV to near-infrared (NIR), while simultaneously enhancing the scattering and absorption of light. We demonstrate the outstanding performance of this substrate by highly sensitive and specific detection of a small organic molecule of 4-mercaptobenzoic acid and living C6 rat glioma cell nucleic acids/proteins/lipids. Specifically, the bSi/Au SERS-active substrate offers a unique opportunity to investigate the malignant transformation of living cells using characteristic protein disulfide Raman bands as a marker.

lena.golubewa@ftmc.lt

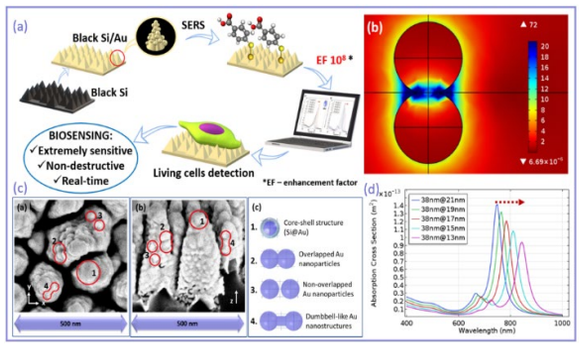


Fig. 3. (a, c) Design of a bSi-based gold-sputtered SERS-active substrate for the detection of trace molecule concentration and living cells. (b, d) FEM simulation results proving high signal enhancement factor due to the local surface plasmon resonance.

## Double charge transfer dominates in carrier localization in low bandgap sites of heterogeneous lead halide Perovskites

Heterogeneous organic-inorganic halide perovskites possess inherent non-uniformities in a bandgap that are sometimes engineered and exploited on purpose, like in a quasi-2D perovskites. In these systems, charge carrier and excitation energy migration to lower-bandgap sites are the key processes governing the luminescence. The question, which of them dominates in particular materials and under specific experimental conditions, still remains unanswered, especially when charge carriers comprise excitons. In this study, transient absorption (TA) and transient photoluminescence (PL) techniques are combined to address the excited state dynamics in quasi-2D and other heterogeneous perovskite structures in a broad temperature range, from room temperature down to 15 K. The data provide clear evidence that the charge carrier transfer rather than the energy migration dominates in heterogeneous quasi-2D perovskite films.

marius.franckevicius@ftmc.lt

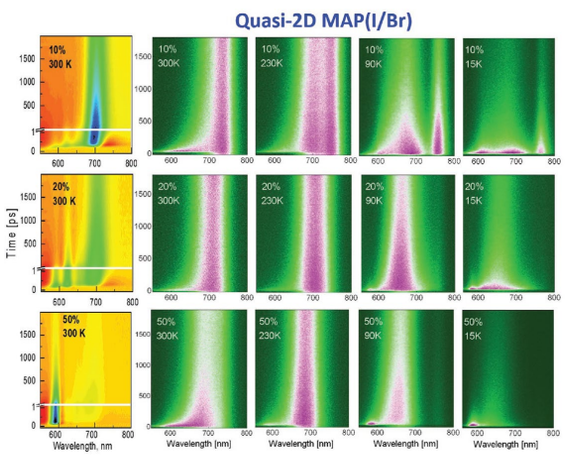


Fig. 4. Evolution of the transient absorption spectra at room temperature and evolutions of photoluminescence spectra at different temperatures measured for quasi-2D MAPI2Br1 samples with 10 %, 20 %, and 50 % of butylammonium (BA) substituting MA.

## Designing a red-emitting viscosity-sensitive BODIPY fluorophore for intracellular viscosity imaging

Viscosity imaging at a microscopic scale can provide important information about biosystems, including the development of serious illnesses. Microviscosity imaging is achievable with viscosity-sensitive fluorophores, the most popular of which are based on the BODIPY group. However, most of the BODIPY probes fluoresce green light, whereas the red luminescence is desired for the imaging of biological samples. Designing a new viscosity probe with suitable spectroscopic properties is a challenging task because it is difficult to preserve viscosity sensitivity after modifying the molecular structure. We managed to develop a new red-emitting, viscosity-sensitive BODIPY fluorophore BP-PH-2M-$NO_2$ which is suitable for reliable intracellular viscosity imaging of lipid droplets in MCF-7 breast cancer cells. The design of BP-PH-2M-$NO_2$ was aided by DFT calculations that allowed a successful prediction of the viscosity sensitivity of fluorophores before synthesis, which has not been done before. In summary, we have created a new red viscosity probe possessing monoexponential fluorescence decay that makes it attractive for lifetime-based viscosity imaging.

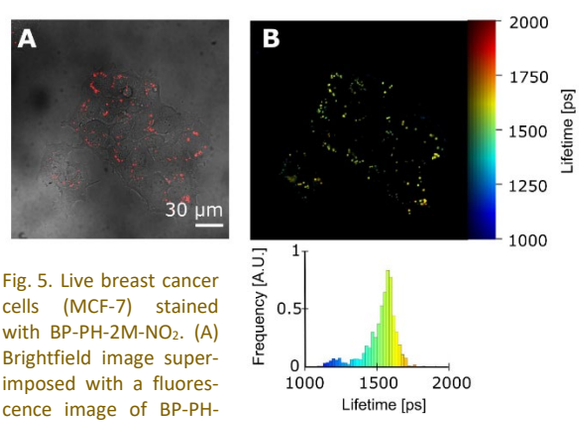


Fig. 5. Live breast cancer cells (MCF-7) stained with BP-PH-2M-$NO_2$. (A) Brightfield image superimposed with a fluorescence image of BP-PH-2M-$NO_2$ showing the staining of endocytotic vesicles. (B) FLIM image with the lifetime histogram at the bottom. The mean lifetime is 1532±74ps corresponding to 123 cP viscosity.

aurimas.vysniauskas@ftmc.lt

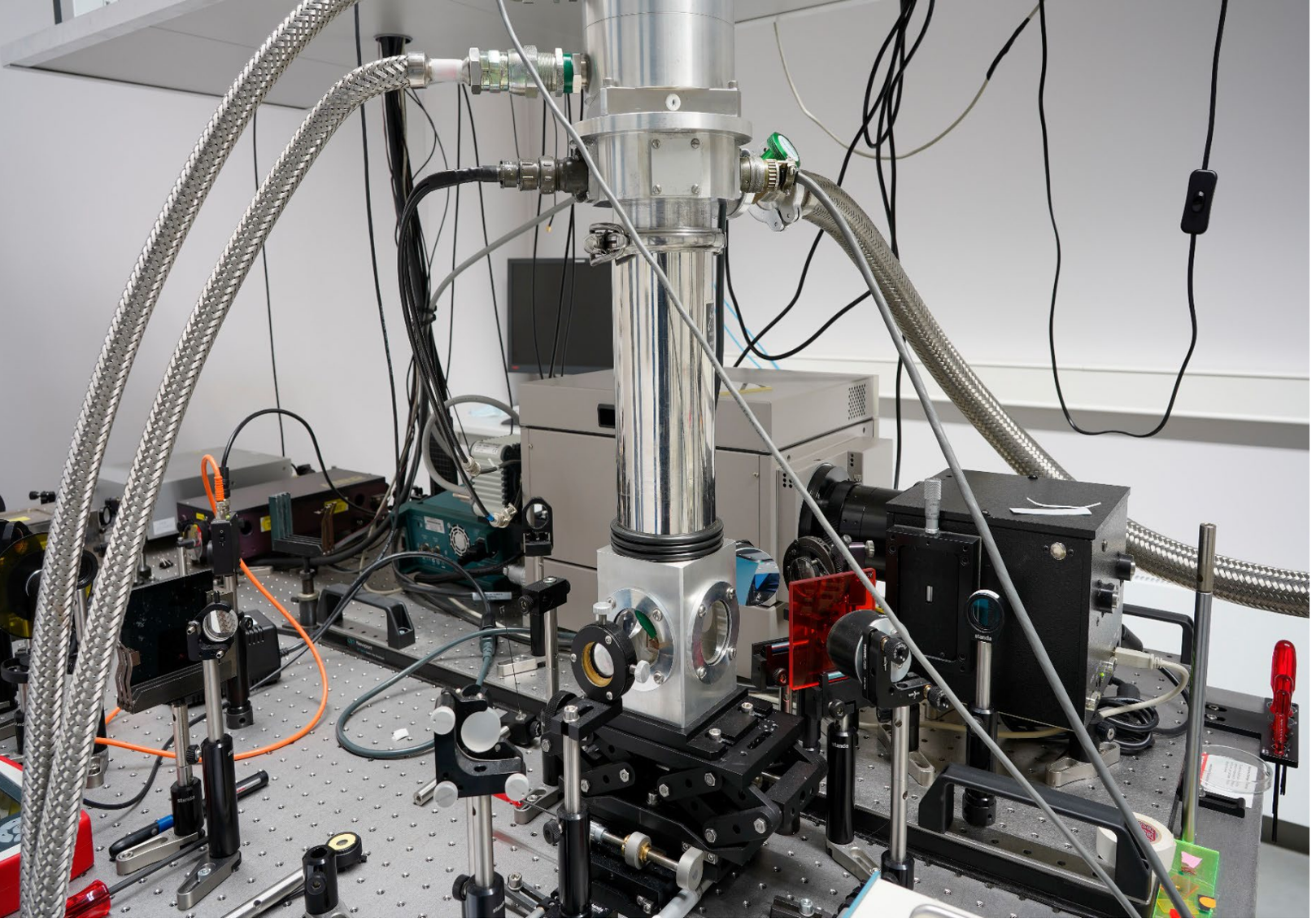

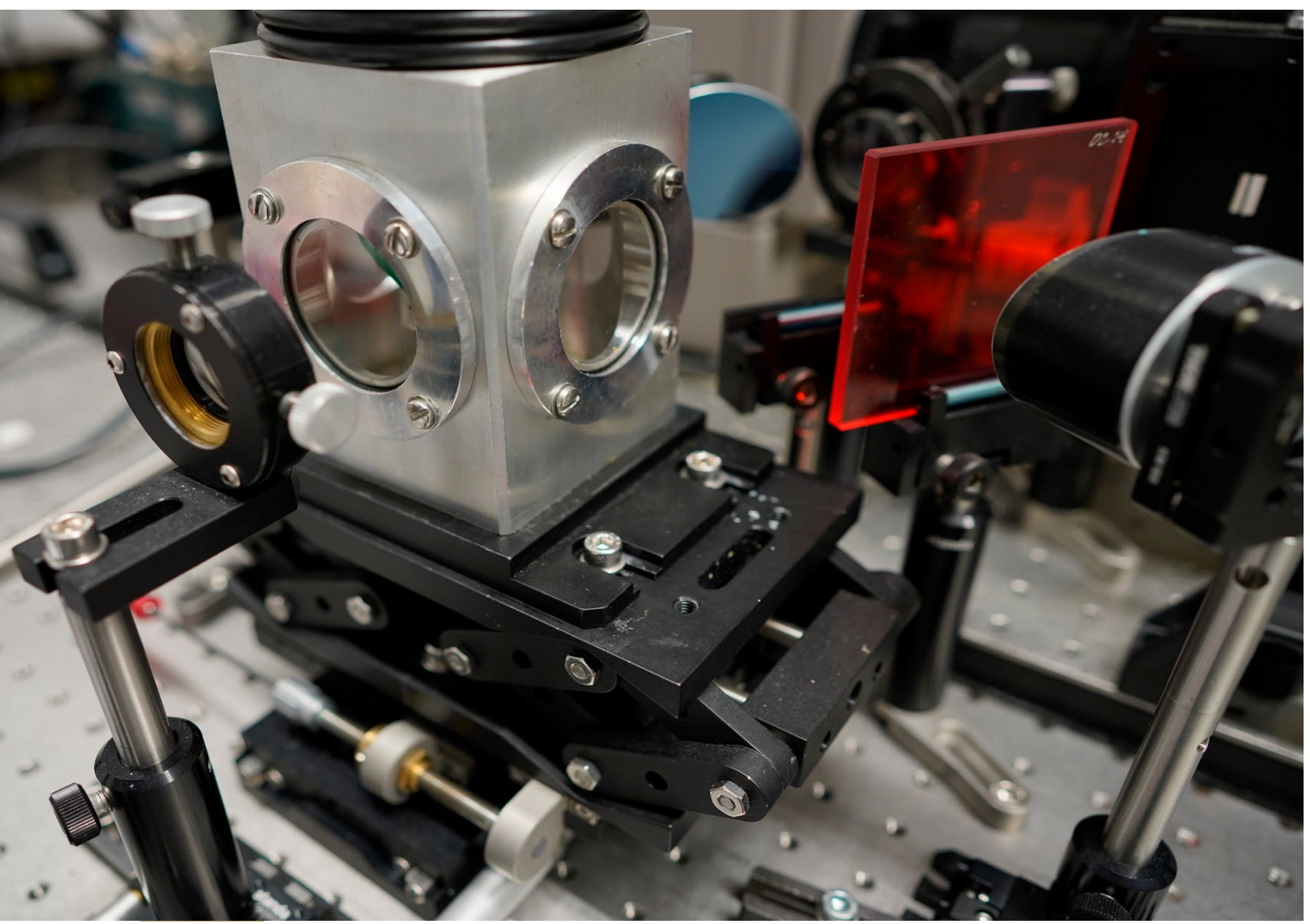

# Nanoengineering

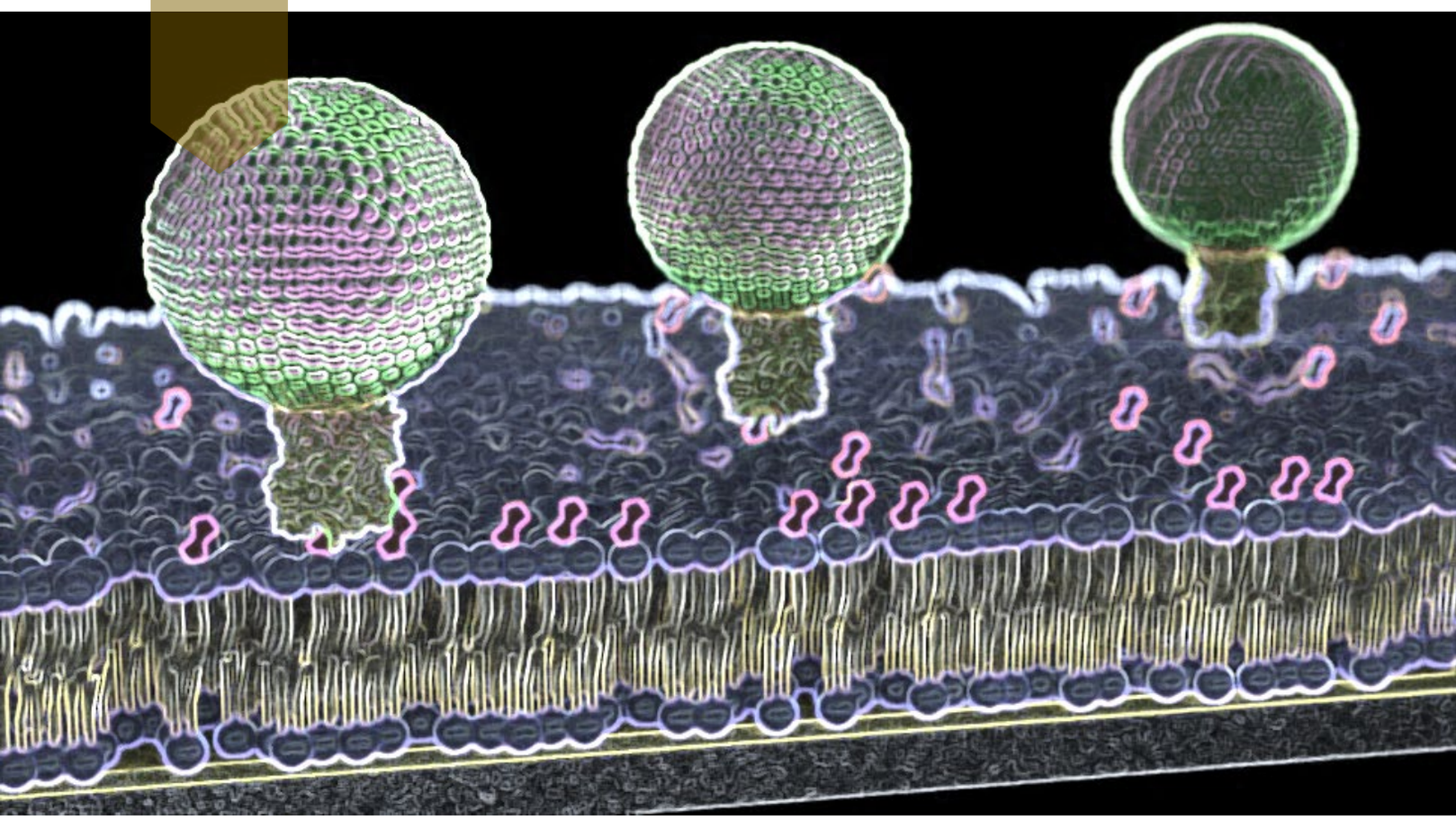

## The Department of Nanoengineering

focuses on new tools and processes for fabrication of functional nanoarchitectures for broad applications: from photonics to life sciences and medicine. One of our long-term interests is the development of reliable miniaturised platforms for biophysical studies at different levels: proteins, single cells and tissues. Also, we aim at establishing cost-effective and easy nanofabrication platforms, suitable for patterning and functionalisation of new nano- and biomaterials. Among our achievements of the past decade we can name high-speed atomic force microscopy and nanolithography, new supramolecular architectures and cell membrane-mimetic assemblies, nanobiochips for single-cell analysis, electrochemical and optical devices for biosensing, micro and nanopatterned hydrogels for tissue engineering.

Another focus of our studies is the development of materials for electrochemical sensing as well as (bio)sensors for food quality monitoring and medical applications. New generation of conducting polymers, composed of B group vitamins or some specific amino acids, is synthesised electrochemically. Such (bio)sensors can be integrated into flexible point-of-care devices due to their biocompatibility and organism friendly nature.

The competences of the department are interdisciplinary, the implementers are physicists, biophysicists, chemists, biologists, biotechnologists, nanotechnologists, etc. This allows fast, cost effective and reliable creation and development of nanoarchitectures for the applications mentioned above.

## Mesoscale surface patterning of self-assembled monolayers with water

The precise patterning of surfaces at nano-, micro- or meso-scale represents an essential step toward fabricating (bio)sensors or (bio)chips. We have developed an experimentally simple and chemically mild method for the formation of spatially-confined surface areas of reactive amine groups on self-assembled monolayers using deprotection of tert-butoxycarbonyl amine protecting group. This is achieved by using the temperature of the substrate elevated to 100 °C and water as a sole chemical. The method is applicable to the surface micro- and meso-scale patterning of reactive amine groups with locally controlled concentration. In contrast to previous reports, our method requires no corrosive or environmentally unfriendly chemicals and is operationally very simple. The proof-of-concept demonstration of a new method was based on the utilization of the new type of in- house developed thiols, forming well-ordered and thermally very stable self-assembled monolayers on gold surface. Spectroscopic evidence of amine deprotection was obtained using reflection adsorption infrared spectroscopy.

edvinas.orentas@ftmc.lt

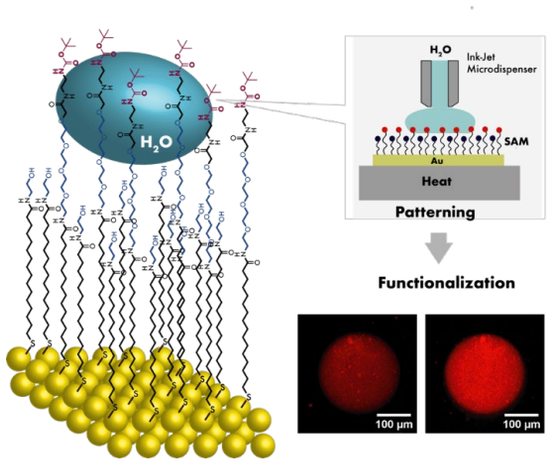


Fig. 1. Schematic representation of the self-assembled monolayer, micro-dispensing of water droplets and functionalization of the surface with quantum dots.

## A novel approach to prepare highly oxidized graphene oxide: structural and electrochemical investigations

Two newly modified Hummers methods include the pre-oxidation of graphite powder by mixtures of $H_3BO_3/H_2SO_4$ and $H_3BO_3/H_2SO_4/CrO_3$. Compared to the traditional Hummers method, these significant improvements substantially enhanced the number of oxygen functionalities in graphene oxide (GO) layers. The Boehm titration showed that GO layers contain such oxygen functionalities as phenolic, ketone, lactone, carboxyl, and epoxy. Quantitative XPS analysis revealed that GO obtained using a pre-oxidation step with $H_2SO_4/H_3BO3/CrO_3$ mixture has higher oxidation degree, C/O = 1.03. Moreover, a greater number of electronegative functional groups, causing the decrease of the zeta potential (-43.3 mV), were observed. The Raman analysis revealed a slightly higher structural disorder in GO layers during the increase of oxidation levels. Further, reduced GO (rGO) obtained from newly synthesized GO was tested in a label-free electrochemical

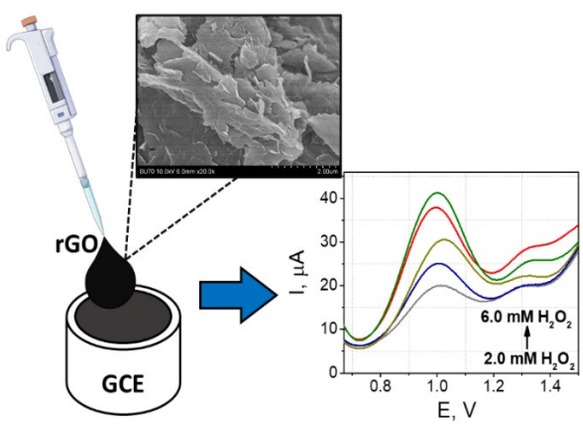


Fig. 2. Electrode modification with newly synthesized rGO as a base for $H_2O_2$ detection.

detection of $H_2O_2$. The electrochemical investigations showed that the samples were prospective for $H_2O_2$ sensing. Thus, the properties of rGO can be tuned by varying the oxidation degree of GO. This might stimulate new developments of rGO-based sensors.

rasa.pauliukaite@ftmc.lt

# Spectroelectrochemistry & organic chemistry

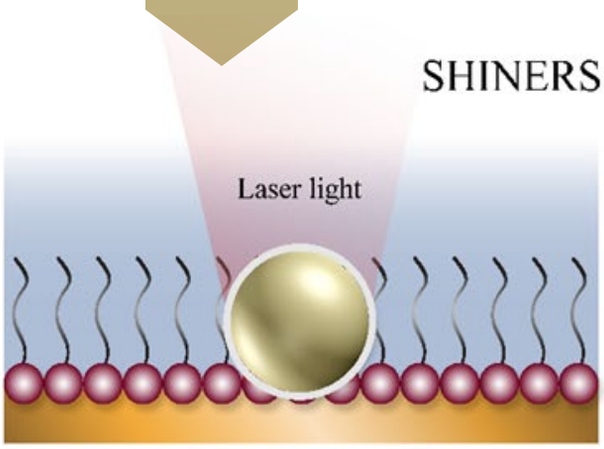


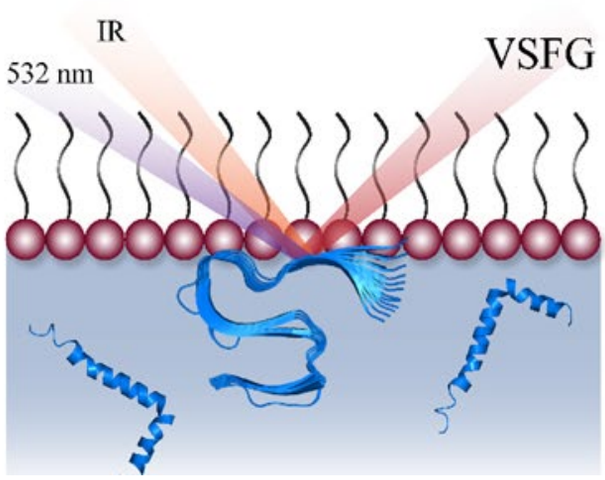


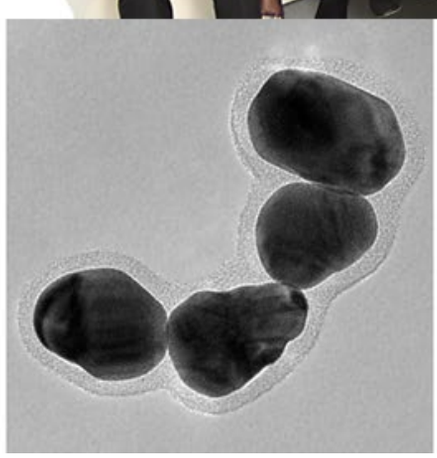

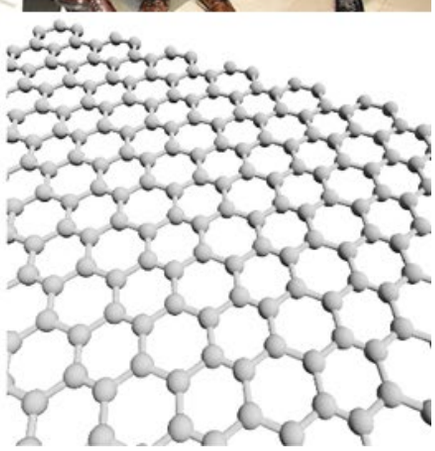

## Spectroscopy of adsorption and biochemical processes at surfaces and interfaces, chromatography of bio-active secondary metabolites in herbal material

Electron transfer reactions, electrocatalysis, functioning of biomolecules, self-assembly, and various biochemical processes take place predominantly at the surfaces and interfaces. To predict and control the way those processes will proceed, a molecular level understanding is required. Our group employs and develops novel spectroscopic techniques that enable to probe complex liquid and solid interfaces that are difficult to study with most common spectroscopic techniques. Shell-isolated nanoparticle enhanced spectroscopy (**SHINERS**) is the most promising vibrational surface-enhanced Raman technique. It was developed in order to overcome the limitations of a substrate use in surface enhanced Raman spectroscopy (Tian et al. 2010). Recently, our group used SHINERS to study potential-induced changes in the molecular structure of self-assembled molecules. We also successfully characterized the surface of functionalized graphene and a biological system of yeast cells using SHINERS. Multiwavelength Raman spectroscopy was employed to get insights into the electrochemical redox transitions of polyaniline and poly(N-methylaniline) in solutions of different acidities. We have used chromatography methods to extract information on bio-active secondary metabolites in herbal material. Vibrational sum-frequency generation spectroscopy (**VSFG**) is a unique technique with an intrinsic surface

specificity. It enables to record the vibrational spectrum explicitly of the surface without any interference with a signal from the bulk material. It is a very versatile technique that can be used to study many different surfaces and interfaces such as solid/air, solid/liquid, and liquid/air. We applied VSFG to study the interaction of Amyloid-β-(1-42) peptide and its aggregates with lipid/water interfaces. The greatest potential of VSFG lies in its ability to measure liquid surfaces with a sensitivity of a few molecular layers. Currently, we are studying the aggregation of proteins and peptides at the surface of model lipid membranes by means of VSFG. The aim of our study is to answer one of the most important questions in biology and chemistry: what is the role of protein-membrane interaction in protein aggregation process?

## Interaction of amyloid-β-(1-42) peptide and its aggregates with lipid/water Interfaces probed by vibrational sum-frequency generation spectroscopy

Interaction between the amyloid-β (Aβ) peptide and the cell membrane is an important factor in the modulation of Aβ aggregation resulting in the development of Alzheimer's disease. We used surface-sensitive vibrational sum-frequency generation (VSFG) spectroscopy to investigate the interaction between model lipid monolayers, and monomeric Aβ(1-42) and its aggregates. Combining VSFG with atomic force microscopy (AFM) and thioflavin T (ThT) fluorescence measurements, we found that only small aggregates with probably a β-hairpin-like structure were adsorbed to zwitterionic lipid monolayer (DOPC). In contrast, larger aggregates with an extended β-sheet structure were adsorbed to a negatively charged lipid monolayer (DOPG). By performing spectral VSFG calculations, we reveal a clear correlation between the amide-II' signal and the degree of amyloid aggregates (e.g., oligomers or (proto)fibrils) of various Aβ (1-42) structures. The combination of the VSFG experiments and calculations substantiated the amide-II(') band as a legitimate amyloid marker.

simona.strazdaite@ftmc.lt

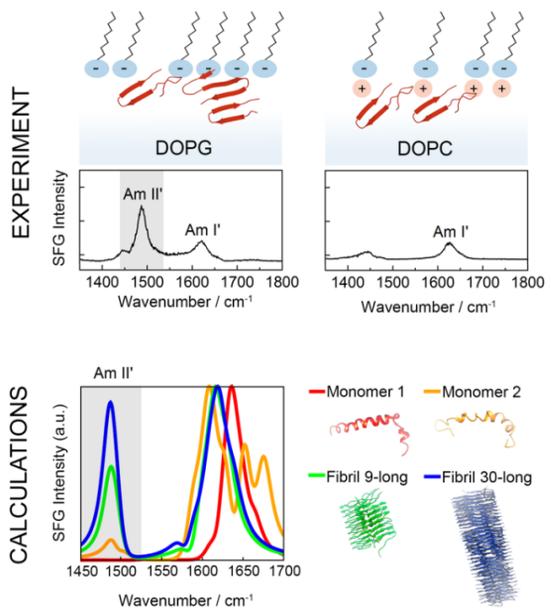


Fig. 1. (Top) Schematic representation of Aβ(1-42) aggregates adsorbed to DOPC and DOPG monolayers. (Bottom) Calculated VSFG spectra for various hypothetical Aβ(1-42) structures, indicating an increase of the amide-II' peak with increasing fibrillation.

## Poly(N-methylaniline) vs polyaniline: an extended pH range of polaron stability as revealed by Raman spectroelectrochemistry

A comparative study of polyaniline (PANI) and poly(N-methylaniline) (PNMA) has been performed by means of Raman spectroelectrochemistry. The dependence of Raman features on electrode potential and solution acidity was studied, and relative content of polaronic and bipolaronic states was evaluated. In an acidic solution, the semioxidized emeraldine form of either PANI or PNMA exists in equilibrium between their polaronic and bipolaronic states. In a neutral or even slightly alkaline solution, this equilibrium for PANI shifts to bipolaron state, resulting in loss of its conductance. For PNMA, however, the relative content of polaronic state appears high enough even in pH-neutral solutions, thus determining a higher conductivity of PNMA in pH-neutral environment as compared to that of PANI.

albertas.malinauskas@ftmc.lt

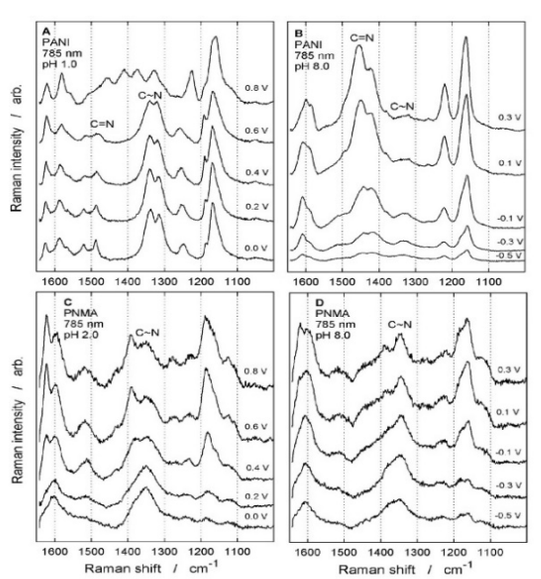


Fig. 2. Resonance Raman spectra obtained at 785 nm laser line excitation from Au electrode modified with a layer of polyaniline (A and B) or poly(N-methylaniline) (C and D) in pH 1.0 (A and C) and pH 8.0 (B and D) solutions at different electrode potentials. The C~N stretching band in the 1300-1400 $cm^{-1}$ spectral region is related to a polaronic state of the polymer.

# Functional materials & electronics

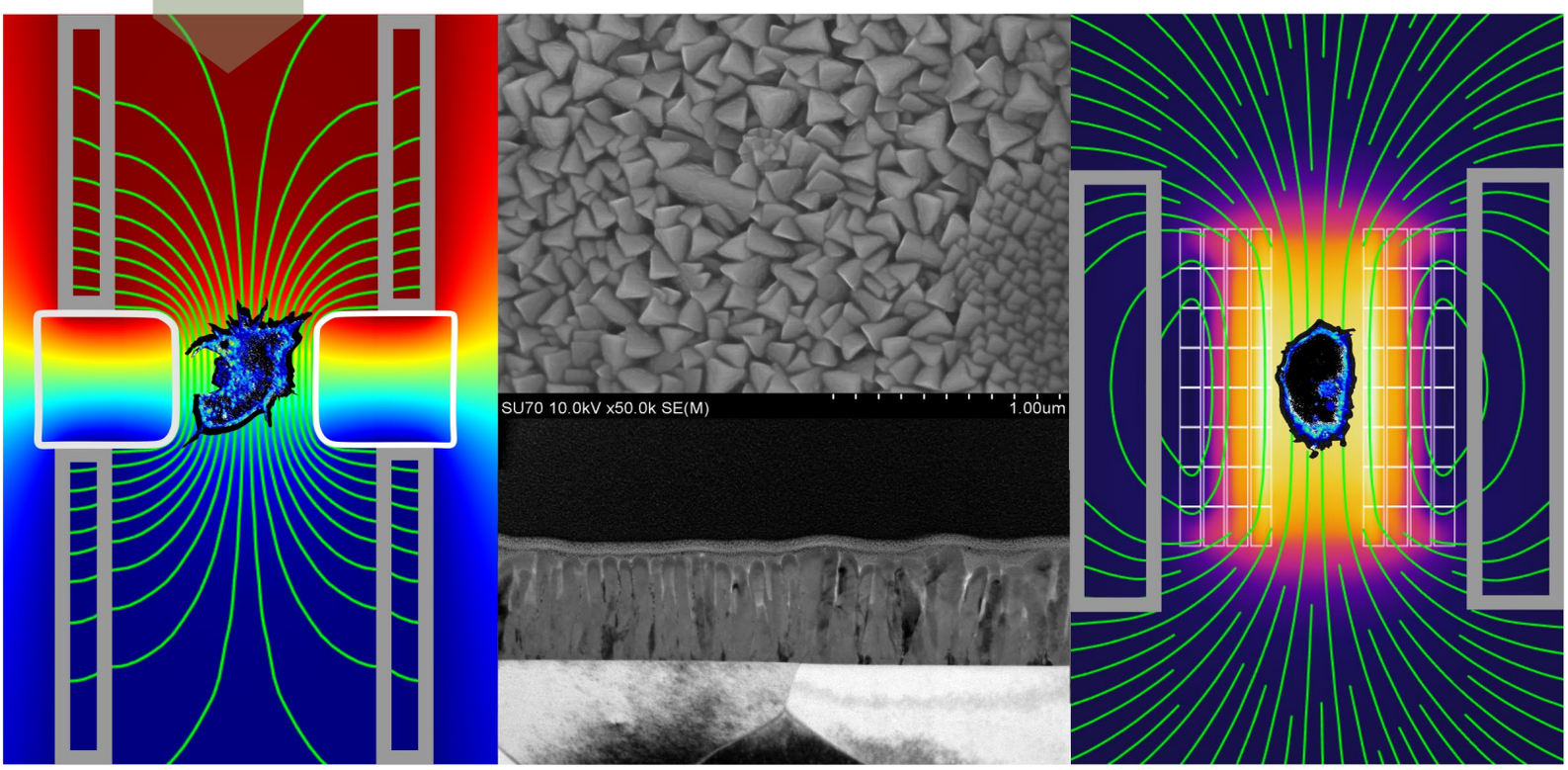


(Left) Electric field distribution in cross-flow treatment chamber during cell electroporation. (Right) Magnetic field distribution in pulsed coil magnet. (Middle) Electron scanning microscopy and transmission electron microscopy images of magnetoresistive La-Sr-Mn-O nanostructured film.

In the last decade the increasing demand of various sensors and sensor systems has resulted in the development of novel technologies for fabrication of advanced functional materials, thin films and nanostructures. The department of Functional materials and electronics is developing the growth technologies of advanced materials and thin films with special properties enabling to use them in various areas of applications. The physical, chemical and biological properties are investigated and combined in developed components and systems. The numerical calculations as well as experimental investigations of prepared structures and biological cells are performed using various computational tools and experimental techniques, and responses of these materials to external stimuli (electrical, magnetic, light, microwaves, etc.) are studied for a wide range of applications.

## Electroporation assisted improvement of freezing tolerance in yeast cells

Prolonged storage of frozen dough worsens the structure of thawed dough. The main reason is the inhibition of yeast activity. In this study we investigated applicability of pulsed electric field (PEF) treatment for introduction of cryoprotectant into yeast cells. We showed that pre-treatment of cells suspended in a trehalose solution improves freezing tolerance and results in a higher viability after thawing. The viability increased raising electric field strength (from 3 to 4.5 kV/cm) and incubation time (from 0 to 60 min) after exposure. The viability of untreated cells dropped to 10%, while the pre-treatment with PEF and trehalose tripled the viability.

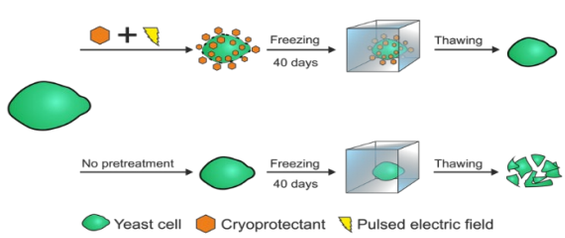


Fig. 1. Schematic overview of the developed new technology of permeabilization assisted improvement of freezing tolerance.

povilas.simonis@ftmc.lt

## Possible synergism between antimicrobial photodynamic therapy and pulsed electric fields for biofilm treatments

Currently, microbial biofilms have been the cause of a wide variety of infections in the human body, reaching 80% of all bacterial and fungal infections. The biofilms present specific properties that increase the resistance to antimicrobial treatments. Thus, the development of new approaches is urgent, and antimicrobial photodynamic therapy (aPDT) has been shown as a promising candidate. The aPDT involves a synergic association of a photosensitizer (PS), molecular oxygen and visible light, producing highly reactive oxygen species (ROS) that cause the oxidation of several cellular components. This therapy attacks many components of the biofilm, including proteins, lipids, and nucleic acids present within the biofilm matrix causing inhibition even in the cells that are inside the extracellular polymeric substance (EPS). Recent advances in designing new PSs to increase the production of ROS and the combination of aPDT with other therapies, especially pulsed electric fields (PEF), have contributed to enhanced biofilm inhibition. The PEF has proven to have antimicrobial effect once it is known that extensive chemical reactions occur when

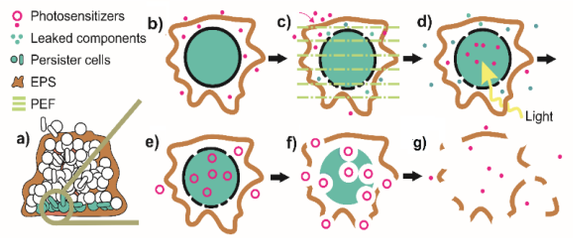


Fig. 2. Hypothetical mechanism of action by the association of aPDT and PEF. (a) Mature biofilm. (b) Persister cells surrounded by EPS, and the PS binding with the EPS. (c) Application of PEF, permeabilizing the PS diffusion through the EPS and cell membrane. (d) Application of visible light, corresponding to the PS absorption. (e) PS activation promoting ROS production. (f) The disruption of EPS and the death of the microbial cells, even the persister cells. (g) PS returns to its ground state.

electric fields are applied. This type of treatment kills microorganisms not only due to membrane rupture, but also due to the formation of reactive compounds including free oxygen, hydrogen, hydroxyl and hydroperoxyl radicals. Thus, the synergism of aPDT and PEF can potentiate the production of ROS and overcome the main defense mechanisms of a biofilm.

wanessa.melo@ftmc.lt

## Evaluation of kinetics and thermodynamics of interaction between immobilized SARS-CoV-2 nucleoprotein and specific antibodies by total internal reflection ellipsometry

During the pandemic, different methods for SARS-CoV-2 detection and COVID-19 diagnostics were developed, including antibody and antigen tests. For a better understanding of the interaction mechanism between SARS-CoV-2 virus proteins and specific antibodies, total internal reflection ellipsometry (TIRE) based evaluation of the interaction between SARS-CoV-2 nucleoprotein (SCoV2-rN) and anti-SCoV2-rN antibodies (and the determination of SCoV2-rN/anti-SCoV2-rN complex formation) was performed. The results show that the appropriate mathematical model, which takes into account the formation of an intermediate complex, can be applied for the evaluation of SCoV2-rN/anti-SCoV2-rN complex formation kinetics. The calculated steric factor indicated that SCoV2-

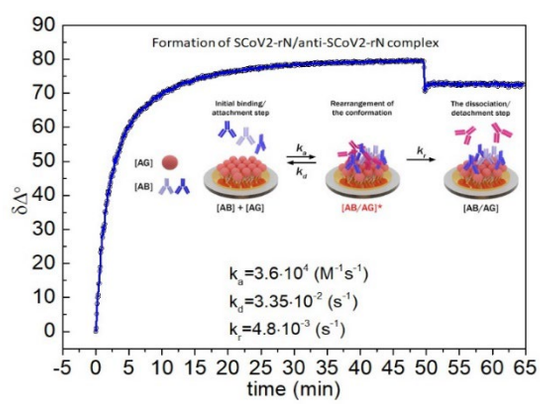


Fig. 3. Application of TIRE for SARS-CoV-2 nucleoprotein and specific anti-body analysis.

rN/anti-SCoV2-rN complex formation has very strict steric requirements. The estimated Gibbs free energy ($\Delta G_{Form}$) for SCoV-rN and anti-SCoV-rN binding was determined as –34 kJ/mol. The reported findings are useful for the design of new analytical systems for the determination of anti-SCoV2-rN antibodies.

ieva.plikusiene@ftmc

## Investigation of electromagnetic acceleration of type II superconductors

The behavior of type-II superconducting armatures, accelerated by a pulsed magnetic field generated by a single-stage pancake coil, was investigated. We performed a numerical finite element study and an experimental study of the magnetic field dynamics at the edge of the pancake coil. The payload was a $YBa_2Cu_3O_{7-x}$ superconducting disc cooled down to 77 K. The magnetic field measurements were performed using a CMR-B-scalar sensor developed at the FTMC, which was able to measure the absolute magnitude of the magnetic field and was specifically manufactured in order to increase the sensor's sensitivity up to 500 mT. It was observed that the motion and the magnetic field dynamics agreed well with the numerical simulations. The numerical study showed that a higher critical current density of the superconductor increased the mechanical energy transferred to the superconducting armature. This energy, however, had a limit for a given accelerating coil current pulse and armature starting position. Superconducting armatures were compared to normal metal armatures, and the regimes of superconductors superiority were identified.

vilius.vertelis@ftmc.lt

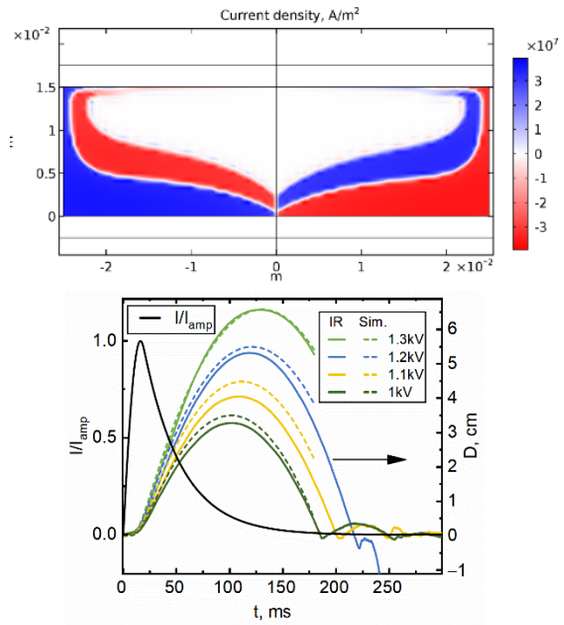


Fig. 4. (Top) Current density distribution within the superconducting armature after a magnetic field pulse. (Bottom) Trajectories of the superconducting armature and the driving current waveform.

## Magnetoresistance of nanostructured La-Sr-Mn-Co-O films and its relaxation

It was demonstrated that electrical transport and magnetic properties of nanostructured $La_{1-x}Sr_xB_zO_3$ films to a large extent depend on B-site doping. The Co substitution for Mn in B site decreases the metal-insulator transition temperature $T_m$ and increases the resistivity maximum $\rho_m$. The enhanced and almost temperature-insensitive values of magnetoresistance (MR), in comparison to manganite LSMO film, were obtained in a wide range of temperatures (5-200 K). The magnetic memory effects were investigated as resistance relaxation processes after the switch-off of the magnetic field pulse. The observed 'fast' (~300 μs) resistance relaxation was analyzed by using the Kolmogorov–Avrami–Fatuzzo model, taking into account the reorientation of magnetic domains into their equilibrium state, while the 'slow' process (>ms) was explained by using the Kohlrausch–Williams–Watts model considering the interaction of the magnetic moments in disordered grain boundaries. It was concluded that Co-doped nanostructured manganite films, demonstrating higher sensitivity and lower memory effects in comparison to the LSMO films, could be used for the development of pulsed magnetic field sensors operating at low temperature.

nerija.zurauskiene@ftmc.lt

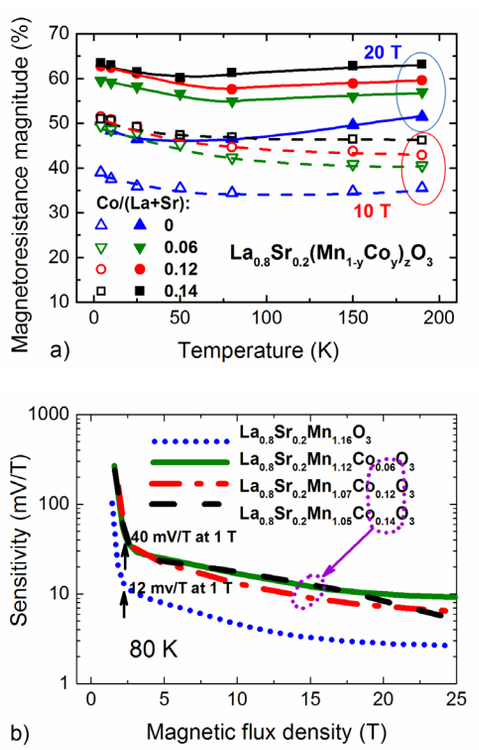


Fig. 5. (a) Temperature dependences of MR and (b) sensitivity dependences on magnetic flux density for La-Sr-Mn-Co-O films with different Co content.

## Cesium-containing triple cation perovskite solar cells

The coating of silicon solar cell (SC) with a thin perovskite layer (PL) absorbing high energy photons allows to considerably decrease the negative effect of hot carriers. The PL must be a good absorber of the visible light and be transparent to the infrared light. The addition of cesium makes the triple cation perovskite compositions more thermally stable, as they have less phase impurities and are less sensitive to processing conditions. The experimental study of the structure, photoluminescence and optical properties of PLs $Cs_x(MA_{0.17}FA_{0.83})_{(1-x)}$ $Pb(I_{0.83}Br_{0.17})_3$ with x=0-0.15, as well as photoelectric properties of SCs fabricated on their base, was carried out to evaluate the utility of the layers for the fabrication of monolithic perovskite/silicon tandem SCs. It is demonstrated that addition of cesium almost does not influence the transparency of the PLs in the infrared range but significantly improves the photovoltaic performance of the perovskite SCs. It was found that the SC with 10% of cesium

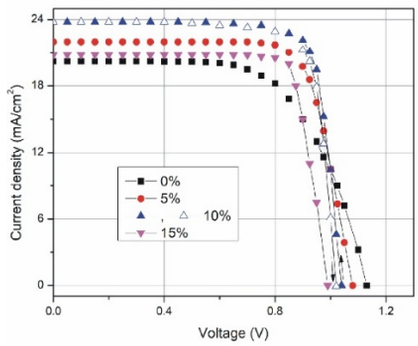


Fig. 6. Current voltage characteristics of perovskite SCs with different cesium concentrations.

in the PL has the highest value of short circuit current, fill factor and power conversion efficiency. It demonstrates the best power conversion efficiency of 20%, and therefore such layers can find application as suitable tandem partners for silicon SCs.

steponas.asmontas@ftmc.lt

# New prototypes

## MB “Aerozolių tėkmė” and FTMC developed “Aerosol whistle” for detection of air-borne pathogens

‘Aerosol whistle’ is a handheld tool designed to collect and concentrate aerosols in exhaled air of a person. The functional design of this new tool enables to generate two contra directional air streams which separates and collects aerosol particles in precise point. More than 20 prototypes were tested during design and testing stages. The tool enables sample collection for further diagnostic applications.

eivydas.andriukonis@ftmc.lt

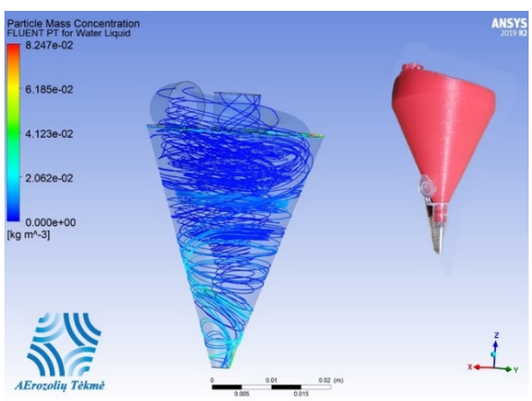


Fig. 7. (Right) Early working ‘Aerosol whistle’ prototype. (Center) Simulation of cyclonic airflow by computational fluid dynamics method.

## New device prototype, CMR-B-Scalar Meter-50-10MS, for measurement of magnetic field magnitude developed by MB ‘MAGSENSAS’ and FTMC

Prototypes of absolute value magnetic field (B-Scalar) meters were developed in the FTMC for measuring variable and continuous magnetic fields (MFs). The technology of these MF meters was elevated to the level of technology readiness 8 (TRL8). The system consists of measurement module and flexible or semi-flexible probe. Design and manufacturing technology of MF sensors, based on nanostructured manganite films, electronic module and software of the meter were improved and optimized. The system is able to measure the magnitude of permanent, pulsed or alternating magnetic flux density ranging from 0.01 T to 50 T. The measurement frequency range is from 0 to 100 kHz. Devices can be triggered in Pulse, Edge and External modes. Several MF measurement systems were produced and tested in real operating conditions.

Fig. 8. B-Scalar magnetic field measurement modules with semi-flexible probe. The project was project supported by MITA (Project Nr. 01.2.2-MITA-K-702-06-0012).

The device is supplemented by technical documentation, including sensors formation and probe fabrication technology, electronic module fabrication technology, meter software and technical description as well as manual instructions of MF measurement system.

voitech.stankevic@ftmc.lt

# Nanostructures for applications

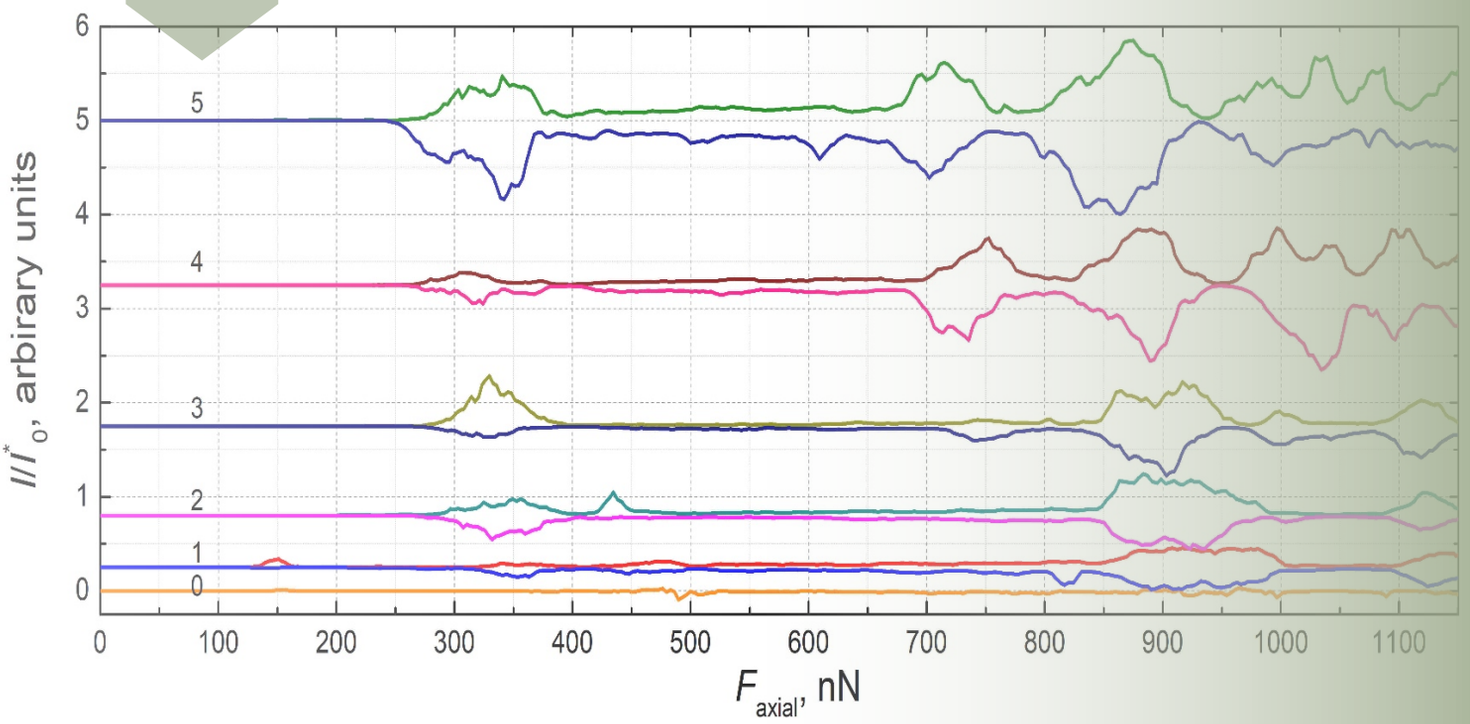


## Hybrid 2D / 3D systems for intelligent receptors

Dedicated problem solutions and original combination of technologies are the strongest preferences for our research and development (R&D) activities. In the long-term run we are focused on the applied systems that combine the fundamentals of the electronical and photonical phenomena, technologies of the semiconductors and optoelectronic devices and the methods of the intelligent information analysis. Our primary concern is to develop the key modules for the systems that are acceptable to convert the physical and chemical characteristics of the processes, materials, things, persons and etc., into a digital stream representing the core information for the decision making and the feedback loop control. Generally speaking, our modules are expected to function as photonic receptors (the data gathering nodes) providing specific information about the targets in the network of the internet of things (IoT) and Internet of Everything (IoE).

The semiconductor technology and the compatible fabrication methods are used for development of advanced materials, devices and integration approaches. Our special efforts are devoted to combine thin films of the usual three dimensional (3D) materials with the two-dimensional (2D) materials. We are absolutely sure that the 2D/3D hybrid structures can lead to highly interesting features of hybrid devices including new ways for integration of diverse functionalities within a compact autonomous system. We plan to include semiconductor lasers, detectors, photovoltaic-based powers sources, and an output signal circuit in these compact systems. Our R&D path to the working prototypes includes three tightly related stages.

First, synthesis and investigation of the functional materials and related structures. The technology studies create the basis for the strictly controlled technologies of the elements with the two-dimensional (2D) materials in the device fabrication route. There are two classes of the 2D materials, namely graphene and transient metal disulphides (TMDs), that are within the focus of our R&D activities. We found that vertical arrangements with graphene can combine mechanical, electronic and photonic effects within a multi-parameter receptor acceptable to monitor a complex external influence. In the headline figure, a combination of mechanical, electronic and electrical changes is illustrated for a van der Waals vertical structure by the electrical current responses to a monotonous increase in the magnitude of

axial force under ultra-low driving voltage. Since the structure can change the parameters of a light beam, interesting possibilities for multi-functional hybrid system are expected.

Second, innovative solutions for prototypes of hybrid devices and their technologies. An exciting way to control the interaction between the electromagnetic waves and the metamaterials was accepted being highly interesting for development of special visualisation systems. There are two primary targets in our scientific and technology studies, namely (i) relationship between the optical – electrical parameters and the core characteristics of the layers and (ii) relationship between the technology conditions and the device parameters. We use the results for development of the IR laser systems in the joint R&D projects.

Third, development and testing of the prototypes of the devices and integrated systems. The primary target of this part of the work is to get a solution of the problems that address the needs of potential producers and end-users. For example, an interesting method to control the surfaces of wood during a special treatment was demonstrated on the working industrial line in the joint project carried out by the FTMC and a private company.

In the present stage, we practically obtained the critical mass of the technology infrastructure required for the high technology level manufacturing of the prototypes of the semiconducting photonic systems and, therefore, we are focused on the project with the technology readiness levels up to the prototypes of devices and the pilot technologies.

arunas.setkus@ftmc.lt

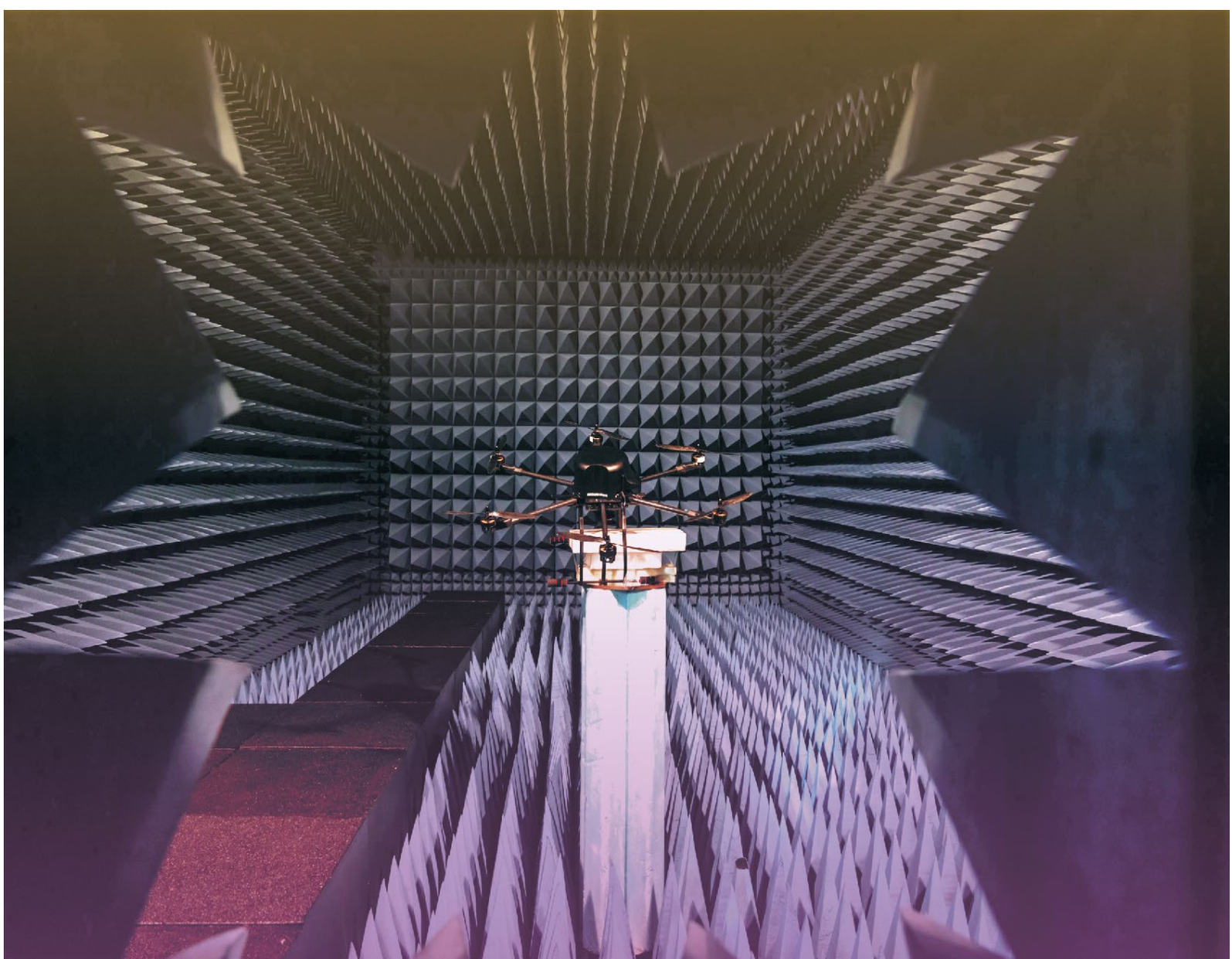

# Astrophysics

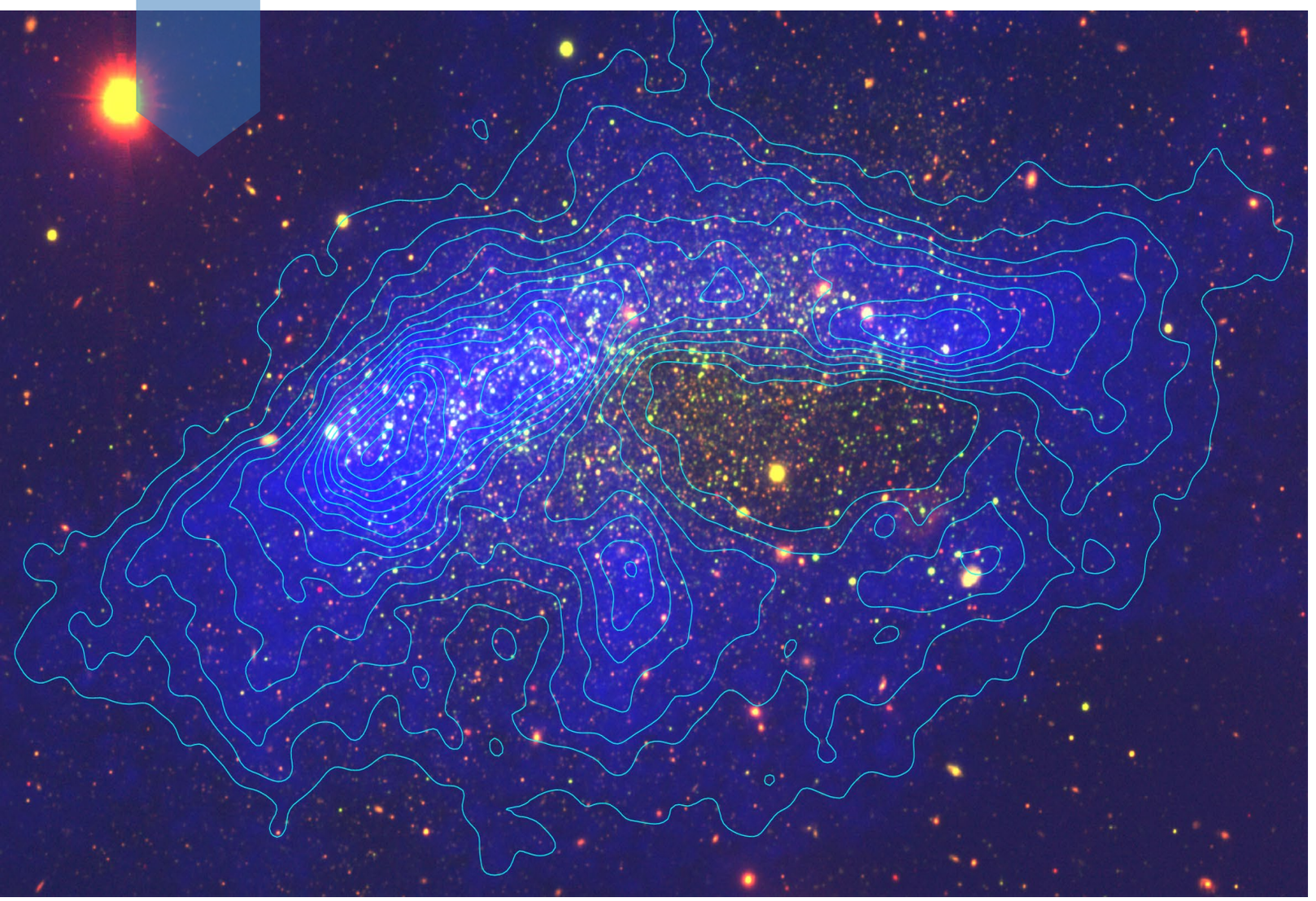

We study complex systems, from star clusters to galaxies, by employing ground- and space-based observations, as well as numerical simulations

## Photometry of star clusters in M31

This study investigates degeneracy and stochasticity problems in determination of the age, mass, extinction, and metallicity of partially resolved or unresolved star clusters in external galaxies using Hubble Space Telescope broadband photometry. We present new aperture photometry results for a sample of star clusters from the M31 Panchromatic Hubble Andromeda Treasury (PHAT) survey. We employed two methods of aperture photometry. The first method is ordinary aperture photometry to measure total cluster fluxes. The second method is proposed to avoid the brightest foreground and background stars that project onto large apertures. This method employs smaller apertures, adapted to cover the central part of clusters, and applies an aperture correction, derived for the *F475W* passband, to other passbands. We present two catalogues of star cluster aperture photometry (produced by applying ordinary aperture photometry and new adaptive aperture photometry methods) with estimated uncertainties for a sample of 1181 star clusters from the M31 PHAT survey. Compared to the M31 PHAT fundamental star cluster aperture photometry catalogue published by Johnson et al., there are changes of cluster centre coordinates, aperture sizes, and sky background estimates.

rima.stonkute@ftmc.lt
vladas.vansevicius@ftmc.lt

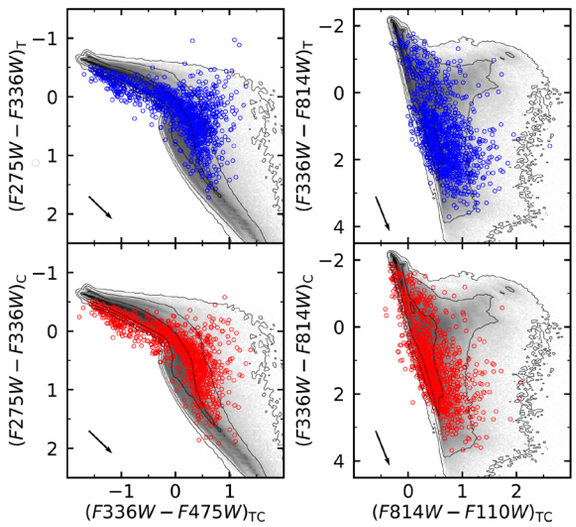


Fig. 1. Colour-colour diagrams show star cluster photometry results: (upper panels, blue dots) total (T) aperture photometry; (bottom panels, red dots) colour (C) aperture photometry. Distributions of star cluster models with masses from $10^2$ to $10^5$ $M_\odot$ are plotted in the background (gray density contours). Colour indices indicated on the X-axis are constructed from T magnitudes in upper panels and C magnitudes in bottom panels. Arrows in the lower-left corners of panels indicate the extinction vectors of $A_V$ = 1, assuming the standard Milky Way extinction law.

## Unveiling galaxy activity histories

Active galactic nuclei (AGN) – sources of extreme luminosity in the centres of galaxies, powered by gas falling on to the central supermassive black hole – tend to drive massive outflows that push gas out of their galaxies. The properties of these outflows correlate rather well with AGN luminosity, albeit with a large scatter around the analytically predicted correlations. This scatter may be explained by the fact that outflows evolve on million-year timescales, while AGN episodes last ~0.1 million years on average. Therefore, a single outflow has most likely been inflated by multiple AGN episodes. In principle, the properties of the outflow contain information about the variations of AGN luminosity that occurred during its evolution. Therefore, outflow properties can be used to track the galaxy's activity history over the past several million years. We used a 1D numerical model to track the evolution of AGN outflows in a large sample of model galaxies. As expected, outflow properties correlate better with the long-term average of AGN luminosity rather than instantaneous value, and the distribution of outflow parameters at a given AGN luminosity agrees well with the observed scatter. We trained a neural network to distinguish between AGN luminosity histories based on the outflow properties; the network can determine the duty cycle of the AGN, as well as the likely properties of outflow geometry and galaxy gas content, with relative errors < 15%.

kastytis.zubovas@ftmc.lt

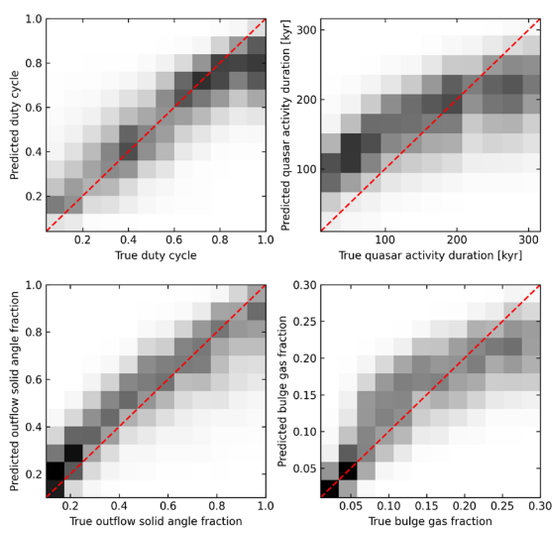


Fig. 2. Neural network test results, comparison of predicted (vertical axis) versus true (horizontal axis) values of (top, left) AGN duty cycle, (top, right) single AGN episode duration, (bottom, left) fraction of solid angle subtended by outflow, (bottom, right) gas fraction in the host galaxy bulge.

# Modeling

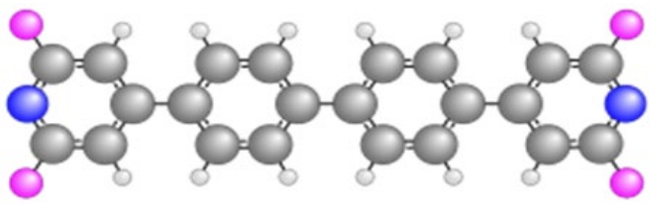

## Generation of vector Bessel vortices with high-order S-waveplates for laser microprocessing applications

Thorough research of high-order vector Bessel-Gauss beams from a perspective of a theory, experimental realizations and application to transparent material laser micro-machining is performed. The efficient, stable, high-quality and power vector Bessel-Gauss beam generation using two geometric phase-based optical elements, high-order S-waveplate and axicon, in combination with simple optical elements such as lenses, waveplates and polarizers, is demonstrated. Ultrashort pulse vector Bessel-Gauss beams were used to induce modifications in the glass, creating three-dimensional tubular structures of type I and type II modification in D263T glass. Samples containing tubular modifications were tested for etch selectivity in the femtosecond laser-induced chemical etching (FLICE) method with KOH solution by etching throughout channels.

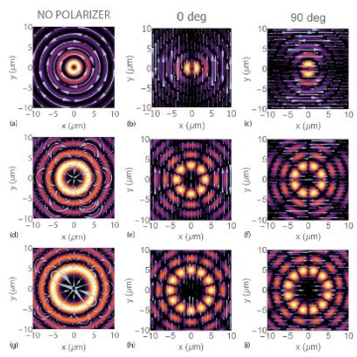


Fig. 1. Numerically calculated transverse intensity profiles of vector Bessel-Gauss beams of orders (a) n=1, (d) n=4, (g) n=6 and their linearly polarized constituents (b, c, e, f, h, i). Gray arrows depict stream lines of electric field.

sergejus.orlovas@ftmc.lt

## Generation of an optical needle beam with a laser inscribed Pancharatnam–Berry phase element under imperfect conditions

Beams exhibiting long focal lines and small focal spot sizes are desired in a variety of applications and are called optical needles. We consider an optical element based on the space-domain Pancharatnam–Berry phase (PBP), to generate a high-power optical needle with a smooth and constant on-axis intensity profile. Our implementation is based on a type 2 modification of bulk transparent glass material, resulting in the formation of nanogratings with slow axes aligned perpendicular to the grating corrugation. We investigate both numerically and experimentally the stability of an optical needle generation under imperfect conditions. Influences of misalignments in the optical schema are investigated numerically and experimentally.

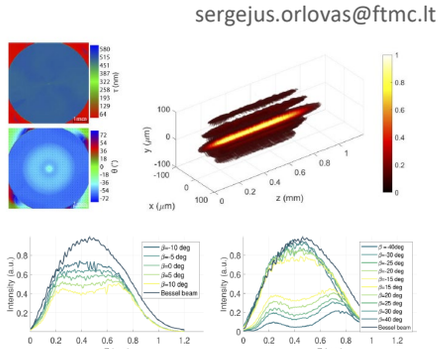

Fig. 2. Distribution of the retardance τ and the slow axis θ in the PBP element manufactured by Altechna R&D. (Top) The 3D intensity distribution in the optical needle created by the combination of the PBP element, the linear polarizer and the axicon. (Bottom) Distortions in the optical needle caused by the azimuthal misalignment between the polarizer and the PBP element for various values of the mismatch angle $\beta$.

sergejus.orlovas@ftmc.lt

## Spatially displaced and superposed Bessel beams for transparent material laser micro-processing

Invariant Bessel-Gauss beams have attracted a great interest in transparent material microprocessing applications. However, many of these applications need asymmetric beams to induce directional cracking. We investigate analytically, numerically and experimentally a beam that was generated by spatially displaced axicon halves, which induce noncylindrical symmetry in the beam phase profile. These beams demonstrate applicability to micro-machining processing of transparent material.

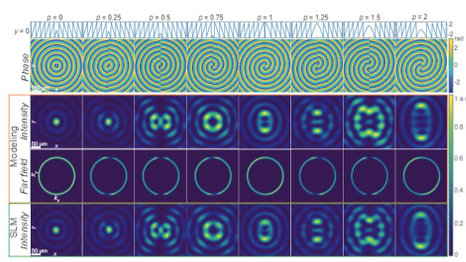


Fig. 3. Intensity patterns of non-diffracting beams as a function of the spatial displacement between two halves of axicon masks. The displacement $p$ is given in steps of quarter period. The phase period $r_0$ = 80 µm and the Bessel beam cone half-angle $\theta_c = 0.74^0$. Bottom rows depict intensity distribution of experimentally generated beams.

sergejus.orlovas@ftmc.lt

## Vibrational and vibronic structure of isolated point defects: the nitrogen-vacancy center in diamond

One of the goals of the Electronic structure theory group is theoretical spectroscopy of solid-state systems. The group develops computational techniques to calculate optical spectra of deep-level defects. The electronic structure and lattice vibrations are described by means of density functional theory calculations. One of the important test systems for the methodology is the so-called nitrogen-vacancy center in diamond (Fig. 1). This defect has been recently used for quantum-technological applications such as quantum sensing, quantum communication, and even quantum computing. In this work, a methodology to calculate luminescence and absorption lineshapes (normalized spectra) of essentially isolated defects was presented. In particular, a new technique to include the multi-mode dynamical Jahn-Teller effect was proposed. The description of this effect is important in order to account for the contribution of asymmetrical e modes to the spectra. The resulting lineshapes are in a very good agreement with experiments regarding both the overall structure and fine

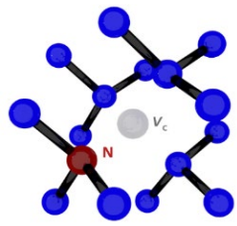


Fig. 1. The nitrogen-vacancy center in diamond.

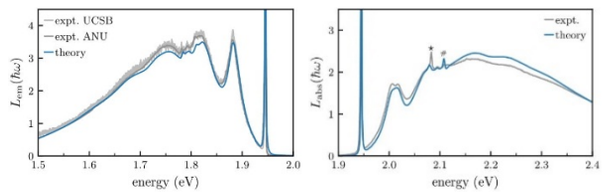


Fig. 2. Calculated (left) luminescence and (right) absorption lineshapes at nitrogen-vacancy centers in diamond (blue curves), compared to experimental ones (gray curves).

details of the spectra (Fig. 2). The developed methodology will be useful for the identification of defects with unknown chemical structure and the understanding of electron-phonon coupling at defects in general.

audrius.alkauskas@ftmc.lt

## Photoionization of negatively charged nitrogen-vacancy centers in diamond: theory and ab initio calculations

Over the past two years, the Electronic Structure Theory group has also developed numerical techniques to calculate absolute photoionization cross sections for point defects in solids. The methodology has been applied to the negatively charged nitrogen-vacancy center in diamond (Fig. 3). Converged values of the photoionization cross section as a function of energy have been obtained by using band unfolding and interpolation in the primitive Brillouin zone. For the specific case of the nitrogen-vacancy center, the ionization threshold from the excited 3E state has been calculated for the first time. It was shown that, contrary to the popular belief in the literature, right after the photoionization the nitrogen-vacancy center transitions into the metastable 4A2 level of the neutral defect.

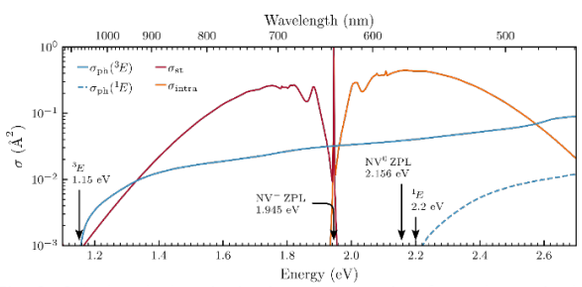


Fig. 3. Calculated photoionization cross section from the excited state 3E (blue curve), cross section for stimulated emission (dark red curve), and cross section for absorption (orange curve) for nitrogen-vacancy centers in diamond.

This process naturally leads to a spin polarization in the 4A2 manifold, explaining electron spin resonance experiments. The developed methodology is expected to be used for other point defects in solids.

lukas.razinkovas@ftmc.lt

## Modeling of high-temperature ordered structures with weak intermolecular bonds

The self-assembly of a hydrogen bond ‘donor– acceptor’ system with fluorinated pyridyl groups, 4,4’ -bis(2,6-difluoropyridin-4-yl)-1,1’ -biphenyl (BDFPBP), is studied to explain the emergence of different ordered structures bonded by weak C– H··· F and C– H··· N bonds. BDFPBP on Au(111) is known to assemble into four molecular arrangements: a herringbone phase at room temperature and three other structures at 450– 460 K. In our model, we assume partial deprotonation of donor sites in phenyl and pyridyl rings during heating. Therefore, we choose seven types of BDFPBP molecules (one intact and six with differently damaged donor sites) and suggest the mechanisms of their bonding. Using density functional theory, we estimate the energies of different hydrogen-bonding motifs for intact and

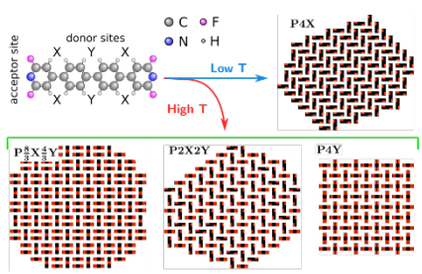


Fig. 4. (Top, left) BDFPBP molecule and (top, right and bottom) four self-assembled structures obtained by MC modeling. Black rectangle represents the molecule with differently damaged (red boxes) donor sites.

damaged molecules. We also perform Monte Carlo (MC) simulations for homo- and bimolecular ensembles to obtain all experimentally observed molecular phases. In addition, we reveal several new structures and their coexistences with the phases known from experiments.

evaldas.tornau@ftmc.lt

# Electrochemical material science

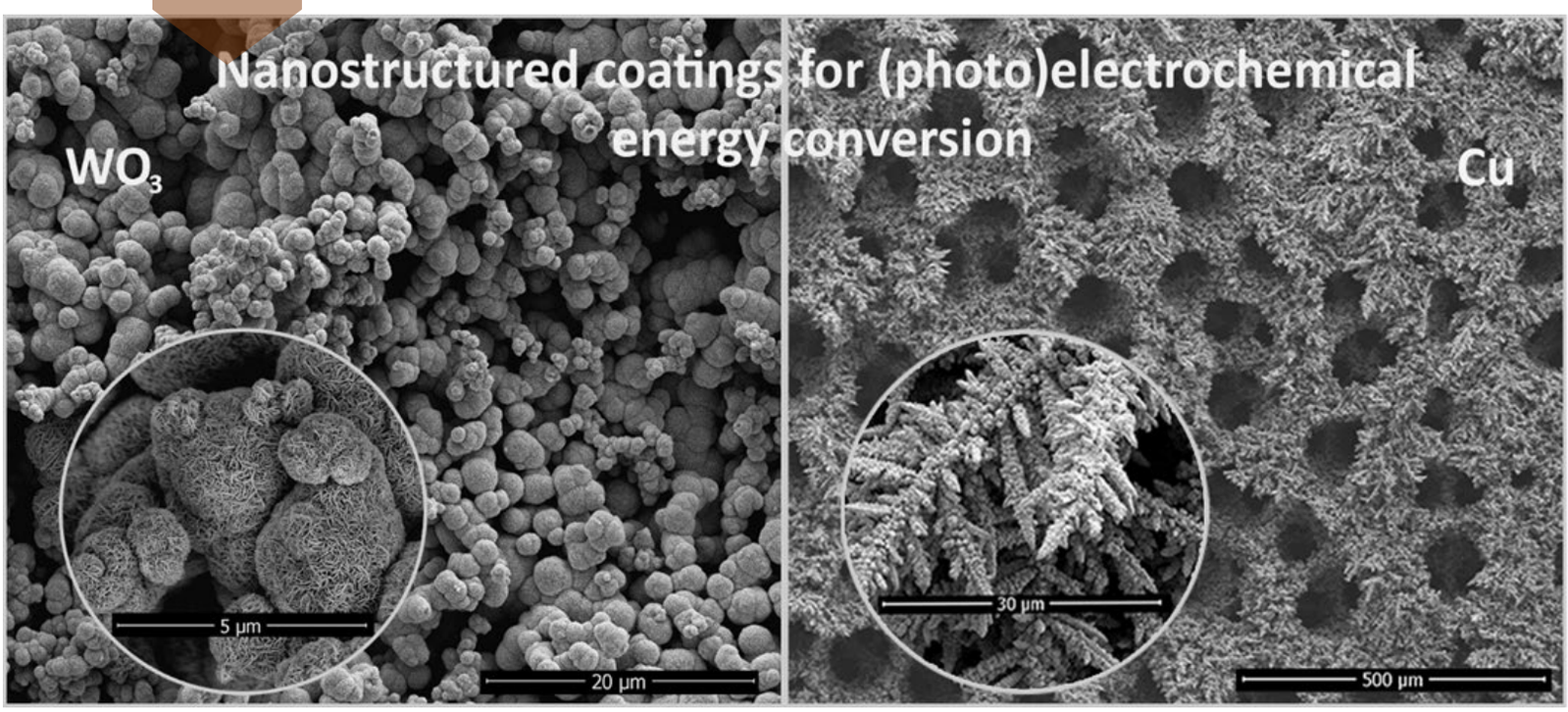


## Technologies for electrochemical energy conversion and storage, solar-driven electrochemistry, smart coatings

The search and development of novel energy storage means is recognized as one of the key tasks in modern science. Electrochemical energy conversion and storage technologies offer attractive solutions for many current renewable energy related problems. The R&D activities in this area in Departments of Electrochemical Material Science and Chemical Engineering and Technology are focused on the development and profound understanding of materials, processes and devices for safe, sustainable and low-cost aqueous Na-ion batteries for stationary energy storage applications (NaAquaCell project), photoelectrochemical production of hydrogen and strong oxidants suitable for water treatment (CatWatSplit project), electrochemical synthesis of silicon nanostructures and other materials, including superparamagnetic and luminescent nanoparticles with possible applications in photovoltaics, nanomedicine, etc. Electrochemical, chemical as well as physical methods (electrodeposition, atomic layer deposition, magnetron sputtering) are applied for the surface modification and production of smart materials with exceptional electrocatalytic, anticorrosive, magnetic, mechanical or other properties. The integral part of the process of new materials development is a thorough characterization of their structure, morphology and chemical composition. Environmental friendliness and sustainability are imperative for all newly developed technologies. Expertize in electrochemistry and material science is the main driving force in developing innovative sustainable technologies and new applications for circular economy. Anodic coatings on aluminum, fortified by depositing nanothin layers of selected metals and oxides, show very promising tribological characteristics and good biocompatibility. Major focus has also been devoted to the diffusion of organic compounds, such as corrosion inhibitors, antiwear additives, colorants or adhesives, into electrochemically nanostructured coatings. Significant attention has been paid to the properties of natural deep eutectic solvents, which are very promising industrially. These solvents are investigated in great detail during the H2020 project TERMINUS. A critical task of this project, tackled by FTMC Tribology laboratory, targets the development of adhesives for recyclable multilayer packaging. Smart coatings with active corrosion protection ability for metals in aggressive environments are

developed. Corrosion tests are carried out in the Accredited Corrosion Research Laboratory at FTMC, which performs characterization and evaluation of the corrosion-caused changes in metals, alloys, composite coatings, paints and lacquers in natural and artificial atmospheres and can also assess the microbially induced corrosion of materials in ambient atmosphere or model media.

## Investigation of $NaTi_2(PO_4)_3$ – carbon composites as aqueous Na-Ion Battery anodes

Aqueous Na-ion based batteries are considered promising candidates for replacing conventional Li-ion technologies, especially in the field of stationary energy storage. Research and development of novel electrode materials remain the central effort in this area. NASICON-structured phosphate framework (*i.e.* $NaTi_2(PO_4)_3$) has attracted a great deal of attention and remains the most studied negative electrode material for aqueous Na-ion batteries. The active material preparation and carbon composite property tailoring play a critical role in the electrode materials engineering process which governs the performance of the entire electrochemical system. We investigated a series of $NaTi_2(PO_4)_3$-carbon composites prepared using three different sol-gel approaches and three distinct pyrolysis/calcination strategies. The structural and morphological analysis results revealed that both the sol-gel route as well as the thermal treatment strategy have significant effects on the active material purity and degree of crystallinity as well as the content and properties of the carbonaceous phase. Electrochemical investigations of these composites also show strong effects of the structure and carbon matrix morphology on the electrochemical performance and degradation of these materials when employed as aqueous Na-ion battery negative electrodes.

skirmante.tutliene@ftmc.lt

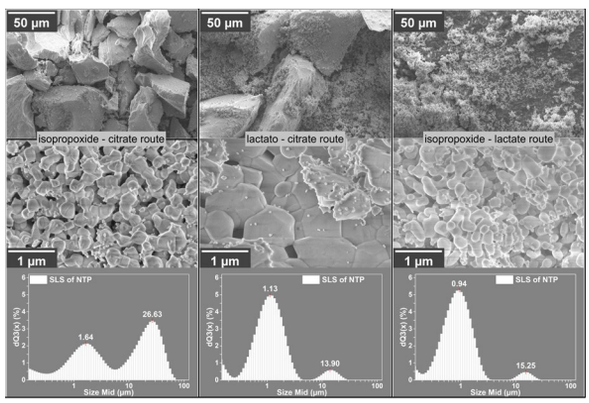


Fig. 1. SEM images and particle size distribution histograms (SLS) of carbon-free NTP materials derived by different sol-gel routes (isopropoxide-citrate, lactate-citrate, isopropoxide-lactate, respectively).

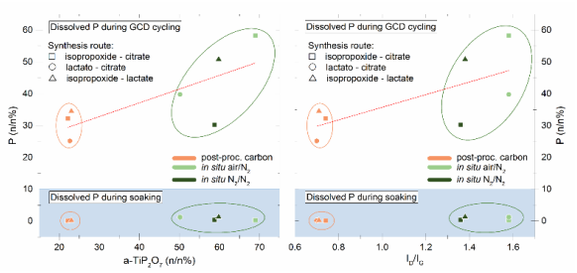


Fig. 2. ICP-OES determined phosphorus content in the electrolyte after soaking the electrodes in solution for ca. 24 h (blue area) or after 100 galvanostatic charge/discharge cycles at 1C rate (white area) with respect to (left) content of a-$TiP_2O_7$ phase; (right) degree of structural disorder in carbon phase.

## Yeast-based microbial biofuel cell mediated by 9,10-phenantrenequinone

Microbial fuel cells can be efficiently used for simultaneous cleaning of wastewater and generation of electricity. This research demonstrates the applicability of Baker yeast cells in the design of microbial biofuel cells. The applicability the 9,10-phenantrenequinone (PQ) as a redox mediator in the design of yeast-based microbial cell (MFC) for the improvement of charge transfer through the yeast cell membrane and cell wall towards the electrode was evaluated. Differently modified graphite electrodes ((i) non-modified, (ii) yeast-modified, (iii) modified by PQ and yeast) were evaluated. The modified electrodes were evaluated as anodes of MFC. Maximal open circuit potential was 178 mV at 7.8 mM of glucose and 23 mM of potassium ferricyanide. Maximal power of BFC calculated at the same conditions was registered at 56 mV, and it reached 22.2 mW/m$^2$ (at 30 mM of glucose).

inga.vilkonciene@ftmc.lt

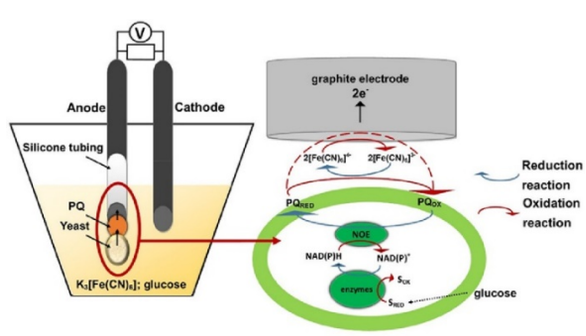


Fig. 3. The two redox mediator-based system with first adsorbed PQ and then immobilized yeast layers on the graphite electrode (graphite/PQ/yeast electrode).

## Atoms vs. ions: intermediates in reversible electrochemical hydrogen evolution reaction

A critical analysis of the mechanism of reversible hydrogen evolution reaction based on thermodynamics of hydrogen processes, considering atomic and ionic species as intermediates, is performed. Clear distinction between molecular hydrogen evolution/oxidation ($H_2ER$ and $H_2OR$) and atomic hydrogen evolution/oxidation (HER and HOR) reactions is made. Presented analysis implies that reversible $H_2$ evolution is a two-electron transfer process, which proceeds via the stage of adsorbed hydrogen molecular ion $H_2^+$ as intermediate, rather than $H_{ad}$ as postulated in the Volmer-Heyrovsky-Tafel mechanism. We propose that $H_2$ formation on Pt electrode surface is proceeding via a structural reorganisation inside the $H_3O^+$ ion, where two neighbouring H-atoms, being already at the bond separation, form a bond. The energy costly and asymmetric process of hydrogen evolution/oxidation via H-atoms contradicts the reversibility of standard and reversible hydrogen electrodes, which apparently exists in reality and is used in practice. We demonstrate that in theory, two slopes of potential vs. lg(current) plots are feasible in the reversible region of $H_2$ evolution (2.3RT/F ≈ 60 mV and 2.3RT/2F ≈ 30 mV) which is corroborated by the results of electrocatalytic hydrogen evolution studies.

jurga.juodkazyte@ftmc.lt

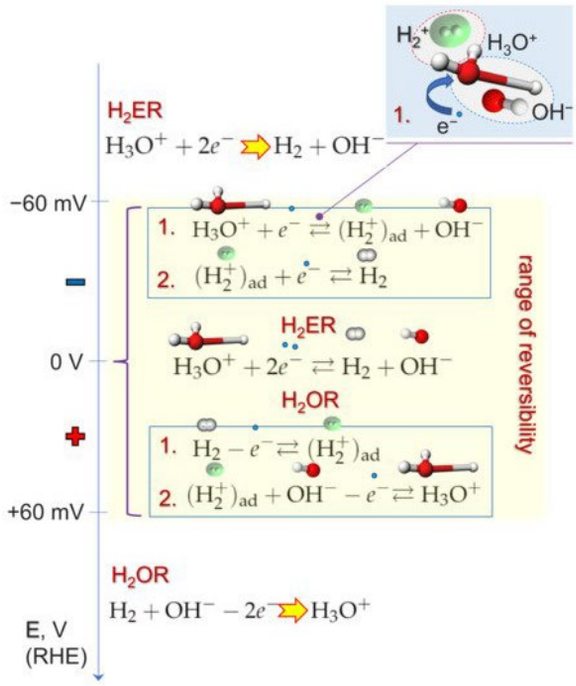


Fig. 4. Hydrogen evolution/oxidation reactions $H_2ER/H_2OR$ in aqueous solutions. Inset: schematics of $H_2^+$ formation using pictorials of chemical structures of the participating species.

## Cysteine-induced hybridization of 2D molybdenum disulfide films for efficient and stable hydrogen evolution reaction

The noble, metal-free materials capable of efficiently catalyzing water splitting reactions currently hold a great deal of promise. In this study, we reported the structure and electrochemical performance of new $MoS_2$-based material synthesized with L-cysteine. A facile one-pot hydrothermal process was developed and an array of densely packed nanoplatelet-shaped hybrid species composed of nanostructured $MoS_2$ and thermally degraded D,L-cysteine amino acid fragments, namely $NH_2$–Cα–C*, were designed for the first time. The crucial role of L-cysteine residue insertion resulting in a surprising catalysis of hydrogen evolution reaction from water attributed to the formation of stable 1T-$MoS_2$ and 2H-$MoS_2$ hybrid material with a low Tafel slope equaled to 32.6 mV dec$^{-1}$.

arunas.jagminas@ftmc.lt

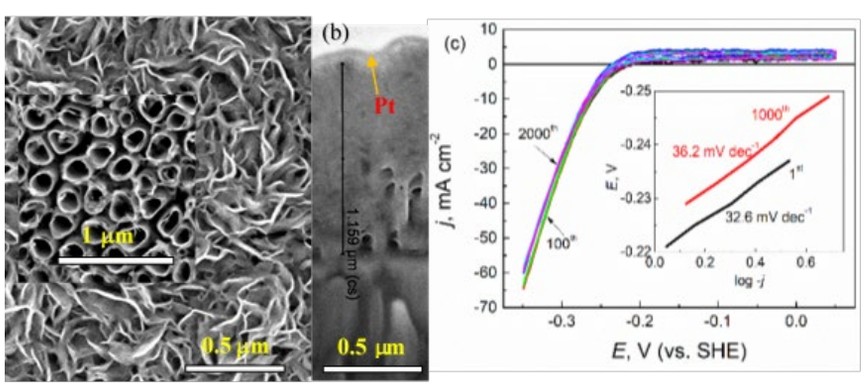


Fig. 5. (a) Top-side and (b) cross-sectional SEM images of hybrid $MoS_2$/cyst film whereas (c) depicts the CV plots in 0.5 M $H_2SO_4$ solution up to 2000 potential scans. Insets: in (a) support SEM view, in (c) Tafel slope for indicated scan.

# Materials for catalysis

## Electroless metal deposition: from fundamental research to application for microelectronics, fuel cells, and other areas

Electroless metal plating is a well-known method for the deposition of metal coatings by a controlled chemical reduction and formation of small (nano-scale) metal particles. The autocatalytic metal ion reduction systems are widely used for decorative and functional purposes, i. e. for deposition of a conductive metal layer on dielectrics, semiconductors, or on conductors with a complicated configuration without external current. The selection of suitable reducing agents and conditions of the reaction (temperature, the concentration of the reacting substances, etc.) plays a very important role in creating stable solutions and obtaining coatings with required characteristics, such as purity and surface roughness. The use of conventional hydrogen-containing reducing agents is connected with environmental and technological problems: (i) the plating bath cannot be recycled, i. e. the reducing agent oxidizes irreversibly; (ii) the plating rate and solution stability are not high enough. For these reasons, the search and investigations of the reducing agents of a new type, e. g. charge-transfer reducers, namely the different oxidation state metal-ion redox couples, are actual nowadays, and they are developed and applied in the Department of Catalysis. The main reducing agents used are Ti(III) and Co(II), which oxidize during the electroless plating processes to Ti(IV) and Co(III). An additional advantage of such systems, where no hydrogen is formed during the electroless plating process, is the possibility to reduce the oxidized form of the reducing agent to the initial state. The R&D activities of our department in this area are focused on the development of new electroless metal plating processes as well as fundamental studies of reactions occurring in autocatalytic metal ions reduction systems employing electrochemical quartz crystal microgravimetry. The electroless metal plating method is also successively used for the fabrication of new catalytic materials for fuel cells. The non-noble metal and noble metal catalysts with a low amount of noble metal-supported titanium, titania nanotube arrayed surfaces, carbon, graphene powder, or other supports with enhanced activity towards the oxidation of various fuels, have been developed. The catalysts obtained are promising anode materials and can be used in the practical fuel cells.

## Development of catalysts for water splitting

The electrochemical water splitting is a simple method to produce high purity hydrogen ($H_2$) through a cathodic reaction (hydrogen evolution reaction, HER) and oxygen ($O_2$) through an anodic reaction (oxygen evolution reaction, OER). Bimetallic cobalt (Co)-based coatings were prepared by a facile, fast, and low-cost electroless deposition on a copper substrate (CoFe, CoMn, CoMo) and characterized by scanning electron microscopy with energy-dispersive X-ray spectroscopy and X-ray diffraction analysis. Prepared coatings were thoroughly examined for HER and OER in alkaline solution (1 M potassium hydroxide, KOH) and their activity compared to that of Co and Ni coatings. All five coatings showed the activity for both reactions, and CoMo and Co showed the highest activity for HER and OER, respectively. Namely, the highest HER current density was recorded at CoMo coating with low overpotential (61 mV) to reach a current density of 10 $mAcm^{-2}$. The highest OER current density was recorded at Co coating with a low Tafel slope of 60 $mVdec^{-1}$. Furthermore, these coatings proved to be stable under HER and OER polarization conditions.

aldona.balciunaite@ftmc.lt

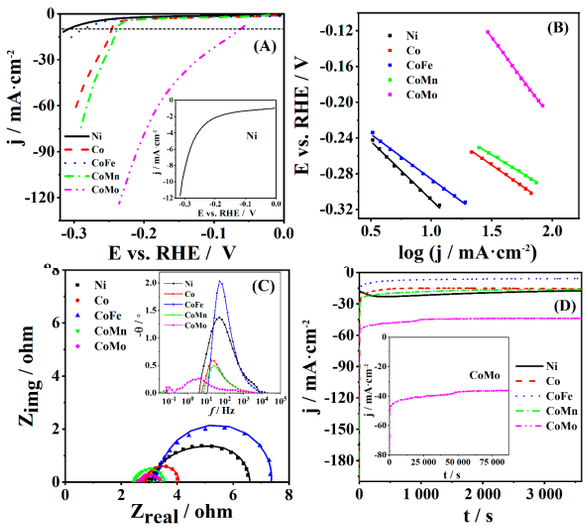


Fig. 1. (A) HER polarization curves (iR-corrected) of five studied coatings at 5 $mVs^{-1}$ with (B) corresponding Tafel plots. (C) Nyquist plots at -0.33 V (amplitude of 5 mV in the 100 kHz–0.1 Hz range) with the corresponding Bode plots in the inset. (D) Chronoamperometric curves at -0.24 V for 1 h with the chronoamperometric curve of CoMo at the same potential for 24 h (inset). All measurements were performed in 1 M KOH.

## Biomass-derived graphene-like catalyst material for oxygen reduction reaction

The number of studies dedicated to renewable energy conversion and storage devices, such as batteries, fuel cells, and photovoltaic systems, has gained utmost importance as pollution levels, caused by large-scale consumption of fossil fuels, have continued to rise year by year. The attention has been paid to development of metal-free and cheap, biomass-derived electrocatalysts for oxygen reduction reaction (ORR). We report a facile strategy to synthesize a cheap and electrochemically active nanocarbon material from the alder wood char. Carbonaceous materials have been obtained by thermochemical activation with NaOH followed by doping with nitrogen using dicyandiamide (DCDA). The morphology of typical wavy and wrinkled layered graphene can be seen in Fig. 2a. The space between the two layers is 0.34 nm (Fig. 2b) which matches the distance between two layers in graphene-like materials. The electrochemical activity towards the ORR was studied in 0.1 M KOH solution by employing the rotating disc electrode (RDE) method (Fig. 3). The results showed that compared to commercial non-sustainable nitrogen-doped graphene, the material synthesized herein shows better activity towards the ORR. The stability compared to commercial Pt/C catalyst was also significantly better.

loreta.tamasauskaite@ftmc.lt

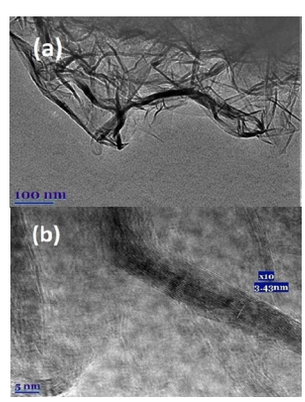


Fig. 2. (a), (b) TEM images of wood-derived N-doped carbon.

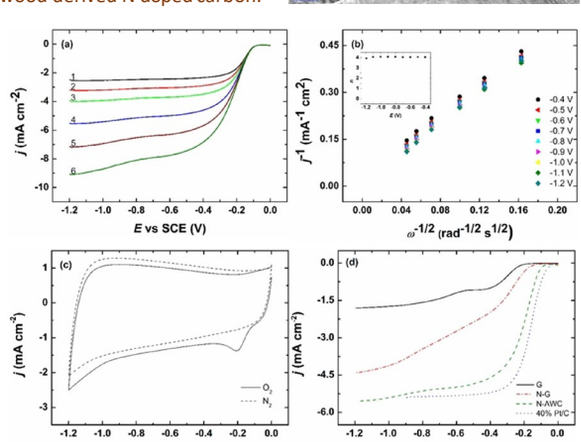


Fig. 3. RDE voltammetry curves for oxygen reduction on GC electrodes modified with different catalyst materials in $O_2$-saturated 0.1 M KOH for v = 10 mV $s^{-1}$ and ω = 1900 rpm.

# Environment

## Sustainable technologies for observation, simulation, prevention and mitigation of climate change and atmospheric pollution

Poor air quality and climate change are closely linked. Reducing air pollution from human activity sources will help to improve air quality and address climate change at the same time. Reducing air pollution and mitigating climate change are increasingly being approached in a more integrated way. The European Green Deal is at the heart of European efforts to achieve sustainability. A modern environmental research relies on solutions that bring together the recent achievements in technologies and sciences that underpin our understanding of the Nature to deliver a sustainable environmental future, economic growth and greater wellbeing. In the Department of Environmental Research the main focus is directed towards investigations of changing atmospheric composition impact on air quality, climate change and ecosystems. By conducting the fundamental and applied research, we are aiming to find long-term solutions, especially in experimental techniques devoted to develop and apply methods determining the dynamics, balance and sources of atmospheric compounds in environmental components by combining mass and size spectrometry, stable isotope analysis and chromatographic methods. *Objectives*: To develop and improve principles, means and technologies of the environment quality evaluation and to ensure the scientific competence in the fields of environmental physics and chemistry, understanding of key factors influencing the climate change and air quality. *Tasks*: Development of technologies, modelling approaches and equipment for the environment protection quality control as well as methods and experimental basis for the investigation of micro impurities dynamics and balance in the environment components evaluating the impact on climate change by transformation, composition, formation, evolutionary processes of atmospheric chemical compounds. Department is engaged in police-making activity, the creation of the taxonomy, world's first-ever classification system proposed by European Commission for environmentally sustainable

economic activities in accordance with EU sustainability-related policy objectives. Also Department is responsible for EU emission inventory report preparation under the UNECE Convention on Long-range Transboundary Air Pollution (LRTAP) and GHG emissions under United Nations Climate Change Convention (UNFCCC).

## Long-term air pollution trend analysis in the South-eastern Baltic region, 1981–2017

Since the mid-20th century, environmental awareness has started to grow, and the emissions of sulphur and nitrogen components to the atmosphere received considerable attention due to their increasingly harmful effects on ecosystems and human health. Oxides of sulfur ($SO_x$) and nitrogen ($NO_x$), as gaseous emissions, are important precursors of the secondary inorganic aerosols (SIAs), namely, sulfate ($SO_4^{2-}$), nitrate ($NO_3^-$) and ammonium ($NH_4^+$). The concentration of all the analyzed S- and N- species at the Preila background station decreased during the 1981–2017 period except for that of the nitrate (Fig. 1). The analysis has shown that despite the immense decrease of sulfur dioxide and sulfate concentrations, 95 % and 79 % respectively, sulfate still has a considerable share in particle formation. The share of sulfate concentration in the sea-related particles increased up to 22%.

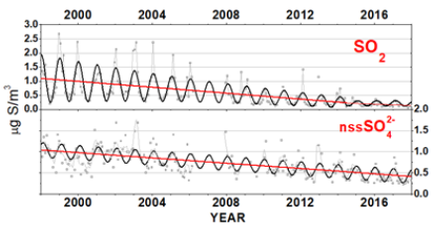


Fig. 1. Time-series of gaseous and particulate sulphur-related air pollutants, 1998–2017. Monthly means (grey point and line) of gaseous $SO_2$ and particulate non-sea salt $SO^+_4$ with slope (red line for s.sgn. trend) and sine (black line, damped sine for $SO_2$) approximations.

lina.davuliene@ftmc.lt

## Intercomparison and characterization of 23 Aethalometers under laboratory and ambient air conditions: procedures and unit-to-unit variabilities

The impact of black carbon (BC) on climate, health, and human activities prioritizes the observation of BC mass concentration and its optical properties in different environments. The intercomparisons of Aethalometers (AEs) were conducted in three laboratory workshops at the World Calibration Centre for Aerosol Physics (WCCAP) in Leipzig, Germany. AE33 collects the aerosol sample in two spots (S1 and S2) on the filter (Fig. 2). The average unit-to-unit variability in the measurements of eBC mass concentrations (880 nm) reported by the 23 instruments was −2.0 % for soot before maintenance and −1.0 % after the maintenance activities (Fig. 3). The results of this intercomparison activity show that relatively small unit-to-unit variability of AE33-based particle light absorbing measurements is possible with well-maintained instruments. It is crucial to follow the guidelines for maintenance activities and use a proper filter tape in the AE33 to ensure high quality and comparable BC measurements in international observational network.

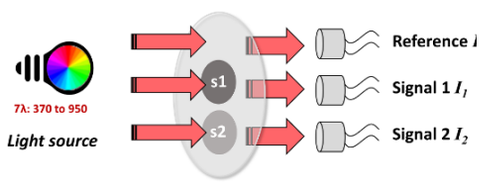


Fig. 2. Schema of the optical chamber in AE33.

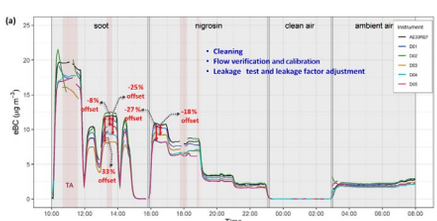


Fig. 3. Time-series of eBC mass concentrations at 880 nm.

vadimas.dudoitis@ftmc.lt

## Coast of Eastern Antarctica as the source of atmospheric mercury during austral summer

Mercury is a toxic element of global concern. Anthropogenic sources of mercury to the atmosphere include coal-fired power plants, iron and steel industries, cement industries and metal smelters. Automated gold amalgamation + CVAAS method was successfully applied for the investigation of Antarctic environment for the first time. Little-varying gaseous elemental mercury (GEM) concentrations, on average 1.08 ng/m$^3$, were recorded during the ship cruise from Cape Point towards Prydz Bay, which was in good agreement with other research. Elevated concentrations (up to 2.36 ng/m$^3$) were detected both during day and night when the air masses were coming from the Eastern Antarctic coast (Fig. 4). Much lower concentrations (down to 0.17 ng/m$^3$) were detected when the air masses were steeply descending from the free troposphere above the coast, or coming from deeper of the continent (Fig. 5). Data analysis allows us to conclude that the Antarctic coast in this region acted as a temperature-driven local source of mercury in the given observation time (Austral Summer, January–February, 2015).

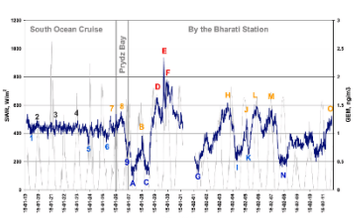


Fig. 4. Time series of GEM concentration during the entire campaign along with short wave radiation and air temperature.

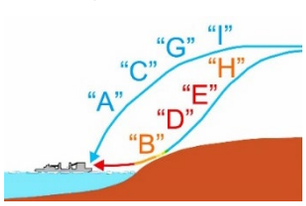


Fig. 5. Schema of how different vertical trajectories of air parcel movement may have affected the GEM concentrations measured at the sampling point.

andriejus.urba@ftmc.lt

# Nuclear


## Nuclear research for applications today and innovative technologies for future

The Department of Nuclear Research develops and applies known and innovative methods in the fields of nuclear fuel cycle technologies, experimental nuclear and mass spectroscopy, ion beam application for material analysis and modification as well as applications of lasers for generation of ionizing radiation for different purposes. Optimization of nuclear facility radioactive waste management and comprehension of processes of radionuclides transport through engineering barriers to enable nuclear facility safety are key applications of nuclear research carried out. The special attention is also paid to environmental impact assessment of energy generating facilities, elemental and isotopic analysis of groundwater, food fabrics and products, and also industrial stocks, medical samples with sensitivity up to 1 ppq. Application of stable isotope ratio analysis ($\delta^{13}C$, $\delta^{15}N$, $\delta^{18}O$ and $\delta^{34}S$) in environmental, biomedical and food samples stimulates new promising technologies. $^{14}C$ measurements open the potentially new field of activity related to carbon dating and analysis of triple carbon ratio for dedicated samples. Complementary information on material properties (magnetic properties, oxidation and corrosion of iron compounds) is determined by Mössbauer spectroscopy (combining with data of vibrating sample magnetometer for better characterization of multiferroics). Development of ion beam methods for material analysis and modification is important part of our activities having intersection both with semiconductor materials and applications for lasers. Investigation of organic scintillator films opens new possibilities of simple scintillator material application for detection and spectroscopy of ionizing radiation particles. The principles of the high energy electromagnetic radiation generation are investigated using ultrashort laser pulses, taking into consideration the possibility of their practical applications.

## Structural and radiological investigation of spent RBMK-1500 reactor graphite

The comprehensive understanding of both structural and radiological characteristics of nuclear graphite is very important when dealing with irradiated graphite waste management strategy or treatment options prior to its final disposal. The experimental results of morphological and structural analysis of the irradiated graphite samples by using SEM, Raman spectroscopy and theoretical evaluation of primary displacement damage, as well as the experimental and theoretical evaluation of the neutron flux (comparing measured and calculated $\delta^{13}C$ values) and activation in the spent graphite was assessed. The results indicate that structural changes are uniform enough in all the analyzed samples. This result correlates with obtained neutron flux values varying from $7.3\times10^{13}$ n/cm$^2$s to $1.5\times10^{14}$ n/cm$^2$s. Neutron irradiated graphite exhibits significant reduction in crystallites size, when compared to the raw RBMK graphite, though the amorphous fraction is very low in both samples from the central and peripheral zone of the RBMK-1500 reactor core (Fig. 1). However, the distribution of radionuclides is non-homogeneous in the irradiated RBMK-1500 reactor graphite matrix; the main γ-ray emitters are $^{60}Co$ and $^{137}Cs$. $^{14}C$ specific activity was measured by using improved version of rapid analysis method for $^{14}C$ activity determination (Table 1). This study is important for all irradiated RBMK type reactors.

Table. 1. Experimentally determined mass and $^{14}C$ activity of graphite samples.

| Sample No | Sample mass, μg | | $^{14}C$ activity, Bq | $^{14}C$ activity, $\times10^5$ Bq/g |
|---|---|---|---|---|
| | By weighing | By $CO_2$ amount | | |
| No 1 | 190 | 186 | 44 ± 3 | 2.3 ± 0.1 |
| No 2 | 422 | 400 | 115 ± 7 | 2.7 ± 0.2 |
| No 3 | 380 | 373 | 95 ± 5 | 2.5 ± 0.1 |
| No 4 | 204 | 210 | 40 ± 2 | 2.0 ± 0.1 |
| No 5 | 414 | 388 | 79 ± 5 | 1.9 ± 0.1 |

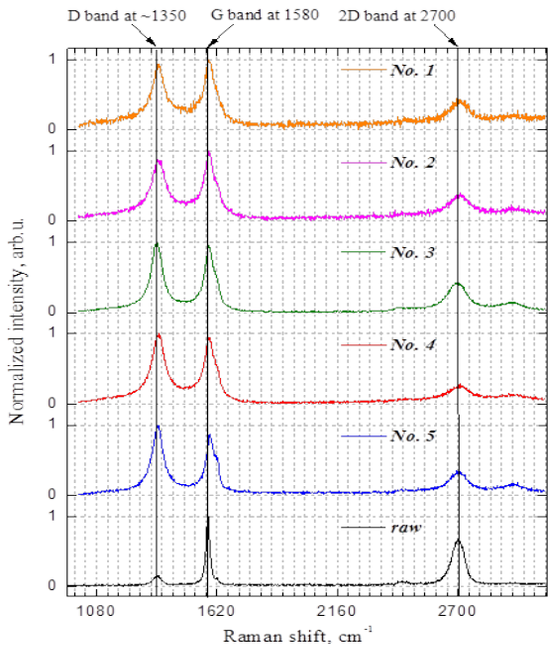


Fig. 1. The Raman spectra of graphite samples obtained from different locations of RBMK-1500 reactor. The excitation wavelength is 532 nm (0.3 mW).

elena.lagzdina@ftmc.lt

## Mössbauer spectroscopy for investigation of Y–Gd–Mn perovskites

Mössbauer spectroscopy revealed the effects of Gd substitution in yttrium manganite on its structural, magnetic and morphological properties. The structure of $YMnO_3$ can be stable hexagonal and metastable orthorhombic, while $GdMnO_3$ is orthorhombic. Several magnetic transitions (at 44, 23 and 6 K), related to changes of antiferromagnetic order of Mn and Gd spins, are observed in $GdMnO_3$. The hexagonal $YMnO_3$ has higher temperature (75 K) of magnetic ordering. Under gradual substitution of Y by Gd, the sol-gel synthesized perovskites change their structure from hexagonal to orthorhombic. Small amount of $^{57}Fe$ substituting Mn was used to perform the Mössbauer spectroscopy studies. We obtained that the magnetic ordering occurs at 36, 39 and 70 K for $Y_xGd_{1-x}Mn_{0.97}Fe_{0.03}O_3$ with x = 0, 0.4 and 1, respectively (Fig. 2). Moreover, the change in magnetic ordering below 23 K for $GdMn_{0.97}Fe_{0.03}O_3$ may be associated with the increase in hyperfine field probability of distribution. Partial substitution of Y at x=0.4 leads to additional spectra broadening even at very low temperature.

kestutis.mazeika@ftmc.lt

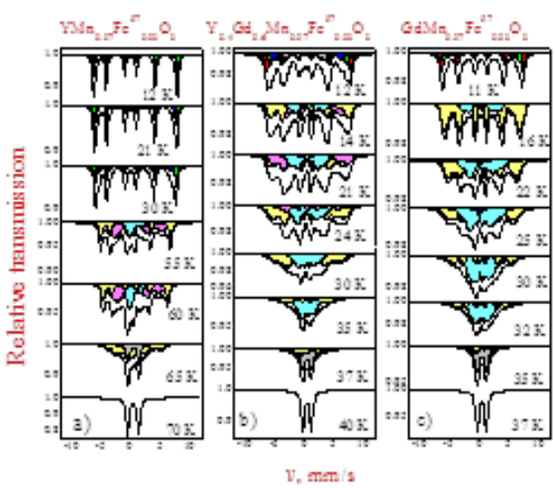


Fig. 2. (a) Mössbauer spectra of $YMn_{0.97}Fe_{0.03}O_3$, (b) $Y_{0.4}Gd_{0.6}Mn_{0.97}Fe_{0.03}O_3$ and (c) $GdMn_{0.97}Fe_{0.03}O_3$ (c) at indicated temperatures.

## Development of online sulfur trapping system for graphitization of biological samples

The dating of the carbon content incorporated in the apatite of cremated bones is very low (0.5–1% by weight) and problematic even for such an advanced technique as accelerator mass spectrometry (AMS). The graphitization of cremated bones by an online Carbonate Handling System (CHS) coupled to Automated Graphitization Equipment (AGE-3) can be complicated due to sulfur impurities in the samples. An online sulfur trap was created for the purification of $CO_2$ during graphitization of samples with the CHS-AGE-3 system for radiocarbon measurements with AMS. It is an alternative to the purification of $CO_2$ gas in a quartz tube filled with cobaltous oxide and silver wool. Optimal operating parameters of the sulfur trap were experimentally determined by varying temperature from 20º to 600ºC. High graphitization efficiency was obtained starting from 100ºC, and further increase of temperature to 600 ºC resulted in graphitization yield improvement of 4-6%. Based on graphitization yield and $^{14}C$ analyses, our proposed $CO_2$ purification line was successful in removing sulfur impurities and did not contaminate samples due to the continuous flushing of the trap with helium gas. The processing blank and reproducibility of applied online graphitization system are satisfactory and allow the production of high-quality graphite target of cremated bone samples for 14C analysis.

justina.sapolaite@ftmc.lt
zilvinas.ezerinskis@ftmc.lt

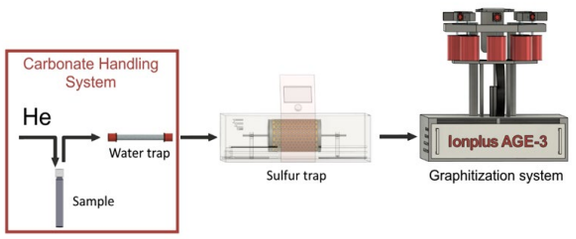


Fig. 3. Schematic view of graphitization line of cremated bones at Mass Spectrometry Laboratory.

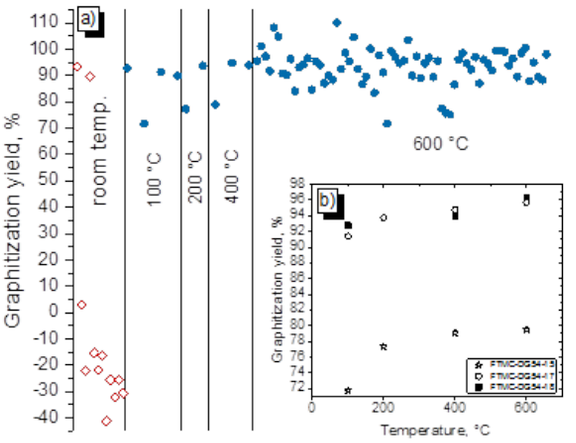


Fig. 4. (a) Graphitization yield of samples with a sulfur trap at temperature above 100°C (blue circles) and room temperature (red diamonds). (Inset) Graphitization yield of the three cremated bone samples at different temperatures.

## Development of the structural analysis methods using high-energy ion beams

Open source modelling technique, GEANT4 software, is a tool to simulate Rutherford backscattering (RBS) spectra and improve the analysis of investigated samples. The described model simulates particle tracks in the sample and evaluates the backscattering spectra based on the scattering cross sections and the energy loss on the way out of the sample. The simulated backscattering cross sections are in good agreement with the recommended ones, as are the multiple scattering induced energy spread values when compared to the Depth code values. Proton and alphas stopping powers agree with the Stopping and Range of Ions in Matter (SRIM-2013) and the RBS spectra coincide well with other simulations (SIMNRA and WINDF), when SRIM stopping powers are used.

danielius.lingis@ftmc.lt

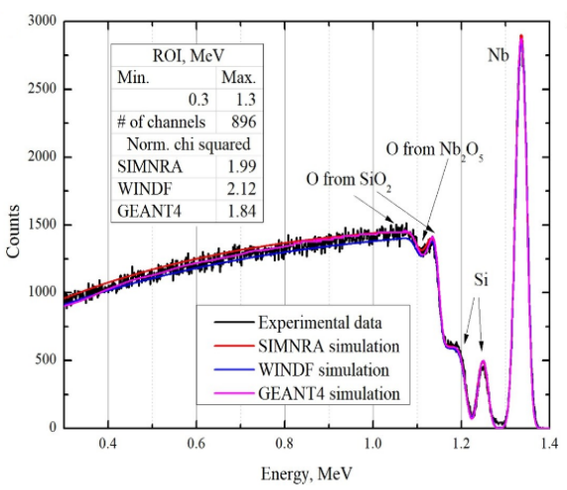


Fig. 5. Experimental and calculated spectra of proton RBS from $SiO_2/Nb_2O_5/SiO_2$ sample.

## Model of radiocarbon cycling processes for nuclear power plant environmental impact assessment

Lake Drūkšiai with water residence time of 3–4 year and undisturbed sediment layers is a unique system to assess the impact of Ignalina nuclear power plant (INPP) on the aquatic ecosystem with a sufficiently high temporal resolution. We constructed a model of radiocarbon cycling processes in an ecosystem of the lake which evaluates the $^{14}C$ specific activity vertical distribution in two organic sediment fractions: alkali-soluble and alkali-insoluble. Our modeling proved that during the first 15 years of operation since 1983 14C annual aqueous releases from the INPP were in a form of a water dissolved inorganic carbon, and it varied in the range of $2.4 \div 3.7 \times 10^8$ Bq/year. The results showed one episode of elevated releases from the INPP in 2000–2001, which changed the interaction between the two organic sediment fractions for the period of 2000–2006. After 2006, the ecosystem recovered to its original state indicating the clean-up of the lake.

ruta.bariseviciute@ftmc.lt

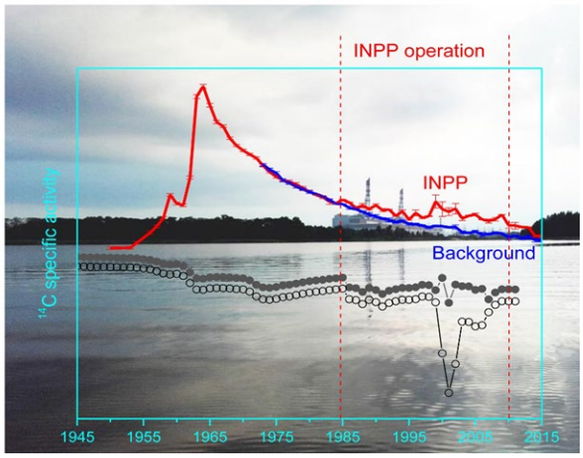


Fig. 6. Measured and calculated values of $^{14}C$ specific activity in the alkali-soluble and alkali-insoluble sediment fractions.

## Isotope method to track climate-induced changes in marine ecosystem

Changes of ocean climate strongly affect organisms and ecosystems, and the causes, consequences and underlying mechanisms need to be documented. In the Baltic Sea, a marginal sea under severe eutrophication stress, a longer productive season and changes in the phytoplankton community over the last few decades have likely impacted diet and condition of keystone species, from individual to population level. The stable isotopes ($\delta^{13}C$, $\delta^{15}N$, and derived isotope niche metrics) were used to trace energy and nutrient flows in archived samples of blue mussel (Mytilus edulis trossulus) spanning 24 yr (1993–2016). We test if long-term changes in isotope and elemental composition in mussels, can be explained by changes in abiotic and biotic variables. Changes in isotope composition were best explained by nitrogen-fixing cyanobacteria, increase in terrestrial organic carbon from land runoff (reflecting precipitation) and decrease in dissolved inorganic nitrogen (indicative of successful eutrophication mitigation) and biomass of a mixotrophic ciliate species. It was revealed that altered trophic relationships from climate-induced changes in the productivity base may strongly impact keystone species, with potential knock-on effects on ecosystem functions.

andrius.garbaras@ftmc.lt

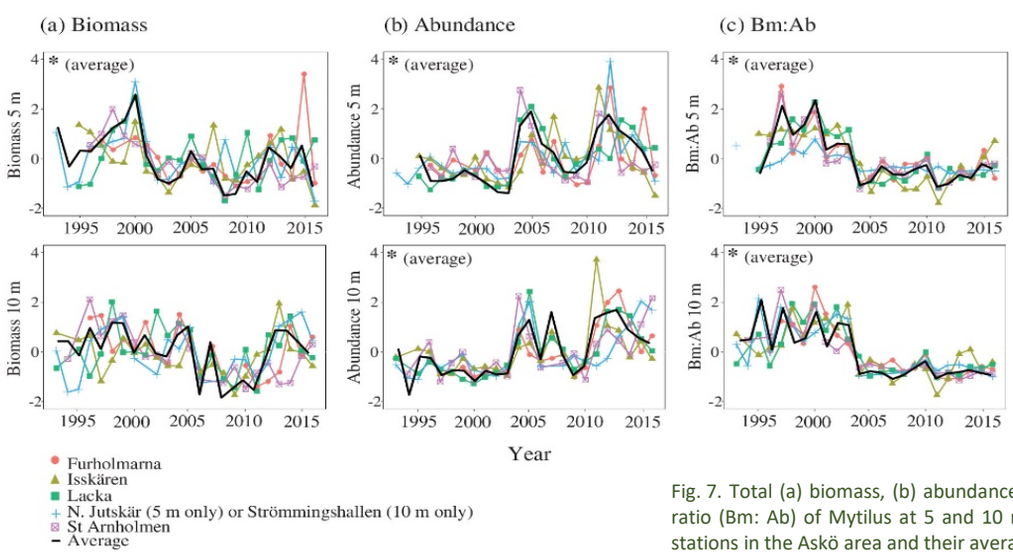


Fig. 7. Total (a) biomass, (b) abundance, (c) biomass: abundance ratio (Bm: Ab) of Mytilus at 5 and 10 m depth for five different stations in the Askö area and their average (black line).

# Textile technologies


## Green deal in textile

Research of Textile Departments is based on the requirements for Green Deal Concept seeking to adopt environmentally friendly processes for Textile technologies and products. The EUREKA **project *Eco Design Casual Garments from Biodegradable and Natural Fibers Based on the Principles of the Circular Economy* is ongoing and** fabrics from plant-derived thermoplastic polylactic acid, organic wool, hemp fibres, etc. are used as alternative to the currently prevailing synthetics. Environmentally friendly organic chemicals are applied for innovative finishing of the fabrics as well. Industry partners from Lithuania and partners from the Netherlands take part in this project to develop sustainable, eco-design fashion garments. More energy-efficient solutions for finishing processes in textile were developed by investigating and adapting linear non-thermal plasma source created by the research and development partner JSC *Nova Fabrica*. The development and investigation of smart personal protective equipment (PPE) remains the core of the research of Textile Departments. The project *Strengthening of The Researcher's Interdisciplinary Competences Directing Them towards the Development of Smart Protective Textile Products* has just finished, and the prototype of smart bulletproof garment with EMR shielding properties and integrated active thermoregulation system was developed. The ACAMS II project funded by European Defence Agency is continued as well. Four prototypes of soldier camouflage systems were developed and field tests were performed. The aim to simultaneously demonstrate adaptive protection of camouflage in the VIS, TIR and radar ranges has been fulfilled. Research and certification services due to Covid-19 pandemic have also found its place in the activity of FTMC Textile Departments. The protective clothing certifying body was established and certification of category II and III of PPE according to the requirements of the Regulation (EU) 2016/425 of the European Parliament and of the Council are now performed. The scope of accreditation was extended and includes protective clothing against harmful biological agents.

## Enhancement of thermal performance of the paraffin-based microcapsules intended for textile applications

Phase changing materials (PCMs), microcapsules MPCM32D, consisting of a polymeric melamine-formaldehyde (MF) resin shell surrounding a paraffin core (melting point: 30-32 °C), have been modified by introducing thermally conductive additives on their outer shell surface, using a layer-by-layer self-assembly method. As additives we used multiwall carbon nanotubes (MWCNTs) and poly(3,4-ethylenedioxyoxythiophene)-poly (styrene sulphonate) (PEDOT: PSS) in different parts by weight (1wt.%, 5wt.% and 10wt.%). The main aim of this modification was to enhance the thermal performance of the microencapsulated PCMs intended for textile applications. The morphologic analysis of the newly formed coating of MWCNTs or PEDOT: PSS was performed by SEM (Fig. 1). The heat storage and release capacity were evaluated changing MPCM32D shell modification (Fig. 2). To evaluate the influence of the modified MF outer shell to the thermal properties of paraffin PCM, a thermal conductivity coefficient ($\lambda$) of these unmodified and shell-modified microcapsules was also measured and compared. Based on the identified optimal parameters of the thermal performance of the tested PCM microcapsules, a 3D warp knitted spacer fabric from PET was treated by dip coating method with a composition containing 5wt.% MWCNTs or 5wt.% PEDOT: PSS shell-modified microcapsules MPCM32D and acrylic resin binder. To assess the dynamic thermal behaviour of the treated fabric samples, the IR heating source and IR camera were used. The knitted fabric after the dip coating with 5wt.% MWCNTs or 5wt.% PEDOT: PSS in shell-modified paraffin microcapsules MPCM32D revealed much faster heating and significantly slower cooling compared to the fabric treated with the unmodified microcapsules. After

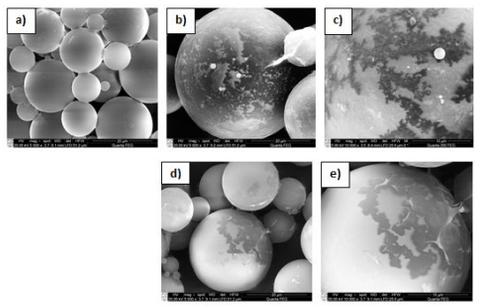


Fig. 1. SEM morphologic analysis of microcapsules MPCM32D: (a) unmodified, magnification 5000x; (b, c) with 5wt.% MWCNTs shell-modified, magnification 5000x and 10000x; (d, e) with 5wt.% PEDOT: PSS shell-modified, magnification 5000x and 10000x.

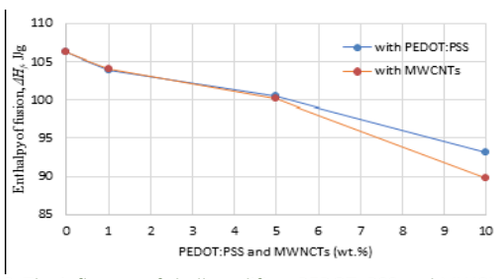


Fig. 2. The influence of shell modifiers PEDOT: PSS and MWCNTs on fusion enthalpy of paraffin PCM microcapsules.

modification of the outer shell of the microcapsules MPCM32D with 5wt.% of used add-on's, the thermal conductivity of the investigated knitted fabric has improved in comparison to the unmodified fabric samples. This confirms the positive influence of used thermally conductive enhancing additives to the heat transfer rate in textile sample containing these modified paraffin PCM microcapsules.

audrone.sankauskaite@ftmc.lt

## Investigation of pedot: pss composition coated fabrics intended for microwave shielding and absorption

This study presents the investigation of the electromagnetic properties and resistance performance of electrically conductive fabrics coated with composition containing the conjugated polymer PEDOT:PSS. The developed fabrics were intended for electromagnetic radiation (EMR) shielding in microwave range and for absorbing microwaves in radar operating range, to act as radar absorbing materials (RAM). The measurements of reflection and transmission of the developed fabrics were performed in a frequency range of 2–18 GHz, which covers the frequencies relevant to the application. Four types of fabrics with different fiber composition (I group - polyamide; II group - polyamide/cotton; III group - wool and IV group - para-aramid/viscose) were selected and coated with conductive paste using screen printing method. It was found that EMR shielding effectiveness (SE) as well as absorption properties depend not only on the amount of conductive paste topped on the fabric, but also resides in the construction parameters of fabrics (Fig. 1). Depending on structural parameters of the fabric, such as density, mass per unit area, type of weave, a layer of shield (or coating) just sticks on the fabric surface or penetrates into fabric, changing the shield thickness and herewith affecting the SE results. Meanwhile, the fiber composition of fabrics influences mostly bonding between fibers and polymer coating. To improve the resistance performance of the developed samples, a conventional textile surface modification technique,

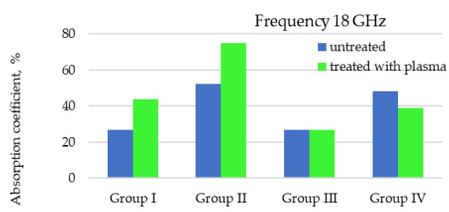


Fig. 3. Absorption ability of tested samples at 18 GHz frequency.

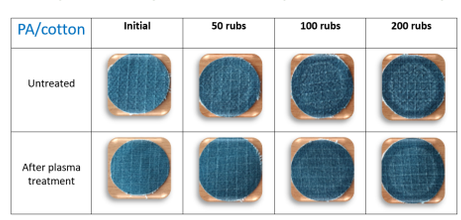


Fig. 4. Polyamide/cotton coated fabric samples after being subjected to abrasion in the Martindale abrasion tester.

atmospheric plasma treatment, was applied. Initially, before and after plasma treatment the fabrics were evaluated by aqueous liquid repellency test, measuring the contact angles for the water solvent. The influence of plasma treatment on resistance performance of coated fabrics was evaluated by subjecting the plasma treated and untreated samples to abrasion in the Martindale abrasion apparatus and to multiplex washing cycles. Applied plasma treatment visibly improved abrasion resistance as a result of better adhesion of the coating (Fig. 2).

vitalija.rubeziene@ftmc.lt

# Metrology


## National Metrology Institute of Lithuania

'Man's knowledge of nature, the universe, and how to adapt nature to his purpose, advances in step with his ability to measure precisely'

Metrology is the science of measurement and its application. In metrology one has to deal with correctness, accuracy and reliability of measurement results. The core of metrology lies in the validation of the result, particularly by specifying its actual limitations.

FTMC Metrology Department (MD) was authorized to perform and implement functions of the National Metrology Institute (NMI) since 1 July 2014. The MD has implemented and peer-reviewed Quality Management System (QMS) fulfilling the requirements of international standard ISO/IEC 17025:2017 which is recognised by EURAMET. The last year NMI of Lithuania became one of eight NMIs of Nordic-Baltic countries which established European Metrology Network (EMN) *Smart Specialisation in Northern Europe.* The MD maintains the national standards in seven areas of measurements.

**Time and Frequency Standard Laboratory (TFSL)** is reproducing values of the unit of time, the second (*s*), and the unit of frequency, hertz (*Hz*). The mission of TFSL is representation of Lithuanian Coordinated Universal Time UTC(LT), ensuring the traceability of the magnitudes reproduced to the International System of Units (SI), disseminating them to Lithuanian scientific establishments, personal and legal bodies by calibrating their working standards and measurement devices, disseminating Lithuanian time scale, and other relevant means. The TFSL in cooperation with the JSC *BaltStamp* provides qualified time stamping services, which meet the eIDAS regulations and the ETSI standards. The time stamping service is issuing up to two million time stamps per month for Lithuanian governmental organisations and European users.

The mission of the **Electrical Standards Laboratory (ESL)** is maintaining and developing the standards of unit of voltage, the volt (*V*), and unit of resistance, the ohm (*Ω*), ensuring their traceability to the SI, calibrating working standards and measurement devices, pursuing research in the field of measurement of voltage, resistance and electrical current.

The mission of the **Temperature Unit Standard Laboratory (TUSL)** is in realization of the international temperature scale ITS-90 and the value of the unit of temperature, the kelvin (*K*), ensuring their traceability to SI. Lithuanian National Standard of the temperature unit (in the range from -195°C to +961,78° C) is of the primary level and the reference point of the freezing point of Cu (+1084,62 °C) is the secondary level.

The Government of the Republic of Lithuania transferred the **National Standards of Mass and Length Laboratory (NSMLL)** to FTMC in 2019. The mission of the national gauge blocks standard is maintaining and transferring length unit (in the range from 0,5 mm to 100 mm with 0,0001 mm uncertainty) ensuring its metrological traceability to the SI system. The mission of the national mass unit standard is maintaining and developing the standards of mass unit ensuring the traceability to the SI system in the range from 1 mg to 20 kg with uncertainty from 0,4 mg to 3,2 mg. Reference equipment of NSMLL can also measure the magnetic properties and density of weights.

The reliable, traceable and accurate chemical measurements in different sectors of biotechnology, healthcare, safety and environment protection can be provided by the **Laboratory for Metrology in Chemistry (LMiC)**. In 2021 LMiC provided more than 380 different chemical measurements for the local and foreign companies. Last year LMiC together with the project partner started a new research project *01.2.1-LVPA-K-856-01-0120* "*Development of in-combo methods for the evaluation of the safety of compounds for humans and environment and development of products prototypes based on them*". The project develops prototypes for new products characterizing chemical compounds - AQUASOL (water solubility), PERMSKIN (compound dermal permeability), HERG (hERG channel inhibition) and PGP (P-gp substrate specificity) for chemistry, cosmetics and pharmaceutical industry, national environmental protection and chemical monitoring agencies. Another areas of laboratory interests are a new regional metrological capacity for certification of reference materials according the requirements of ISO 17034 standard and research in the field of volatile organic compounds for different applications.

The **Ionizing Radiation Metrology Laboratory (IRML)** participated in the IAEA-TEL-2021-03 *World-wide open Proficiency Test on determination of anthropogenic and natural radionuclides in water, Japanese bamboo and simulated swipe samples* organized by International Atomic Energy Agency (IAEA). IRML started the activities within the EMPIR 2020 joint project 20SIP02 which has the aim to disseminate the pre-selection and free release measurement technology developed within former European research projects to end-users from nuclear facilities, preferably in decommissioning, or waiting for decommis-sioning. The calibrations, ensuring traceability to the National Standard of Ra-223, Tc-99m and I-131, were carried out for Lithuanian hospitals and other customers, Ignalina Nuclear Power Plant (under decommissioning now) in particular. In 2020 the IRML organized the intercomparison for local laboratories of gamma-ray emitters and low-activity measurement in water.

## Efficiency calibration and performance testing of LSC cocktails as an indicator of the technological start of a new NPP

The instrument of liquid scintillation (LSC) coctails was efficiency calibrated for the tritium activity determination in river water samples by the direct measurement, and different LSC cocktails were evaluated. The combined standard uncertainty was around 6% at the coverage factor $k = 1$. The obtained mean values for the background tritium, total beta- and $^{137}Cs$ activity concentrations in the Neris River samples were 1.5 $Bq \cdot L^{-1}$, 25 $mBq \cdot L^{-1}$, and 3.3 $mBq \cdot L^{-1}$, respectively.

arunas.gudelis@ftmc.lt

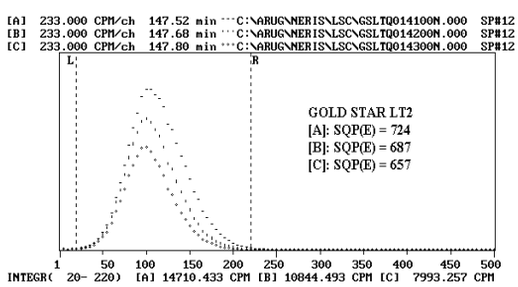


Fig. 1. Effect of quenching for the LSC cocktail (GSLT) at the sample-to-cocktail ratio of 10:10 mL. The spectra [B] and [C] are measured with added 20 and 40 µl of quenching agent, respectively. The SQP(E)=724 refers to the typical sample prepared with the GSLT cocktail.

## On national standard of electric resistance

The Lithuanian national standard of electric resistance is maintained as the basis of calibration and measurement capabi-lities. The stability and uncertainty of the resistance values, realized since 2004 using the calibrated values of the standard resistors to predict their future behaviour, as well as the influence of environmental conditions and the recovery of a standard resistor which underwent a mechanical disturbance, are discussed.

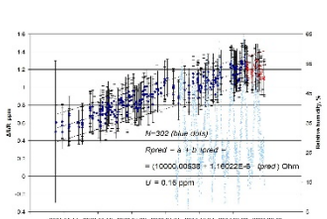

Fig. 2. Calibration history with prediction lines and uncertainties for the 10 kΩ Tegam SR104 standard resistor.

We concluded that the standard resistors of ESL feature stable and well-predicted (by linear regression) drift of resistance.

emilis.urba@ftmc.lt

# Open access facilities



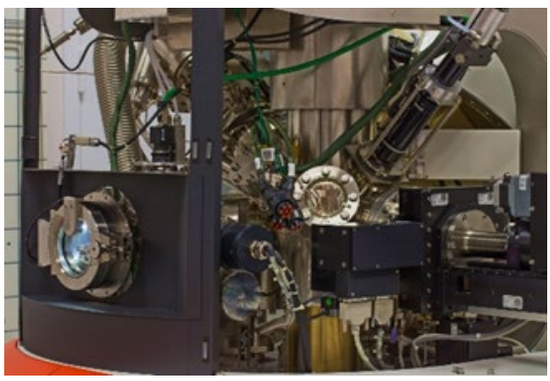

## Electron microscopy, X-ray spectroscopy and XRD open-access center (OAC)

OAC offers open access facilities for characterisation of solid material surface structure, morphology, inner and crystalline structure, chemical and phase composition. The OAC infrastructure has been improved significantly during last 10 years, and now is equipped with modern electron microscopes (FE-SEM-FIB and TEM), X-ray diffractometers, X-ray fluorescence (WD-XRF), X-ray photoelectron (XPS) and Auger electron spectrometers. The OAC provides characterisation services of solid materials for customers from academic institutions and industry in Lithuania and abroad. Among the customers, there are universities of Southampton, Hoseo (South Korea), Riga, Vilnius and Kaunas. OAC provided structure characterisation services for such companies as Translucent Inc (from Palo Alto), IQE (North Carolina), Brolis Semiconductor, Altechna, Optolita and many others. For more information, please visit https://litexbeam.ftmc.lt.

## Prototype formation and integration

### Clean room technology for prototyping of semiconductor-based devices

Based on a collaboration between the Departments for Physical Technologies and Optoelectronics, a complete cycle of the clean room (CR) micro-processing line has started to function. It is ready to produce the working models and the demonstration prototypes of chemical and photo-sensitive devices as single units and as limited batches of products. The prototyping of innovative devices is based on a few key enabling technologies including the PECVD/CVD for the synthesis of 2D materials, namely graphene and MoS2, multi-mode magnetron sputtering for deposition of multicomponent functional films and molecule beam epitaxy for GaAs based optoelectronic devices.

The CR services include: 1) CR (ISO7–ISO5 about 300 $m^2$) operations, 2) photolithography, 3) laser lithography, 4) wet chemical processing, 5) thermal processing, 6) metal and oxide coatings, 7) assemblage and testing.

### Characterisation and testing of prototypes

The R&D projects in the OAC can range from proof of concepts (TRL – Technological Readiness Level- 3), validation of technologies in the laboratory (TRL 4) or relevant environment (TRL 5), and up to demonstration in a relevant environment (TRL 6). In specific cases, collaboration can reach prototyping in an operational environment (TRL 7). For this, we use the methods acceptable to characterise the components and devices at the nanometre scale level and the level of the complete unit.

The characterization includes: 1) topography, force spectroscopy, tunnelling current spectroscopy by scanning probe microscopy, 2) standard I-V and C-V characteristics in the dc- and ac-modes by the probe station, 3) photovoltaic parameters with the A1.5 solar source by special set-up, 4) gas response in the synthetic atmosphere under strictly controlled conditions by gas flow control system. We also carry out special set of tests to determine the response and resistivity to the microwave irradiation.

# BALTFAB processing technologies

is a joint open user facility between departments of Laser technologies and Nanoengineering, offering a full range of nano/ micro and macro fabrication as well as laser patterning, marking and cutting on any required material. State of the art laser microfabrication workstations are equipped with full variety of industrial ns-, ps- and fs- lasers. The BALTFAB team include experts to set-up, test and develop laser micromachining processes and systems. Soft nano-lithography tools for rapid creation of nano-structures are tested to be live cell compatible. The patterns are routinely applied to improve the bio-compatibility of medical devices. The team is developing tools for detection of molecules on surfaces, to fasten the testing and evaluation of cells or drugs. More: see www.baltfab.com

Services include: 1) Laser processing: in-Glass marking; laser beam interference ablation; laser direct writing; ultrashort pulse laser ablation. 2) Molecular: dip pen nanolithography; microcontact printing; piezoelectric inkjet printing; colloidal nanolithography. 3) Analytical: bio AFM; electrochemical sensors; imaging surface plasmon ellipsometry.

Available equipment: Multi-axis workstations with ultrashort pulse lasers for experimentation, rent and user training services. Dip pen nanolithography and imaging ellipsometry for creating and imaging of molecular surfaces.

# Converse and chemical coatings

specializes in aluminium and its alloys anodization, galvanic precious metals plating and related fields. The services provide: electrodeposition of protective, decorative as well as technical converse (anodic) coatings, structural etching of decoration elements, adsorption colouring of anodized surfaces, modify-cation of aluminium and its alloys surfaces with a passivation film that ensures the required conductivity, protection and other properties, chemical deposition of passivation coatings onto alloy steels.

Available equipment: Experimental equipment for environment-friendly galvanic processes, anodizing line.

# Microwave transmission, reflection and absorption

In the new microwave anechoic chamber we developed a setup for microwave transmission and reflection measurement in a frequency range from 1 GHz to 18 GHz. Measured sample is placed in the aperture of the absorbing panel. Using this technique, it is possible to measure microwave properties of various modern materials: windowpanes, absorbing textiles, shielding materials, etc.

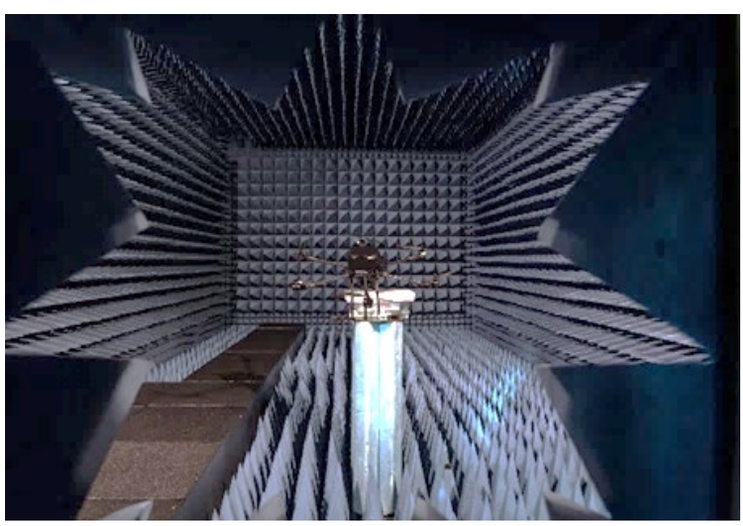

# Projects

European Commission project “Advancing Science and TEchnology thRough dIamond Quantum Sensing”

**A. Alkauskas**

ASTERIQS

European Commission project “European Joint Research Programme in the management and disposal of radioactive waste”

**R. Plukienė**

EURAD

European Commission project “In-built Triggered Enzymes to Recycle Multi-layers: an Inovation for Uses in Plastic-packaging”

**S. Asadauskas**

ResearchExecutive Agency (REA) project “Chalcopyrite-perovskites for infrared photovoltaics”

**R. Kondrotas**

IRPV

Research Executive Agency (REA) “Dirac Semimetals based Terahertz Components”

**G. Valušis**

DiSeTCom

Science for Peace and Security Programme project “Tuned optical sensors for detection and identification of airborne hostile agents”

**A. Rodin**

HOSTITUNOP

European Space Agency (ESA) project “Bismide-based Intersubband Devices for Mid-Infrared Applications”

**J. Devenson**

BISMIRA

Research Executive Agency (REA) project “Terahertz Photonics for Communica-tions, Space, Security, Radio-Astronomy, and Material Science”

**I. Kašalynas**

TERAOPTICS

European Space Agency (ESA) project “Terahertz Time Domain Gas-Phase Spectroscopy”

**R. Adomavičius**

Horizon 2020 programme project “PRE-DISposal management of radioactive waste“

**R. Plukienė**

PRE-DIS

European Space Agency (ESA) project “Optical fiber-based source of entangled photons for satellite-based quantum communications”

**V. Tomkus**

EPhOS

Horizon 2020 programme project “Fostering the PAN-European infrastructure for empowering SMEs digital competences in laser-based advanced and additive manufacturing”

**G. Račiukaitis**

PULSATE

Horizon 2020 programme project “Laser-plasma based source 3D Tomography for cargo inspection”

**G. Račiukaitis**

MULTISCAN 3D

Horizon 2020 programme project “Innovation fostering in accelerator science and technology”

**V. Tomkus**

# Events

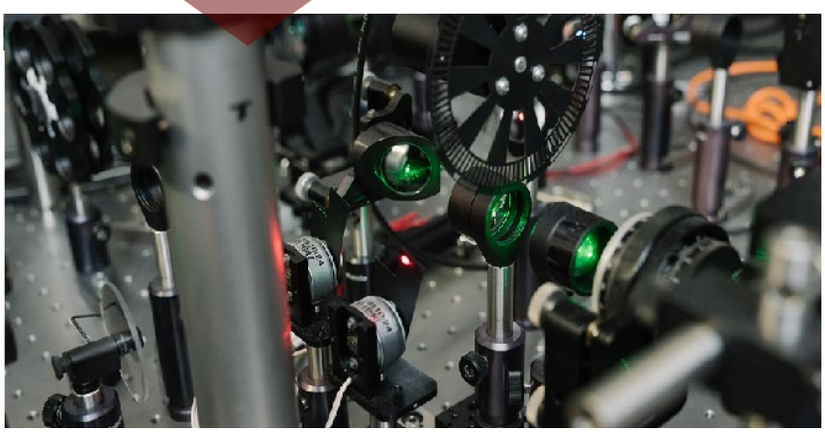

## New technology developed in FTMC

Researchers at the Department of Laser Technologies of FTMC have developed a technology for electroconductive circuit fabrication on dielectrics, allowing replacement of the indium tin oxide (ITO) electrode in touch-screen production. SSAIL - Selective Surface Activation Induced by Laser - a promising technology for solving emerging production issues for electrical conductors on polymers, glass and ceramics.

## FTMC signed the Memorandum with EC Joint Research Center on participation in the European Technology Transfer Offices Circle

FTMC is expanding its involvement in international networks in order to innovate and commercialize research results. Last year FTMC became a member of the European Association of Research and Technology Organisations (EARTO) in Brussels and this year joined the European Technology Transfer Offices Circle (TTO).

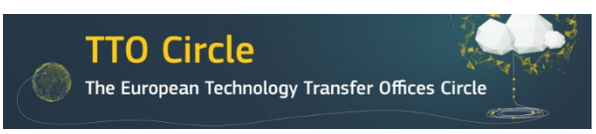


European TTO was established in 2014 and brings together key members of EARTO - European scientific research and technology organisations leading in nanoelectronic and nanoengineering, photonics and optics, chemistry and materials research, digital technologies.

## Scientists from FTMC were awarded Lithuanian Sciences Prizes

On February 4, the Commission for Lithuanian Sciences Prizes announced the winners of 2020. Six prizes were awarded this year and two of them went to five scientists from FTMC. The prize in the field of physical sciences was awarded to Gediminas Niaura and Albertas Malinauskas for the cycle of works “Research into the Molecular Structure and Functionality of Materials by Vibrational Spectroscopy Methods”. In the field of technological sciences, the Lithuanian Science Prize was awarded to Gediminas Račiukaitis, Mindaugas Gedvilas and Paulius Gečys for the cycle of works “Interaction of Ultrashort Laser Pulses with Material and its Application in Laser Micromachining”.

## Three joint initiatives will be funded under an internal Green Deal funding scheme

This year three projects were selected for small scale initiatives under Green Deal topics. The projects involve researchers from all three RTO Lithuania member-institutes – FTMC, Lithuanian Energy Institute and The Lithuanian Research Centre for Agriculture and Forestry.

The main goal of **BioDegra** project (A. Ramanavičius, Ž. Kryževičius and N. Striūgas) is to form large-area, inexpensive and biodegradable carbon-based electrodes serving as anodes of microbial biofuel cells, placed in a soil and populated by living microorganisms which are involved into the generation of electricity.

**ExtraIMTA** project (A. Stirkė, E. Bakšienė and L. Marcinauskas) is related to more efficient use of resources due to growing population. Since more than half of fish stocks are fully exploited, the aquaculture can help to fill the gaps. During inland aquaculture, huge amounts of water rich in nutrients are used in waste. Growing of algae in the "processed" water can lead to the waste- to resource transformation.

The objective of **NUTREC** project (K. Barčauskaitė, M. Urbonavičius and I. Ignatjev) is to determine how to recover the nutrients necessary for plants from secondary raw materials. Simulated wastewater containing nutrients (N, P) and biomass combustion ash are planned to be used as a raw material to produce struvite. Process development would contribute to the strategy of reducing environmental pollution, sustainable use of materials, and preservation of our planet.

## Elected new president of Lithuanian laser association

In an annual meeting of Lithuanian laser association, new members of the board and its president (chairman) were elected. Gediminas Račiukaitis, head of laser technology department of FTMC was elected a new president of the LLA.

## L´Oréal Baltic For Women in Science award for scientist from FTMC

Dr. Ieva Plikusienė received this year's L´Oréal Baltic For Women in Science Young Talents award. L´Oréal Baltic For Women in Science award is provided in collaboration with the national UNESCO embassy and Lithuanian Academy of Sciences. Ieva´s innovative work provides a deeper understanding of the novel coronavirus that causes COVID-19 diseases as she focuses on evaluating SARS-CoV-2 proteins' interaction with specific antibodies using spectroscopic ellipsometry. This year Ieva was elected the Young Academy member of the Lithuanian Academy of Sciences.


Photo by T. Kauneckas

## Visit of A. Armonaitė to FTMC and GMC

On August 13, the Minister of Economy and Innovations of Lithuania Aušrinė Armonaitė visited Saulėtekis scientific centers, FTMC and Vilnius University Life sciences center (GMC), and communicated with the scientists. Together with FTMC director Gintaras Valušis and GMC director Gintaras Valinčius she discussed business-science partnership and development of innovations in our country. Armonaitė emphasized the necessity to use better our achievements in science and business.

## FTMC was visited by Minister of Foreign Affairs of Poland

On September 6, was the 30 years anniversary of recreation of diplomatic relations between Lithuania and Poland. To commemorate this important date, the Minister of Foreign Affairs of Poland Zbigniew Rau visited Lithuania. Among other important events, the Minister and the Polish ambassador to Lithuania Urszula Doroszewska visited FTMC and was met by scientific community. The honorary guests got acquainted with the scientific activities of the Center and existing scientific relations between Polish and Lithuanian scientists. The development and extension of these bilateral relations was discussed.

## Delegation of American – Lithuanian Business Council in FTMC

On September 22, the members of the American – Lithuanian business council (ALBC) from business and military industries of USA visited FTMC. The scientists of the Center had a good opportunity to communicate with businessmen representing the sectors of information technology, cybersecurity, biotechnology, pharmacy and human resources which are planning to or already implemented their activities in Lithuania, also with the guests from the USA Embassy and Lithuanian Ministry of Foreign Affairs. The guests were acquainted with the main fields of FTMC activity, the competencies of FTMC scientists, their experience in R&D and collaboration with industrial partners. The possibility of partnership and joint projects between FTMC and high technology business entities in the USA was discussed.

## 44th Lithuanian National Conference in Physics – science and high technologies

On October 6-8, the FTMC hosted 44th Lithuanian National Conference in Physics (LNFK 2021). The conference, organized every two years by the Lithuanian Physical Society, has a long standing tradition. It reviews the most important achievements of Lithuanian physicists in the last two years. This year the conference due to pandemics was organized in a hybrid way. It comprised 6 plenary, 13 invited and more than 60 oral presentations in fifteen fields of physics and physics education and gathered above 200 presenters (90 participants on youtube online sessions, 100 participants in the FTMC Hall and 27 participants via Zoom), in total 30 h of online broadcasting. The conference also included lectures of fifteen well-known, leading, and accomplished scientists. This conference also provided the opportunity for BSc, MSc and PhD students to present their scientific achievements to a larger audience, get constructive criticism and useful advice.

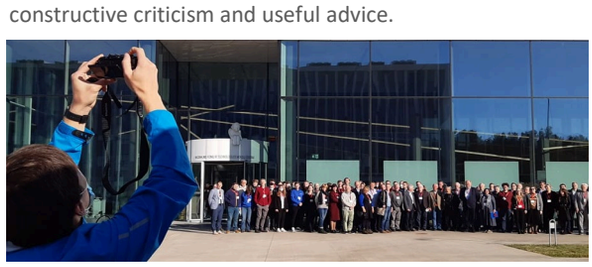

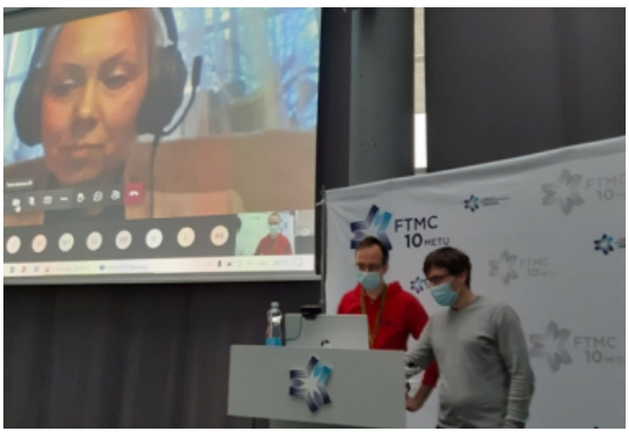


## 11th conference for PhDs and young researchers

On October 20 – 21, the 11th conference for doctorants and young researchers (FizTeCh 2021) was held in FTMC. The participants were welcomed by an encouraging talk of FTMC director Gintaras Valušis. During the conference young scientists in physics, chemistry, material engineering, electricity and electronics presented their scientific results and discussed the possibilities of their application.

## Memorandum between FTMC and National Sun Yat-Sen University

During the visit of Taiwan business delegation in Lithuania, on October 27 the FTMC and the Center for Crystal Researches of the National Sun Yat-Sen University of Taiwan signed the memorandum of understanding. According to the director of FTMC Gintaras Valušis, this memorandum is an important step extending the international scientific activities of the Center. It paves the way to scientific and technological collaboration in the fields of material science and material engineering, solid state physics and technology, optoelectronics and electrical engineering. Photo by K. Vanagas.


## The British Ambassador to Lithuania Received the Patronage Award of FTMC

The Ambassador of the United Kingdom to Lithuania Brian Olley received the Patronage Award of the FTMC as a symbol of respect and gratitude. In the wake of the global coronavirus pandemic, the FTMC initiated the tripartite Lithuanian, UK and Ukrainian research project to control the spread of COVID-19 and other infections. With the support and care of Ambassador Brian Olley, the Foreign, Commonwealth & Development Office provided funding for a research study and helped to purchase innovative laboratory equipment. The aerodynamic aerosol particle size spectrometer allowed FTMC researchers to evaluate the filtration efficiency of protective masks and the reliability of textile combinations in the most penetrating (~ 0.3 µm) aerosol particle size range. Photo by D. Jokubauskis.

## Egidijus Auksorius received Marius Jakulis Jason/MJJ Foundation Grant and prof. Arvydas Janulaitis Foundation Grant

FTMC researcher Egidijus Auksorius was awarded the personal science grant from Marius Jakulis Jason (MJJ) foundation for developing novel microscopy methods to image the human eye in vivo and the grant from prof. Arvydas Janulaitis foundation which helped to develop the Optical Coherence Tomography laboratory in FTMC. These two private foundations are focused on attracting scientists from abroad and helping them to establish their research in Lithuania.

## Renata Butkutė won LRT Annual Awards 2021

Renata Butkutė, the top-level specialist in material engineering at Optoelectronic Technology laboratory, FTMC was awarded the *LRT Annual Awards 2021* in the category *Discovery of the Year* for the development of unique materials, bismides, and scientific leadership in the world. Bismides are innovative semiconductor compounds exhibiting unique optoelectronics properties which provide the solutions for wide range of applications (security, environmental protection, communication, preventive medicine). The integration of bismide quantum structures in semiconducting microlasers could enhance the performances of NIR sensing systems operating on GaAs platform in the wavelength range of 1.0 µm -1.55 µm. Renata's leadership, scientific excellence, technological know-how and innovative activity impacts Lithuanian science in photonics field. Photo by E. Blaževič.

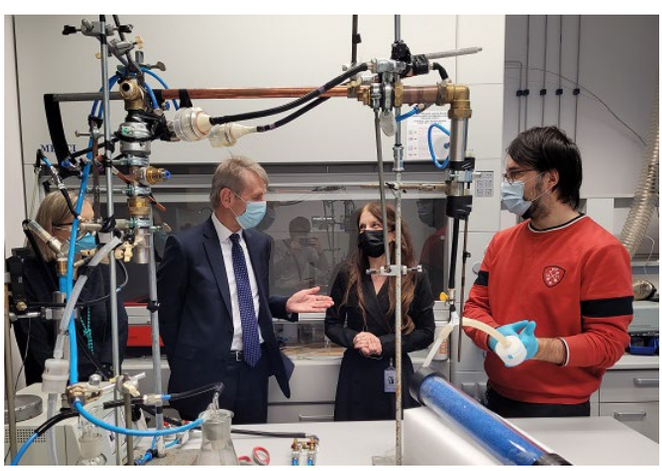

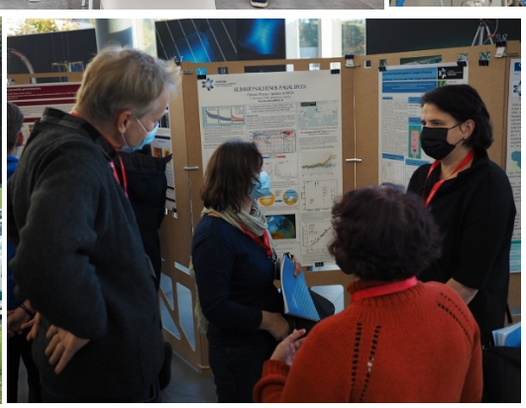

# Awards

## Leonas Valkūnas
### *– for life achievements*

For significant contribution to the development of molecular exciton theory. For research of photosynthetic excitons, the path moving new generations of scientists towards quantum biology.

## Gediminas Niaura
### *– for scientific achievements*

For outstanding achievements within recent years, for broad range of scientific interests covering chemistry, physics and materials engineering. For creation of scientific atmosphere. For being driving and inspiring force of the team.

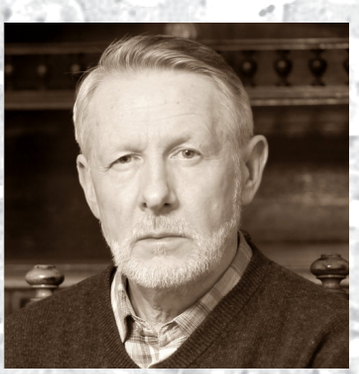

## Remigijus Juškėnas
### *– for innovational activity*

For successful development of Department of Characterisation of Materials Structure. For extension of scientific services to international scale. For precision of measurements, high standard of work, exceptional attitude and responsibility.

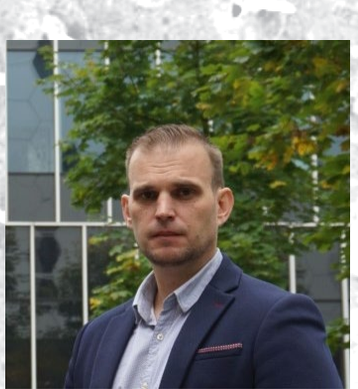

## Žilvinas Ežerinskis
### *– breakthrough of the year*

For encouraging achievements in mass spectrometry and different applications. For the leadership of young and successful team.

## Audronė Barkauskienė
### *– for scientifically invisible work*

For years of honest, diligent and patient work, professionalism and responsibility in managing personnel documents of FTMC community. For grateful acceptance in the Department of Law and Personnel, delightful smile and subtle understanding.

## Marija Gutauskienė
### *– special award for contribution to transformation*

For tremendous and versatile contribution to transformation of FTMC into a public entity, for precision, patience and encouraging spirit.

## Arvydas Eugenijus Janulaitis
### *– FTMC Patronage award*

For generosity, sincere support and essential contribution in development of Optical Coherence Tomography Laboratory.

# Doctoral theses

**VIDMANTAS TOMKUS**

Microstructural and optical properties of metal oxide optical coatings deposited by ion beam sputtering and their application in UV spectral range. (T008)

*Scientific supervisor: dr. K. Regelskis*

**POVILAS ŠIMONIS**

Microstructural and optical properties of metal oxide optical coatings deposited by ion beam sputtering and their application in UV spectral range. (N003)

*Scientific supervisor: dr. A. Stirkė*

**ANDRIUS SAKAVIČIUS**

Dependence of the properties of the nanometer-thin layered structures containing graphene on the layout and the ambient conditions. (T008)

*Scientific supervisor: dr. A. Šetkus*

**TADAS BARTULEVIČIUS**

Compact high pulse energy fiber laser systems for industrial and scientific applications. (N 002)

*Scientific supervisor: dr. A. Michailovas*

**LINA GRINEVIČIŪTĖ**

Nanostructured optical coatings for the manipulation of laser radiation. (T008)

*Scientific supervisor: dr. R. Drazdys*

**VILIUS VERTELIS**

Magnetic field diffusion in metallic and superconducting cylinders, (N 002).

*Scientific supervisor: prof. habil.dr. S. Balevičius*

**EDITA SODAITIENĖ**

Removal of anionic and cationic pollutants by groundwater water treatment waste. (N003)

*Scientific supervisor: dr. A. Gefenienė*

**VAKARIS RUDOKAS**

Magnetoresistive properties of nanostructured manganite-cobaltite films (N 002)

*Scientific supervisor: prof. dr. N. Žurauskienė*

**MINDAUGAS KAMARAUSKAS**

Intentional modification of silicon photovoltaic devices by deep surface structuring and two dimensional material coatings. (T008)

*Scientific supervisor: dr. A. Šetkus*

**LUKAS RAZINKOVAS**

Vibrational properties and photoionization of color centers in diamond: theory and *ab initio* calculations. (N 002)

*Scientific supervisor: prof., dr. A. Alkauskas*

**KAROLIS MADEIKIS**

Investigation of the ultrafast fiber and hybrid laser systems and their nonlinear wavelength conversion methods in the infrared spectral region. (N 002)

*Scientific supervisor: dr. A. Michailovas*

**ALINA LEŠČINSKAITĖ**

Stellar populations in the dwarf irregular galaxy Leo A. (N 002)

*Scientific supervisor: prof. dr. V. Vansevičius*

**LAURYNAS VESELIS**

High energy hybrid femtosecond lasers based on Yb doped fibers and YAG crystals. (N 002)

*Scientific supervisor: dr. A. Michailovas*

**GIEDRIUS SINKEVIČIUS**

Research of piezoelectric ringing supperssion in pockels cells. (T001)

*Scientific supervisor: prof. dr. A. Baškys*

**IRENA BALČIŪNAITĖ**

Characterization of natural silicate gar-nets by means of non-destructive testing methods. (N003)

*Scientific supervisor: prof. habil. dr. E. Norkus*

# Publications

## with FTMC affiliations in 2021 in the top quartiles (Q1-O4) journals

1. Abdelkader, M.; Noman, M.T.; Amor, N.; Petru, M.; Mahmood, A. Combined use of modal analysis and machine learning for materials classification // *Materials*. ISSN 1996-1944. 2021, vol. 14, iss. 15, art. no. 4270, p. 1-15.
2. Adamov, R.B.; Pashnev, D.; Shalygin, V.A.; Moldavskaya, M.D.; Vinnichenko, M.Y.; Janonis, V.; Jorudas, J.; Tumėnas, S.; Prystawko, P.; Krysko, M.; Sakowicz, M.; Kašalynas, I. Optical performance of two dimensional electron Gas and GaN:C buffer layers in AlGaN/AlN/GaN heterostructures on SiC substrate // *Applied sciences*. eISSN 2076-3417. 2021, vol. 11, iss. 13, art. no. 6053, p. 1-14.
3. Adomaitienė, E.; Ašmontas, S.; Bumelienė, S.; Tamaševičius, A. V. Controllability of the unijunction transistor based integrate-and-fire electronic spiking neuron // *AEÜ - International journal of electronics and communications*. ISSN 1434-8411. 2021, vol. 133, art. no. 153666, p. 1-8.
4. Adomavičiūtė-Grabusovė, S.; Ramanavičius, S.; Popov, A.; Šablinskas, V.; Gogotsi O.; Ramanavičius, A. Selective enhancement of SERS spectral bands of salicylic acid adsorbate on 2D Ti3C2Tx-based MXene film // *Chemosensors*. ISSN 2227-9040. 2021, vol. 9, art. no. 223, p. 1-18.
5. Anbinderis, M.; Ašmontas, S.; Čerškus, A.; Gradauskas, J.; Lučun, A.; Šilėnas, A.; Sužiedėlis, A. Sensitive planar microwave diode on the base of ternary AlxGa1-xAs semiconductor compound// *Sensors*. ISSN 1424-8220. 2021, vol. 21, 13, art. no. 4487, p.1-17.
6. Andriukonis, E.; Celiešiūtė-Germanienė, R.; Ramanavičius, S.; Viter, R.; Ramanavičius, A. From microorganism-based amperometric biosensors towards microbial fuel cells // *Sensors*. eISSN 1424-8220. 2021, vol. 21, no. 7, art. no. 2442, p. 1-23.
7. Ardaravičius, L.; Kiprijanovič, O.; Alsalman, H.; Young Kwak, J. Self-heating controlled current–voltage and noise characteristics in grapheme // *Journal of physics D: Applied physics*. ISSN 0022-3727. 2021, vol. 54, iss. 18, art. no. 185101, p. 1-8.
8. Asadauskas, S.; Stalnionis, G.; Bikulčius, G.; Jankauskas, S.; Staišiūnas, L.; Matijošius, T. Nanoscale deposition of group IVB elements on anodized surfaces to reduce friction // *Materials today communications*. ISSN 2352-4928. 2021, vol. 29, art. no. 103008, p. 1-12.
9. Astrauskas, I.; Považay, B.; Baltuška, A.; Pugžlys, A. Influence of 2.09-µm pulse duration on through-silicon laser ablation of thin metal coatings // *Optics and laser technology*. ISSN 0030-3992. 2021, vol. 133, art. no. 106535, p. 1-6.
10. Ašmontas, S.; Čerškus, A.; Gradauskas, J.; Grigucevičienė, A.; Leinartas, K.; Lučun, A.; Petrauskas, K.; Selskis, A.; Sužiedėlis, A.; Širmulis, E.; Juškėnas, R. Cesium-containing triple cation perovskite solar cells // *Coatings*. eISSN 2079-6412. 2021, vol. 11, iss. 3, art. no. 279, p. 1-12.
11. Auksorius, E.; Borycki, D.; Wojtkowski, M. Multimode fiber enables control of spatial coherence in Fourier-domain full-field optical coherence tomography for in vivo corneal imaging // *Optics letters*. ISSN 0146-9592. 2021, vol. 46, no. 6, p. 1413-1416.
12. Auksorius, E. Fourier-domain full-field optical coherence tomography with real-time axial imaging // *Optics letters*. ISSN 0146-9592. 2021, vol. 46, no. 18, p. 4478-4481.
13. Badokas, K.; Kadys, A.; Mickevičius, J.; Ignatjev, I.; Skapas, M.; Stanionytė, S.; Radiunas, E.; Juška, Giedrius; Malinauskas, Tadas. Remote epitaxy of GaN via graphene on GaN/sapphire templates // *Journal of physics D: applied physics*. ISSN 0022-3727. 2021, vol. 54, iss. 20, art. no. 205103, p. 1-8.
14. Balčiauskas, L.; Skipitytė, R.; Garbaras, A.; Stirkė, V.; Balciauskiene, L.; Remeikis, V. Isotopic niche of syntopic granivores in commercial orchards and meadows // *Animals*. ISSN 2076-2615. 2021, vol. 11, iss. 8, art. no. 2375, p. 1-13.
15. Balčiauskas, L.; Skipitytė, R.; Garbaras, A.; Stirkė, V.; Balčiauskienė, L.; Remeikis, V. Stable isotopes reveal the dominant species to have thewidest trophic niche of three syntopic Microtus voles // *Animals*. ISSN 2076-2615. 2021, vol. 11, iss. 6, art. no. 1814, p. 1-14.
16. Balčiauskas, L.; Balčiauskienė, L.; Garbaras, A.; Stirkė, V. Diversity and diet differences of small mammals in commensal habitats // *Diversity*. ISSN 1424-2818. 2021, vol. 13, iss. 8, art. no. 346, p. 1-13.
17. Balčiūnaitė, A.; Sukackienė, Z.; Antanavičiūtė, K.; Vaičiūnienė, J.; Naujokaitis, A.; Tamašauskaitė-Tamašiūnaitė, L.; Norkus, E. Investigation of hydrogen generation from sodium borohydride using different cobalt catalysts // *International journal of hydrogen energy*. ISSN 0360-3199. 2021, vol. 46, iss. 2, p. 1989-1996.
18. Balčiūnaitė, A.; Zabielaitė, A.; Upskuvienė, D.; Tamašauskaitė-Tamašiūnaitė, L.; Stalnionienė, I.; Naruškevičius, L.; Vaičiūnienė, J.; Selskis, A.; Juškėnas, R.; Norkus, E. Platinum nanoparticles modified copper/titanium electrodes as electrocatalysts for borohydride oxidation // *Materials*. eISSN 1996-1944. 2021, vol. 14, iss. 24, art. no. 7663, p. 1-15.
19. Balčiūnaitė, I.; Ignatjev, I.; Kaminskas, D.; Niaura, G.; Norkus, E. Characterization of natural silicate garnets by means of non-destructive testing methods // *Chemija*. ISSN 0235-7216. 2021, vol. 32, no. 3-4, p. 107-126.
20. Baltrukonis, J.; Ulčinas, O.; Orlovas, S.; Jukna, V. High-order vector Bessel-Gauss beams for laser micromachining of transparent materials // *Physical review applied*. ISSN 2331-7019. 2021, vol. 16, no. 3, art. no. 034001, p. 1-6.
21. Barisevičiūtė, R.; Maceika, E.; Juodis, L.; Pabedinskas, A.; Šapolaitė, J.; Ežerinskis, Ž.; Butkus, L.; Remeikis, V. Modeling of 14C vertical distribution in bottom sediments of the Ignalina nuclear power plant cooling reservoir // *Water*. eISSN 2073-4441. 2021, vol. 13, iss. 10, art. no. 1397, p. 1-15.
22. Barkauskas, J.; Gaidukevič, J.; Niaura, G. Thermal reduction of graphite oxide in the presence of nitrogen-containing dyes // *Carbon letters*. ISSN 1976-4251. 2021, vol. 31, iss. 6, p. 1097-1110.
23. Belosludtsev, A.; Buinovskis, D. Significant increase of UV reflectivity of SiC galvanometer mirror scanners for the high-power laser applications // *Optics and laser technology*. ISSN 0030-3992. 2021, vol. 140, art. no. 107027, p. 1-6.
24. Belosludtsev, A.; Bitinaitis, I.; Baltrušaitis, K.; Rodin, A. Investigation of the laser cleaning process for IBS grids in optical coating technology // *The international journal of advanced manufacturing technology*. ISSN 0268-3768. 2021, vol. 114, iss. 9-10, p. 2863-2869.
25. Bieliūnas, V.; Stončius, S. Fine-tuning the bicyclo [3.3.1] nona-2,6-diene ligands:second generation 4,8-substituted dienes for Rh-catalyzed asymmetric 1,4-addition reactions // *ChemCatChem*. ISSN 1867-3880. 2021, vol. 13, iss. 17, p. 3815-3823.
26. Bliujienė, A.; Peseckas, K.; Šapolaitė, J.; Ežerinskis, Ž.; Bagdzevičienė, J.; Babenskas, E.; Taraškevičius, R.; Suzdalev, S.;

Vybernaitė-Lubienė, I.; Pabedinskas, A.; Butkus, L.; Petrauskas, G. Manufacture of the well-known Central and Northeastern European eye fibulae: previously unknown tricks of the trade // *Radiocarbon*. ISSN 0033-8222. 2021, vol. 63, no. 5, p. 1369-1386.

27. Bočkuvienė, A.; Žalnėravičius, R.; Sereikaitė, J. Preparation, characterization and stability investigation of lycopene-chitooligosaccharides complexes // *Food bioscience*. ISSN 2212-4292. 2021, vol. 40, art. no. 100854, p. 1-9.

28. Bogužaitė, R.; Ratautaitė, V.; Mikoliūnaitė, L.; Pudžaitis, V.; Ramanavičienė, A.; Ramanavičius, A. Towards analytical application of electrochromic polypyrrole layers modified by phenothiazine derivatives // *Journal of electroanalytical chemistry*. ISSN 1572-6657. 2021, vol. 886, art. 115132, p. 1-10.

29. Braver, J.; Valkūnas, L.; Gelžinis, A. Quantum–classical approach for calculations of absorption and fluorescence: principles and applications // *Journal of chemical theory and computation*. ISSN 1549-9618. 2021, vol. 17, iss. 11, p. 7157-7168.

30. Braver, J.; Valkūnas, L.; Gelžinis, A. Stark absorption and Stark fluorescence spectroscopies: Theory and simulations // *Journal of chemical physics*. ISSN 0021-9606. 2021, vol. 155, iss. 24, art. no. 244101, p. 1-16.

31. Braver, J.; Valkūnas, L.; Gelžinis, A. Derivation of the stationary fluorescence spectrum formula for molecular systems from the perspective of quantum electrodynamics // *Lithuanian journal of physics*. ISSN 1648-8504. 2021, vol. 61, no. 2, p. 110-123.

32. Būdienė, J.; Guclu, G.; Oussou, K. F.; Kelebek, H.; Selli, S. Elucidation of volatiles, anthocyanins, antioxidant and sensory properties of cv. Caner pomegranate (Punica granatum L.) juices produced from three juice extraction methods // *Foods*. ISSN 2304-8158. 2021, vol. 10, iss. 7, art. no. 1497, p. 1-14.

33. Bužavaitė-Vertelienė, E.; Vertelis, V.; Balevičius, Z. The experimental evidence of a strong coupling regime in the hybrid Tamm plasmon-surface plasmon polariton mode // *Nanophotonics*. ISSN 2192-8606. 2021, vol. 10, iss. 5, p. 1565-1571.

34. Chernyakova, K.; Vrublevsky, I.; Jagminas, A.; Klimas, V. Effect of anodic oxygen evolution on cell morphology of sulfuric acid anodic alumina film // *Journal of solid state electrochemistry*. ISSN 1432-8488. 2021, vol. 25, iss. 4, p. 1453-1460.

35. Chmeliov, J.; Elkhouly, K.; Gegevičius, R.; Jonušis, L.; Devižis, A.; Gelžinis, A.; Franckevičius, M.; Goldberg, I.; Hofkens, J.; Heremans, P.; Qiu, W.; Gulbinas, V. Ion motion determines multiphase performance dynamics of perovskite LEDs // *Advanced optical materials*. ISSN 2195-1071. 2021, vol. 9, iss. 24, art. no. 2101560, p. 1-12.

36. Cuesta-Mosquera, A.; Močnik, G.; Drinovec, L.; Müller, T.; Pfeifer, S.; Cruz Minguillón, M.; Briel, B.; Buckley, P.; Dudoitis, V.; Fernández-García, J.; Fernández-Amado, M.; Ferreira De Brito, J.; Riffault, V.; Flentje, H.; Heffernan, E.; Kalivitis, N.; Kalogridis, A.C.; Keernik, H.; Marmureanu, L.; Luoma, K.; Marinoni, A.; Pikridas, M.; Schauer, G.; Serfozo, N.; Servomaa, H.; Titos, G.; Yus-Díez, J.; Zioła, N.; Wiedensohler, A. Intercomparison and characterization of 23 Aethalometers under laboratory and ambient air conditions: procedures and unit-to-unit variabilities // *Atmospheric measurement techniques*. ISSN 1867-1381. 2021, vol. 14, iss. 4, p. 3195-3216.

37. Dansette, P.M.; Eremchev, M.; Michailovas, A. Continuous compensation of the phase mismatch by using temperature gradients for second harmonic generation // *Optics communications*. ISSN 0030-4018. 2021, vol. 484, art. no. 126687, p. 1-8.

38. Daublytė, E.; Zdaniauskienė, A.; Talaikis, M.; Drabavičius, A.; Charkova, T. A facile microwave-assisted synthesis of Ag@$SiO_2$ nanoparticles for Raman spectroscopy // *New journal of chemistry*. ISSN 1144-0546. 2021, vol. 45, iss. 24, p. 10952-10958.

39. Davulienė, L.; Jasinevičienė, D.; Garbarienė, I.; Andriejauskienė, J.; Ulevičius, V.; Byčenkienė, S. Long-term air pollution trend analysis in the South-eastern Baltic region, 1981–2017 // *Atmospheric research*. ISSN 0169-8095. 2021, vol. 247, art. no. 105191, p. 1-14.

40. Deveikis, L.; Vaitkus, J.V.; Čeponis, T.; Gaspariūnas, M.; Kovalevskij, V.; Rumbauskas, V.; Gaubas, E. Profiling of proton beams by fluence scanners // *Lithuanian journal of physics*. ISSN 1648-8504. 2021, vol. 61, no. 2, p. 75-83.

41. Devenson, J.; Norkus, R.; Juškėnas, R.; Krotkus, A. Terahertz emission from ultrathin bismuth layers // *Optics letters*. ISSN 0146-9592. 2021, vol. 46, no. 15, p. 3681-3684.

42. Devižis, A.; Gelžinis, A.; Chmeliov, J.; Diethelm, M.; Endriukaitis, L.; Padula, D.; Hany, R. Carrier tunneling from charge transfer states in organic photovoltaic cells // *Advanced functional materials*. ISSN 1616-301X. 2021, vol. 31, iss. 29, art. no. 2102000, p. 1-8.

43. Diliautas, R.; Beganskienė, A.; Karoblis, D.; Mažeika, K.; Baltrūnas, D. A.; Žarkov, A.; Raudonis, R.; Kareiva, A. Reinspection of formation of BiFe1-xMnxO3 solid solutions via low temperature sol-gel synthesis route // *Solid state sciences*. ISSN 1293-2558. 2021, vol. 111, no. 106458, p. 1-6.

44. Dilys, J.; Stankevič, V.; Łuksza, K. Implementation of extended kalman filter with optimized execution time for sensorless control of a PMSM using ARM cortex-M3 microcontroller // *Energies*. ISSN 1996-1073. 2021, vol. 14, iss. 12, no. 3491, p. 1-16.

45. Dobrovolskas, D.; Kadys, A.; Usikov, A.; Malinauskas, T.; Badokas, K.; Ignatjev, I.; Lebedev, S.; Lebedev, A.; Makarov, Y.; Tamulaitis, G. Luminescence of structured InN deposited on graphene interlayer // *Journal of luminescence*. ISSN 0022-2313. 2021, vol. 232, art. no. 117878, p. 1-7.

46. Dovbeshko, G.; Gnatyuk, O.; Dementjev, A.; Rutkauskas, D.; Kovalska, E.; Baldycheva, A.; Ilchenko, O.; Krasnenkov, D.; Kaplas, T. Coherent anti-stokes Raman scattering spectroscopy (CARS) and imaging of DNA on graphene layers and glass covers // *FlatChem*. ISSN 2452-2627. 2021, vol. 27, art. no. 100243, p. 1-8.

47. Drobysh, M.; Ramanavičienė, A.; Viter, R.; Ramanavičius, A. Affinity sensors for the diagnosis of COVID-19 // *Micromachines*. eISSN 2072-666X. 2021, vol. 12, art. no. 390, p. 1-19.

48. Dronina, J.; Samukaitė-Bubnienė, U.; Ramanavičius, A. The application of DNA polymerases and Cas9 as representative of DNA-modifying enzymes group in DNA sensor design (review) // *Biosensors and bioelectronics*. ISSN 0956-5663. 2021, vol. 175, art. no. 112867, p. 1-11.

49. Dronina, J.; Samukaitė-Bubnienė, U.; Ramanavičius, A. Advances and insights in the diagnosis of viral infections // *Journal of nanobiotechnology*. eISSN 1477-3155. 2021, vol. 19, no. 348, p. 1-23.

50. Dubois, J.L.; Couturier, J.L.; Asadauskas, S.; Labanauskas, L.; Bražinskienė, D.; Blaauw, R. Conversion of fatty acid methyl esters into dibasic esters by metathesis and their lubricant properties // *RSC advances*. eISSN 2046-2069. 2021, vol. 11, iss. 49, p. 31030-31041.

51. Dudutienė, E.; Jasinskas, A.; Čechavičius, B.; Nedzinskas, R.; Jokubauskaitė, M.; Bičiūnas, A.; Bukauskas, V.; Valušis, G.; Butkutė, R. Photoluminescence properties of GaAsBi single quantum wells with 10% of Bi // *Lithuanian journal of physics*. ISSN 1648-8504. 2021, vol. 61, no. 2, p. 142-150.

52. Emir, G.; Dilgin, Y.; Ramanavičienė, A.; Ramanavičius, A. Amperometric nonenzymatic glucose biosensor based on graphite rod electrode modified by Ni-nanoparticle/polypyrrole composite // *Microchemical journal*. ISSN 0026-265X. 2021, vol. 161, art. no. 105751, p. 1-12.

53. Fakharuddin, A.; Franckevičius, M.; Devižis, A.; Gelžinis, A.; Chmeliov, J.; Heremans, P.; Gulbinas, V. Double charge transfer dominates in carrier localization in low bandgap sites of heterogeneous lead halide perovskites // *Advanced functional materials*. ISSN 1616-301X. 2021, vol. 31, iss. 15, art. no. 2010076, p. 1-9.

54. Fujiwara, E.; Orita, R.; Vyšniauskas, A.; Franckevičius, M.; Ishige, R.; Gulbinas, V.; Ando, S. Ultrafast spectroscopic analysis of pressure-induced variations of excited-state energy and intramolecular proton transfer in semi-aliphatic polyimide films // *The journal of physical chemistry B*. ISSN 1520-6106. 2021, vol. 125, iss. 9, p. 2425-2434.

55. Gaidukevič, J.; Aukštakojytė, R.; Navickas, T.; Pauliukaitė, R.; Barkauskas, J. A novel approach to prepare highly oxidized graphene oxide: structural and electrochemical investigations // *Applied surface science.* ISSN 0169-4332. 2021, vol. 567, art. no. 150883, p. 1-12.

56. Garbarienė, I.; Dudoitis, V.; Ulevičius, V.; Plauškaitė-Šukienė, K.; Kilikevičius, A.; Matijošius, J.; Rimkus, A.; Kilikevičienė, K.; Vainorius, D.; Maknickas, A.; Borodinas, S.; Byčenkienė, S. Application of acoustic agglomeration technology to improve the removal of submicron particles from vehicle exhaust // *Symmetry*. ISSN 2073-8994. 2021, vol. 13, iss. 7, no. 1200, p. 1-15.

57. Gedvilas, M.; Stankevič, V.; Račiukaitis, G. The behaviour of sapphire under intense two-colour excitation by picosecond laser // *Lithuanian journal of physics*. ISSN 1648-8504. 2021, vol. 61, no. 2, p. 124-141.

58. Gegevičius, R.; Franckevičius, M.; Gulbinas, V. The role of grain boundaries in charge carrier dynamics in polycrystalline metal halide perovskites // *European journal of inorganic chemistry*. ISSN 1434-1948. 2021, vol. 2021, no 35, p. 3519-3527.

59. Gelžinis, A.; Augulis, R.; Büchel, C.; Robert, B.; Valkūnas, L. Confronting FCP structure with ultrafast spectroscopy data: evidence for structural variations // *Physical chemistry chemical physics*. ISSN 1463-9076. 2021, vol. 23, iss. 2, p. 806-821.

60. German, N.; Ramanavičienė, A.; Ramanavičius, A. Dispersed conducting polymer nanocomposites with glucose oxidase and gold nanoparticles for the design of enzymatic glucose biosensors // *Polymers*. ISSN 2073-4360. 2021, vol. 13, iss. 13, art. no. 2173, p. 1-16.

61. Gollner, C.; Shalaby, M.; Brodeur, C.; Astrauskas, I.; Jutas, R.; Constable, E.; Bergen, L.; Baltuška, A.; Pugžlys, A. Highly efficient THz generation by optical rectification of mid-IR pulses in DAST // *APL photonics*. ISSN 2378-0967. 2021, vol. 6, iss. 4, art. no. 046105, p. 1-6.

62. Golovinas, E.; Rutkauskas, D.; Manakova, E.; Jankunec, M.; Šilanskas, A.; Sasnauskas, G.; Zaremba, M. Prokaryotic Argonaute from Archaeoglobus fulgidus interacts with DNA as a homodimer // *Scientific reports*. ISSN 2045-2322. 2021, vol. 11, art. no. 4518, p. 1-14.

63. Golubewa, L.; Kulahava, T.; Timoshchenko, I.; Shuba, M.; Svirko, Y.; Kuzhir, P. Rapid and delayed effects of single-walled carbon nanotubes in glioma cells // *Nanotechnology*. ISSN 0957-4484. 2021, vol. 32, iss. 50, art. no. 505103, p. 1-11.

64. Gorokhova, E.; El-Shehawy, R.; Lehtiniemi, M.; Garbaras, A. How copepods can eat toxins without getting sick: gut bacteria help zooplankton to feed in cyanobacteria blooms // *Frontiers in microbiology*. eISSN 1664-302X. 2021, vol. 11, art. no. 589816, p. 1-11.

65. Gotovski, P.; Šlevas, P.; Orlovas, S.; Ulčinas, O.; Urbas, A. Generation of an optical needle beam with a laser inscribed Pancharatnam-Berry phase element under imperfect conditions // *Optics express*. ISSN 1094-4087. 2021, vol. 29, iss. 21, p. 33331-33345.

66. Gradauskas, J.; Ašmontas, S. Hot carrier photocurrent through MOS structure //*Applied sciences*. ISSN 2076-3417. 2021, vol. 11, iss. 16, art. no. 7211, p. 1-7.

67. Gradauskas, J.; Dzundza, B.; Chernyak, L.; Dashevsky, Z. Two-color infrared sensor on the PbTe: In p-n junction // *Sensors*. ISSN 1424-8220. 2021, vol. 21, iss. 4, art. no. 1195, p. 1-9.

68. Grybauskaitė-Kaminskienė, G.; Dudkaitė, V.; Bagdžiūnas, G. Photophysical and semiconducting properties of isomeric triphenylimidazole derivatives with a benzophenone moiety // *New journal of chemistry*. ISSN 1144-0546. 2021, vol. 45, iss. 42, p. 19746-19754.

69. Gric, T.; Rafailov, E.U. Non local efects in cone-shaped metamaterials // *Optical and quantum electronics*. ISSN 0306-8919. 2021, vol. 53, art. no. 301, p. 1-8.

70. Gric, T.; Rafailov, E. Absorption enhancement in hyperbolic metamaterials by means of magnetic plasma // *Applied sciences*. eISSN 2076-3417. 2021, vol. 11, iss. 11, art. no. 4720, p. 1-7.

71. Gric, T.; Sokolovski, S. G.; Alekseev, A. G.; Mamoshin, A.; Andrey, D.; Rafailov, E. U. The discrete analysis of the tissue biopsy images with metamaterial formalization: identifying tumour locus // *IEEE journal of selected topics in quantum electronics*. ISSN 1077-260X. 2021, vol. 27, iss. 5, art. no. 4700608, p. 1-8.

72. Griesiūtė, D.; Karoblis, D.; Mikoliūnaitė, L.; Žarkov, A.; Salak, A. N.; Kareiva, A. Chemical solution deposition of La-substituted BiFe0.5Sc0.5O3 perovskite thin films on different substrates // *Coatings*. eISSN 2079-6412. 2021, vol. 11, no. 3, art. no. 307, p. 1-11.

73. Griesiūtė, D.; Sinušaitė, L.; Kizalaitė, A.; Antuzevics, A.; Mažeika, K.; Baltrūnas, D. A.; Tomoyo, G.; Sekino, T.; Kareiva, A.; Žarkov, A. The influence of Fe3+ doping on thermally induced crystallization and phase evolution of amorphous calcium phosphate // *CrystEngComm*. eISSN 1466-8033. 2021, vol. 23, iss. 26, p. 4627-4637.

74. Grinevičiūtė, L.; Nikitina, J.; Babayigit, C.; Staliūnas, K. Fano-like resonances in nanostructured thin films for spatial filtering // *Applied physics letters*. ISSN 0003-6951. 2021, vol. 118, no. 13, art. n. 131114, p. 1-5.

75. Grinevičiūtė, L.; Ramalis, L.; Buzelis, R.; Tolenis, T. Highly resistant all-silica polarizing coatings for normal incidence applications // Optics letters. ISSN 0146-9592. 2021, vol. 46, no. 4, p. 916-919.

76. Grinevičiūtė, L.; Babayigit, C.; Gailevičius, D.; Peckus, M.; Turduev, M.; Tolenis, T.; Vengris, M.; Kurt, H.; Staliūnas, K. Nanostructured multilayer coatings for spatial filtering // *Advanced optical materials*. ISSN 2195-1071. 2021, vol. 9, iss. 9, art. no. 2001730, p. 1-7.

77. Grinevičiūtė, L.; Badorreck, H.; Jensen, L.; Ristau, D.; Jupé, M.; Selskis, A.; Tolenis, T. Impact of deposition conditions on nanostructured anisotropic silica thin films in multilayer interference coatings // *Applied surface science*. ISSN 0169-4332. 2021, vol. 562, art. no. 150167, p. 1-8.

78. Gudelis, A.; Gaigalaitė, L. A preparedness study: efficiency calibration and performance testing of LSC cocktails for determination of tritium in river-water samples as an indicator of the technological start of a new NPP // *Journal of radioanalytical and nuclear chemistry*. ISSN 0236-5731. 2021, vol. 328, p. 471-480.

79. Ibenskas, A.; Tornau, E. Modeling of high-temperature ordered structures with weak intermolecular C–H·F and C–H·N bonds // *Journal of physical chemistry C*. ISSN 1932-7447. 2021, vol. 125, iss. 35, p. 19560-19569.

80. Ibenskas, A.; Šimėnas, M.; Tornau, E. Modeling the dimeric structure of partly deprotonated trimesic acid molecules // *Journal of physical chemistry C*. ISSN 1932-7447. 2021, vol. 125, iss. 13, p. 7466-7475.

81. Indrišiūnas, S.; Svirplys, E.; Jorudas, J.; Kašalynas, I. Laser processing of transparent wafers with a AlGaN/GaN heterostructures and high-electron mobility devices on a backside // *Micromachines*. ISSN 2072-666X. 2021, vol. 12, iss. 4, art. no. 407, p. 1-12.

82. Ioannidis, A.; Gric, T.; Rafailov, E. Controlling surface plasmon polaritons propagating at the boundary of low-dimensional acoustic metamaterials // *Applied sciences*. ISSN 2076-3417. 2021, vol. 11, iss. 14, art. no. 6302, p. 1-8.

83. Ioannidis, A.; Gric, T.; Rafailov, E. The study of the surface plasmon polaritons at the interface separating nanocomposite and hypercrystal // *Applied sciences*. ISSN 2076-3417. 2021, vol. 11, iss. 11, art. no. 5255, p. 1-13.

84. Ioannidis, A.; Gric, T.; Rafailov, E. Looking into surface plasmon polaritons guided by the acoustic metamaterials // *Plasmonics*. ISSN 1557-1955. 2021, vol. 16, iss. 2, p. 1835-1839.

85. Jablonskienė, J.; Šimkūnaitė, D.; Vaičiūnienė, J.; Stalnionis, G.; Drabavičius, A.; Jasulaitienė, V.; Pakštas, V.; Tamašauskaitė-Tamašiūnaitė, L.; Norkus, E. Synthesis of carbon-supported

$MnO_2$ nanocomposites for supercapacitors application // *Crystals*. eISSN 2073-4352. 2021, vol. 11, no. 7, no. 784, p. 1-14.

86. Jagminas, A.; Gaigalas, P.; Bittencourt, C.; Klimas, V. Cysteine-induced hybridization of 2D molybdenum disulfide films for efficient and stable hydrogen evolution reaction // *Materials*. ISSN 1996-1944. 2021, vol. 14, iss. 5, art. no.1165, p. 1-12.

87. Janonis, V.; Balagula, R.; Grigelionis, I.; Prystawko, P.; Kašalynas, I. Spatial coherence of hybrid surface plasmon-phonon-polaritons in shallow n-GaN surface-relief gratings // *Optics express*. ISSN 1094-4087. 2021, vol. 29, iss. 9, p. 13839-13851.

88. Januškevičius, J.; Stankevičiūtė, Ž.; Baltrūnas, D. A.; Mažeika, K.; Beganskienė, A.; Kareiva, A. Aqueous sol-gel synthesis of different iron ferrites: from 3D to 2D // *Materials*. eISSN 1996-1944. 2021, vol. 14, art. no. 1554, p. 1-12.

89. Javorskis, T.; Rakickas, T.; Jankūnaitė, A.; Talaikis, M.; Niaura, G.; Ulčinas, A.; Orentas, E. Meso-scale surface patterning of self-assembled monolayers with water // *Colloids and surfaces A: physicochemical and engineering aspects*. ISSN 0927-7757. 2021, vol. 628, art. no. 127353, p. 1-7.

90. Javorskis, T.; Jurys, A.; Bagdžiūnas, G.; Orentas, E. Synthesis of C - and N-substituted 1,5,2,6-dithiadiazocanes – electrophilic-nucleophilic thioamination (ENTA) reagents // *Advanced synthesis and catalysis*. ISSN 1615-4150. 2021, vol. 363, no. 13, p. 3329-3335.

91. Jelmakas, E.; Kadys, A.; Dmukauskas, M.; Grinys, T.; Tomašiūnas, R.; Dobrovolskas, D.; Gervinskas, G.; Juodkazis, S.; Talaikis, M.; Niaura, G. FIB micro-milled sapphire for GaN maskless epitaxial lateral overgrowth: a systematic study on patterning geometry // *Journal of materials science: materials in electronics*. ISSN 0957-4522. 2021, vol. 32, iss. 11, p. 14532-14541.

92. Judžentienė, A.; Būdienė, J. Mugwort (Artemisia vulgaris L.) essential oils rich in germacrene D, and their toxic activity // *Journal of essential oil research*. ISSN 1041-2905. 2021, vol. 33, iss. 3, p. 256-264.

93. Juknelevičius, D.; Webb, R.; Klapotke, T.; Ramanavičius, A. Low-perchlorate blue-flame pyrotechnic compositions // *Zeitschrift fur naturforschung. Section B*. eISSN 1865-7117. 2021, vol. 76, no. 9, p. 489-494.

94. Juodkazytė, J.; Juodkazis, K.J.; Juodkazis, S. Atoms vs. ions: intermediates in reversible electrochemical hydrogen evolution reaction // *Catalysts*. ISSN 2073-4344. 2021, vol. 11, iss. 9, art. no. 1135, p. 1-12.

95. Juškėnas, R.; Balakauskas, S.; Mockus, Z.; Kanapeckaitė, S.; Kalinauskas, P.; Stalnionis, G.; Naujokaitis, A.; Selskis, A.; Šetkus, A.; Niaura, G. Impact of sulfurization procedure parameters on photoelectrochemical, compositional and structural features of kesterite // *Materials science & engineering B.* ISSN 0921-5107. 2021, vol. 274, art. n. 115483, p. 1-7.

96. Kaare, K.; Yu, E.; Käämbre, T.; Volperts, A.; Dobele, G.; Zhurinsh, A.; Niaura, G.; Tamašauskaitė-Tamašiūnaitė, L.; Norkus, E.; Kruusenberg, I. Biomass-derived graphene-like catalyst material for oxygen reduction reaction // *ChemNanoMat.* ISSN 2199-692X. 2021, vol. 7, iss. 3, p. 307-313.

97. Karaliūnas, M.; Dudutienė, E.; Čerškus, A.; Pagalys, J.; Pūkienė, S.; Udal, A.; Butkutė, R.; Valušis, G. High precision parabolic quantum wells grown using pulsed analog alloy grading technique: Photoluminescence probing and fractional-dimensional space approach // *Journal of luminescence*. ISSN 0022-2313. 2021, vol. 239, art.no. 118321, p. 1-7.

98. Karoblis, D.; Diliautas, R.; Mažeika, K.; Baltrūnas, D.A.; Niaura, G.; Talaikis, M.; Beganskienė, A.; Žarkov, A.; Kareiva, A. Lanthanum and manganese Co-doping effects on structural, morphological, and magnetic properties of sol-gel derived BiFeO3 // *Materials.* ISSN 1996-1944. 2021, vol. 14, iss. 17, art. no. 4844, p. 1-12.

99. Karoblis, D.; Žarkov, A.; Mažeika, K.; Baltrūnas, D.A.; Niaura, G.; Beganskienė, A.; Kareiva, A. YFeO3-GdFeO3 solid solutions: Sol-gel synthesis, structural and magnetic properties // *Solid state sciences*. ISSN 1293-2558.2021, vol. 118, art. no. 106632, p. 1-8.

100. Karoblis, D.; Žarkov, A.; Garškaitė, E.; Mažeika, K.; Baltrūnas, D.A.; Niaura, G.; Beganskienė, A.; Kareiva, A. Study of gadolinium substitution effects in hexagonal yttrium manganite $YMnO_3$ // *Scientific reports*. eISSN 2045-2322. 2021, vol. 11, art. no. 2875, p. 1-14.

101. Karpič, R.; Ostapenko, N.; Ostapenko, Y.; Polupan, Y.; Lazarev, I.; Galunov, N.; Mačernis, M.; Abramavičius, D.; Valkūnas, L. Unusual temperature dependence of the fluorescence decay in heterostructured stilbene // *Physical chemistry chemical physics*. ISSN 1463-9076. 2021, vol. 23, iss. 5, p. 3447-3454.

102. Karpinsky, D.V.; Silibin, M.V.; Zhaludkevich, D.V.; Latushka, S.I.; Sysa, A.V.; Sikolenko, V.V.; Zhaludkevich, A.L.; Khomchenko, V.A.; Franz, A.; Mažeika, K.; Baltrūnas, D.A.; Kareiva, A. Magnetic properties of $BiFeO_3$ – $BaTiO_3$ ceramics in the morphotropic phase boundary: A role of crystal structure and structural parameters // *Journal of magnetism and magnetic materials*. ISSN 0304-8853. 2021, vol. 539, art. no. 168409, p. 1-7.

103. Karpus, V.; Čechavičius, B.; Tumėnas, S.; Stanionytė, S.; Butkutė, R.; Skapas, M.; Paulauskas, T. Optical anisotropy of CuPt-ordered GaAsBi alloys // *Journal of physics D: applied physics*. ISSN 0022-3727. 2021, vol. 54, iss. 50, art. no. 504001, p. 1-8.

104. Kasparavicius, E.; Franckevičius, M.; Malinauskiene, V.; Genevičius, K.; Getautis, V.; Malinauskas, T. Oxidized spiro-OMeTAD: investigation of stability in contact with various perovskite compositions // *ACS applied energy materials*. ISSN 2574-0962. 2021, vol. 4, iss. 12, p. 13696-13705.

105. Kavaliauskaitė, G.; Kuksėnaitė, G.; Gegevičius, R.; Pakštas, V.; Selskis, A.; Strazdienė, V.; Padarauskas, A.; Orentas, E.; Gulbinas, V.; Franckevičius, M. S-methylthiouronium improves the photostability of methylammonium lead iodide perovskites // *ACS applied energy materials*. ISSN 2574-0962. 2021, vol. 4, iss. 7, p. 6466-6473.

106. Kazakevičiūtė-Jakučiūnienė, L.; Druteikienė, R.; Maceika, E.; Lukšienė, B.; Juškėnas, R.; Pakštas, V.; Žukauskaitė, Z.; Gvozdaitė, R.; Tarasyuk, N.. Impact of soil organic matter on Pu migration in five Lithuanian surface soils // *Journal of environmental radioactivity*. ISSN 0265-931X. 2021, vol. 237, art. no. 106702, p. 1-9.

107. Khairullina, E.M.; Panov, M.S.; Andriianov, V.S.; Ratautas, K.; Tumkin, I.I.; Račiukaitis, G. High rate fabrication of copper and copper–gold electrodes by laser-induced selective electroless plating for enzyme-free glucose sensing // *RSC advances*. eISSN 2046-2069. 2021, vol. 11, iss. 32, p. 19521-19530.

108. Kiprijanovič, O.; Ardaravičius, L.; Ašmontas, S. Radiating Barkhausen-type pulses during generation of high-voltage pulse by piezoelectric igniters // *Integrated ferroelectrics*. ISSN 1058-4587.2021, vol. 220, iss. 1, p. 120-131.

109. Kiprijanovič, O.; Ardaravičius, L.; Kwak, J.Y. High-voltage carrier transport measurements in graphene and MoS2 // *Results in physics*. ISSN 2211-3797. 2021, vol. 24, art. no. 104156, p. 1-4.

110. Kirdeikienė, A.; Girčienė, O.; Gudavičiūtė, L.; Jasulaitienė, V.; Selskis, A.; Tutlienė, S.; Skruodienė, M.; Pilipavičius, J.; Juodkazytė, J.; Ramanauskas, R. Self-healing properties of cerium-modified molybdate conversion coating on steel // *Coatings*. ISSN 2079-6412. 2021, vol. 11, iss. 2, art. no. 194, p. 1-15.

111. Klimas, V.; Bittencourt, C.; Valušis, G.; Jagminas, A. Calcination effects of 2D molybdenum disulfides // *Materials characterization*. ISSN 1044-5803. 2021, vol. 179, art. n. 111351, p. 1-9.

112. Konstantinova, M.; Germanas, D.; Gudelis, A.; Plukis, A. Efficiency calibration of high-purity germanium detector using Monte Carlo simulations including coincidence-summing corrections: volume source case // *Lithuanian journal of physics*. ISSN 1648-8504. 2021, vol. 61, no. 1, p. 66-73.

113. Kopūstas, A.; Ivanovaitė, Š.; Rakickas, T.; Pocevičiūtė, E.; Paksaitė, J.; Karvelis, T.; Zaremba, M.; Manakova, E.; Tutkus, M. Oriented soft DNA curtains for single-molecule imaging // *Langmuir*. ISSN 0743-7463. 2021, vol. 37, iss. 11, p. 3428-3437.

114. Krikštaponis, A.; Urbelis, G.; Meškys, R. The first step of biodegradation of 7-hydroxycoumarin in Pseudomonas mandelii 7HK4 depends on an alcohol dehydrogenase-type

enzyme // *International journal of molecular sciences*. eISSN 1422-0067. 2021, vol. 22, no. 4, art. no. 1552, p. 1-18.

115. Kručaitė, G.; Beresnevičiūtė, R.; Tavgenienė, D.; Grigalevičius, S.; Zhang, B.; Gruodis, A.; Charniakova, K.; Karpič, R. Hole-transporting materials based on diarylfluorene compounds containing different substituents: DFT simulation, spectroscopic characterization and applications in organic light emitting diodes // *Optical materials*. ISSN 0925-3467. 2021, vol. 119, art. no. 111345, p. 1-8.

116. Kudrevičius, T.; Plyushch, A.; Ivanov, M.; Svirskas, Š.; Plaušinaitienė, V.; Selskis, A.; Kuzhir, P.; Banys, J. Aqueous tape casting of the 0.7Pb(Mg1/3Nb2/3)O-3-0.3PbTiO(3) ceramic films: Production optimization and properties // *Journal of electroceramics*. ISSN 1385-3449. 2021, vol. 46, iss. 1, p. 20-25.

117. Kumpikaitė, E.; Varnaitė-Žuravliova, S.; Tautkutė-Stankuvienė, I.; Laureckienė, G. Comparison of mechanical and end-use properties of grey and dyed cellulose and cellulose/protein woven fabrics // *Materials.* ISSN 1996-1944. 2021, vol. 14, iss.11, art. no. 2860, p. 1-19.

118. Labutytė, G.; Povilonienė, S.; Šimoliūnas, E.; Gabrielaitis, D.; Skapas, M.; Noreika, A.; Meškys, R.; Časaitė, V. Functionalized protein nanotubes based on the bacteriophage vb_klem-rak2 tail sheath protein // *Nanomaterials.* eISSN 2079-4991. 2021, vol. 11, no. 11, art. no. 3031, p. 1-14.

119. Lapinskaitė, R.; Malatinec, Š.; Mateus, M.; Rycek, L. Cross-coupling as a key step in the synthesis and structure revision of the natural products Selagibenzophenones A and B // *Catalysts*. ISSN 2073-4344. 2021, vol. 11, iss. 6, art. no. 708, p. 1-13.

120. Laurikėnas, A.; Kareiva, A. Investigation of upconversion phenomenon in Y1-xLn3+x(BTC)(DMF)2(H2O) and Y0.8-xYb0.2Ln3+x(BTC) (DMF)2(H2O) metal organic frameworks // *Chemija.* ISSN 0235-7216. 2021, vol. 32, no. 2, p. 63-72.

121. Leščinskaitė, A.; Stonkutė, R.; Vansevičius, V. AGB and RGB stars in the dwarf irregular galaxy Leo A // *Astronomy and astrophysics*. ISSN 0004-6361. 2021, vol. 647, art. no. A170, p. 1-16.

122. Li, L.; Taha Abdelhamid A., Ahmed M.; Geng, M.; Zhang, Z.; Su, H.; Xu, X.; Pan, S.; Hu, H. Ultrasound-assisted gelation of β-carotene enriched oleogels based on candelilla wax-nut oils: Physical properties and in-vitro digestion analysis // *Ultrasonics sonochemistry*. ISSN 1350-4177. 2021, vol. 79, no. 105762, p. 1-10.

123. Lyaschuk, Y.M.; Kukhtaruk, S.M.; Janonis, V.; Korotieiev, V. Modified rigorous coupled-wave analysis for grating-based plasmonic structures with a delta-thin conductive channel: far- and near-field study // Journal of the Optical Society of America A. ISSN 1084-7529. 2021, vol. 38, iss. 2, p. 157-167.

124. Liaugminas, G.; Želudevičius, J.; Regelskis, K. Fiber source of femtosecond pulses at 910–940 nm based on a Mamyshev pulse oscillator and wavelength conversion in a photonic crystal fiber // *Journal of the Optical Society of America B*. ISSN 0740-3224. 2021, vol. 38, iss. 10, p. 2920-2925.

125. Liénart, C.; Garbaras, A.; Qvarfordt, S.; Sysoev, A.Ö.; Höglander, H.; Walve, J.; Schagerström, E.; Eklöf, J.; Karlson, A.ML. Long-term changes in trophic ecology of blue mussels in a rapidly changing ecosystem // *Limnology and oceanography*. ISSN 0024-3590. 2021, vol. 66, iss. 3, p. 694-710.

126. Lymarenko, R.A.; Gailevičius, D.; Meškėlaitė, I.; Grinevičiūtė, L,; Peckus, M.; Staliūnas, K.; Taranenko, V.B. Super-collimation by axisymmetric diffractive metamirror // *Optics letters*. ISSN 0146-9592. 2021, vol. 46, iss.16, p. 3845-3848.

127. Linauskienė, K.; Dahlin, J.; Ežerinskis, Ž.; Isaksson, M.; Šapolaitė, J.; Malinauskienė, L. Occupational exposure to nickel, cobalt, and chromium in the Lithuanian hard metal industry // *Contact dermatitis*. ISSN 0105-1873. 2021, vol. 84, no. 4, p. 247-253.

128. Liu, C.; Yang, Y.; Rakstys, K.; Mahata, A.; Franckevičius, M.; Mosconi, E.; Skackauskaite, R.; Ding, B.; Brooks, K.G.; Usiobo, O.J.; Audinot, J.N.; Kanda, H.; Driukas, S.; Kavaliauskaitė, G.; Gulbinas, V.; Dessimoz, M.; Getautis, V.; De Angelis, F.; Ding, Y.; Dai, S.; Dyson, P.J.; Nazeeruddin, M.K. Tuning structural isomers of phenylenediammonium to afford efficient and stable perovskite solar cells and modules // *Nature communications.* ISSN 2041-1723. 2021, vol. 12, art. no. 6394, p. 1-9.

129. Liustrovaitė, V.; Valiūnienė, A.; Valinčius, G.; Ramanavičius, A. Electrochemical impedance spectroscopy based evaluation of chlorophyll a reconstitution within tethered bilayer lipid membrane // *Journal of the electrochemical society*. ISSN 0013-4651. 2021, vol. 168, iss. 6, art. no. 066506, p. 1-6.

130. Mačiulytė, S.; Mamavičiūtė, I.; Strakšys, A.; Kochanė, T.; Budrienė, S. New poly(urethane-urea) microcapsules from PVA modified with APTES: preparation, characterization and enzyme encapsulation // *Polymer bulletin*. ISSN 0170-0839. 2021, vol. 78, p. 1867-1886.

131. Madeikis, K.; Dansette, P.M.; Bartulevičius, T.; Veselis, L.; Jutas, R.; Eremchev, M.; Danilevičius, R.; Girdauskas, V.; Michailovas, A. Investigation of materials for supercontinuum generation for subsequent nonlinear parametrical and Raman amplification at 1 MHz repetition rate // *Optics & laser technology*. ISSN 0030-3992. 2021, vol. 143, art. no. 107373, p. 1-9.

132. Madeikis, K.; Kananavičius, R.; Danilevičius, R.; Zaukevičius, A.; Januškevičius, R.; Michailovas, A. Hybrid high spectral resolution broadband mid-infrared SFG spectrometer development and demonstration // *Optics express*. ISSN 1094-4087. 2021, vol. 29, iss. 16, p. 25344-25357.

133. Madeikis, K.; Viskontas, K.; Danilevičius, R.; Michailovas, A. All-optical repetition rate stabilization methods for ultrafast Yb-based SESAM mode-locked fiber oscillator // *Optical fiber technology*. ISSN 1068-5200. 2021, vol. 65, no.102636, p. 1-7.

134. Mahmood, A.; Noman, M.T.; Pechočiaková, M.; Amor, N.; Petrů, M.; Abdelkader, M.; Militký, J.; Sozcu, S.; Hassan, S.Z.U. Geopolymers and fiber-reinforced concrete composites in civil engineering // *Polymers.* eISSN 2073-4360. 2021, vol. 13, iss. 13, art. no. 2099, p. 1-34.

135. Maleckaitė, K.; Dodonova, J.; Toliautas, S.; Žilėnaitė, R.; Jurgutis, D.; Karabanovas, V.; Tumkevičius, S.; Vyšniauskas, A. Designing a red-emitting viscosity-sensitive BODIPY fluorophore for intracellular viscosity imaging // *Chemistry – a European journal*. ISSN 0947-6539.2021, vol. 27, iss. 67, p. 16768-16775.

136. Malevich, V.L.; Ziaziulia, P.A.; Norkus, R.; Pačebutas, V.; Nevinskas, I.; Krotkus, A. Terahertz pulse emission from semiconductor heterostructures caused by ballistic photocurrents // *Sensors*. ISSN 1424-8220. 2021, vol. 21, iss. 12, art. no. 4067, p. 1-11.

137. Markauskas, E.; Zubauskas, L.; Gečys, P. Efficient milling and cutting of borosilicate glasses through a thin flowing water film with a picosecond laser // *Journal of manufacturing processes*. ISSN 1526-6125. 2021, vol. 68, p. 898-909.

138. Martins Antunes De Melo, W. De C.; Celiešiūtė-Germanienė, R.; Šimonis, P.; Stirkė, A. Antimicrobial photodynamic therapy (aPDT) for biofilm treatments. Possible synergy between aPDT and pulsed electric fields // *Virulence.* ISSN 2150-5594. 2021, vol. 12, no. 1, p. 2247-2272.

139. Mažeika, K.; Reklaitis, J.; Nicolenco, A.; Vainoris, M.; Tsyntsaru, N.; Cesiulis, H. Magnetic state instability of disordered electrodeposited nanogranular Fe films // *Journal of magnetism and magnetic materials.* ISSN 0304-8853. 2021, vol. 540, art. no. 168433, p. 1-7.

140. Mažeika, K.; Šiliauskas, L.; Skridlaitė, G.; Matelis, A.; Garjonytė, R.; Paškevičius, A.; Melvydas, V. B. Features of iron accumulation at high concentration in pulcherrimin-producing Metschnikowia yeast biomass // *Journal of biological inorganic chemistry*. ISSN 0949-8257. 2021, vol. 26, iss. 2-3, p. 299-311.

141. Mažeikienė, R.; Niaura, G.; Malinauskas, A. Poly(N-methylaniline) vs. polyaniline: An extended pH range of polaron stability as revealed by Raman spectroelectrochemistry // *Spectrochimica acta. Part A: Molecular and biomolecular spectroscopy*. ISSN 1386-1425. 2021, vol. 262, no. 120140, p. 1-9.

142. Meisak, D.; Macutkevič, J.; Selskis, A.; Kuzhir, P.; Banys, J. Dielectric relaxation spectroscopy and synergy effects in

epoxy/MWCNT/Ni@C composites // *Nanomaterials*. eISSN 2079-4991. 2021, vol. 11, iss. 2, art. no. 555, p. 1-16.

143. Melnikas, S.; Ramalis, L.; Kičas, S.; Tolenis, T. Broadband chirped mirrors with a porous top layer for smooth group delay dispersion // *Applied optics*. ISSN 1559-128X. 2021, vol. 60, no. 26, p. 8181-8189.

144. Mikalčiūtė, A.; Vilčiauskas, L. Insights into the hydrogen bond network topology of phosphoric acid and water systems // *Physical chemistry chemical physics*. ISSN 1463-9076. 2021, vol. 23, iss. 10, p. 6213-6224.

145. Miksiunas, R.; Aldonytė, R.; Vailionytė, A.; Jelinskas, T.; Eimont, R.; Stankevičienė, G.; Cėpla, V.; Valiokas, R.; Ručinskas, K.; Janušauskas, V.; Labeit, S.; Bironaitė, D. Cardiomyogenic differentiation potential of human dilated myocardium-derived mesenchymal stem/stromal cells: The impact of HDAC inhibitor SAHA and biomimetic matrices // *International journal of molecular sciences*. ISSN 1661-6596. 2021, vol. 22, iss. 23, art. no.12702, p. 1-25.

146. Milikić, J.; Balčiūnaitė, A.; Sukackienė, Z.; Mladenović, D.; Santos, D.M.F.; Tamašauskaitė-Tamašiūnaitė, L.; Šljukić, B. Bimetallic Co-based (CoM, M = Mo, Fe, Mn) coatings for high-efficiency water splitting // *Materials*. ISSN 1996-1944. 2021, vol. 14, iss. 1, art. no. 92, p. 1-15.

147. Milles, S.; Dahms, J.; Voisiat, B.; Indrišiūnas, S.; Račiukaitis, G.; Lasagni, A.F. Wetting properties of aluminium surface structures fabricated using direct laser interference patterning with picosecond and femtosecond pulses. Journal of laser micro/nanoengineering // *Osaka*. ISSN 1880-0688. 2021, vol. 16, no. 1, p. 1-6.

148. Montvydienė, D.; Jagminas, A.; Jurgelėnė, Ž.; Kazlauskas, M.; Butrimienė, R.; Žukauskaitė, Z.; Kazlauskienė, N. Toxicological effects of different-sized Co–Fe ($CoFe_2O_4$) nanoparticles on Lepidium sativum L.: towards better understanding of nanophytotoxicity // *Ecotoxicology*. ISSN 0963-9292. 2021, vol. 30, iss. 2, p. 277-291.

149. Nacys, A.; Kilmonis, T.; Kepenienė, V.; Balčiūnaitė, A.; Stagniūnaitė, R.; Upskuvienė, D.; Jablonskienė, J.; Vaičiūnienė, J.; Skapas, M.; Tamašauskaitė-Tamašiūnaitė, L.; Norkus, E. One-pot microwave-assisted synthesis of graphene-supported PtCoM (M = Mn, Ru, Mo) catalysts for low-temperature fuel cells // *Catalysts*. ISSN 2073-4344. 2021, vol. 11, iss. 12, art. no. 1431, p. 1-19.

150. Nacius, E.; Gotovski, P.; Ulčinas, O.; Orlovas, S.; Urbas, A.; Jukna, V. Spatially displaced and superposed Bessel beams for transparent material laser microprocessing // *Journal of the Optical Society of America B.* ISSN 0740-3224. 2021, vol. 38, iss. 12, p. 3886-3895.

151. Nevinskas, I.; Mockus, Z.; Juškėnas, R.; Norkus, R.; Selskis, A.; Norkus, E.; Krotkus, A. Terahertz photoconductivity spectra of electrodeposited Thin Bi films // *Materials*. ISSN 1996-1944. 2021, vol. 14, iss. 12, art. no. 3150, p. 1-9.

152. Nevinskas, I.; Norkus, R.; Geižutis, A.; Kulyuk, L.; Miku, A.; Sushkevich, K.; Krotkus, A. Terahertz pulse emission from photoexcited bulk crystals of transition metal dichalcogenides // *Journal of physics D: Applied physics.* ISSN 0022-3727. 2021, vol. 54, iss. 11, art. no. 115105, p. 1-7.

153. Novickij, V.; Stanevičienė, R.; Gruškienė, R.; Badokas, K.; Lukša, J.; Sereikaitė, J.; Mažeika, Kęstutis; Višniakov, N.; Novickij, J.; Servienė, E. Inactivation of bacteria using bioactive nanoparticles and alternating magnetic fields // *Nanomaterials*. ISSN 2079-4991. 2021, vol. 11, iss. 2, art. no. 342, p. 1-16.

154. Novičenko, V.; Ratas, I. Unstable delayed feedback control to change sign of coupling strength for weakly coupled limit cycle oscillators // *Chaos.* ISSN 1054-1500. 2021, vol. 31, art. no. 093138, p. 1-19.

155. Nowok, A.; Szeremeta, A.Z.; Sieradzki, A.; Šimėnas, M.; Snarskis, G.; Vilčiauskas, L.; Maczka, M.; Zubko, M.; Paluch, M.; Pawlus, S. From ambient - to high-pressure dielectric response of perovskite formamidinium manganese formate // *Journal of materials chemistry C*. ISSN 2050-7526. 2021, vol. 9, no. 17, p. 5740-5748.

156. Orlovas, S.; Berškys, J. Generalized Lorenz–Mie theory of photonic wheels // *Journal of quantitative spectroscopy & radiative transfer*. ISSN 0022-4073. 2021, vol. 261, art. no. 107490, p. 1-9.

157. Paddubskaya, A.; Valynets, N.; Maksimenko, S.; Kumar, M.; Baah, M.; Pekkarinen, M.; Svirko, Y.; Valušis, G.; Kuzhir, P. Terahertz absorber with graphene enhanced polymer hemispheres array // *Nanomaterials*. ISSN 2079-4991. 2021, vol. 11, iss. 10, art. no. 2494, p. 1-8.

158. Paek, S.; Khan, S.B.; Franckevičius, M.; Gegevičius, R.; Syzgantseva, O.A.; Syzgantseva, M.A.; Kinche, S.; Asiri, A.M.; Roldán-Carmona, C.; Nazeeruddin, M.K. Cation optimization for burn-in loss-free perovskite solar devices // *Journal of materials chemistry A.* ISSN 2050-7488. 2021, vol. 9, iss. 9, p. 5374-5380.

159. Páez-Pérez, M.; López-Duarte, I.; Vyšniauskas, A.; Brooks, N.J.; Kuimova, M.K. Imaging non-classical mechanical responses of lipid membranes using molecular rotors // *Chemical science*. ISSN 2041-6520. 2021, vol. 12, iss. 7, p. 2604-2613.

160. Pakalniškis, A.; Skapas, M.; Grigoravičiūtė-Puronienė, I.; Ramanauskas, R.; Skaudžius, R.; Kareiva, A. A novel synthetic approach for the preparation of bulk $Bi_3Fe_5O_{12}$ on the $Y_3Ga_5O_{12}$ core // *Integrated ferroelectrics*. ISSN 1058-4587. 2021, vol. 220, no. 1, p. 71-79.

161. Pakalniškis, A.; Skaudžius, R.; Zhaludkevich, D.V.; Zhaludkevich, A.L.; Alikin, D. O.; Abramov, A.S.; Murauskas, T.; Shur, V.Ya.; Dronov, A.A.; Silibin, M.V.; Selskis, A.; Ramanauskas, R.; Lukowiak, A.; Strek, W.; Karpinsky, D.V.; Kareiva, A. Morphotropic phase boundary in Sm-substituted $BiFeO_3$ ceramics: Local vs microscopic approaches // *Journal of alloys and compounds*. ISSN 0925-8388. 2021, vol. 875, art. no. 159994, p. 1-8.

162. Pauraitė, J.; Mainelis, G.; Kecorius, S.; Minderytė, A.; Dudoitis, V.; Garbarienė, I.; Plauškaitė-Šukienė, K.; Ovadnevaite, J.; Byčenkienė, S. Office indoor PM and BC level in Lithuania: The role of a long-range smoke transport event // *Atmosphere*. ISSN 2073-4433. 2021, vol. 12, iss. 8, art. no. 1047, p. 1-15.

163. Pauraitė, J.; Garbarienė, I.; Minderytė, A.; Dudoitis, V.; Mainelis, G.; Davulienė, L.; Uogintė, I.; Plauškaitė-Šukienė, K.; Byčenkienė, S. Effect of spring grass fires on indoor air quality in air-conditioned office building // *Lithuanian journal of physics*. ISSN 1648-8504. 2021, vol. 61, no. 3, p. 191-204.

164. Pham, V.G.; Pham, N.T.; Tran, L.D.; Dinh, T.H.; Vrublevsky, I.; Charniakova, K.; Viet Le, H. Insight into the effect of zinc oxide nanoparticles coated multi-walled carbon nanotubes (ZnO/MWCNTs) on the thermal conductivity of epoxy nanocomposite as an electrical-insulating coating // *Journal of the Australian ceramic society.* ISSN 2510-1560. 2021, vol. 57, iss. 5, p. 1445-1452.

165. Pyragas, K.; Fedaravičius, A. P.; Pyragienė, T. Suppression of synchronous spiking in two interacting populations of excitatory and inhibitory quadratic integrate-and-fire neurons // *Physical review E*. ISSN 2470-0045. 2021, vol. 104, iss. 1, art. no. 014203, p. 1-12.

166. Pyragas, V.; Pyragas, K. Dynamics of a network of quadratic integrate-and-fire neurons with bimodal heterogeneity // *Physics letters A*. ISSN 0375-9601. 2021, vol.416, art. no. 127677, p. 1-7.

167. Plečkaitytė, G.; Petrulevičienė, M.; Staišiūnas, L.; Tediashvili, D.; Pilipavičius, J.; Juodkazytė, J.; Vilčiauskas, L. Understanding and mitigation of $NaTi_2(PO_4)_3$ degradation in aqueous Na-ion batteries // *Journal of materials chemistry A*. ISSN 2050-7488. 2021, vol. 9, iss. 21, p. 12670-12683.

168. Plikusienė, I.; Bužavaitė-Vertelienė, E.; Mačiulis, V.M.; Valavičius, A.; Ramanavičienė, A.; Balevičius, Z. Application of Tamm plasmon polaritons and cavity modes for biosensing in the combined spectroscopic ellipsometry and quartz crystal microbalance method // *Biosensors*. eISSN 2079-6374. 2021, vol. 11, iss. 12, art. n. 501, p. 1-13.

169. Plikusienė, I.; Mačiulis, V.M.; Graniel, O.; Bechelany, M.; Balevičius, S.; Vertelis, V.; Balevičius, Z.; Popov, A.; Ramanavičius,

A.; Ramanavičienė, A. Total internal reflection ellipsometry for kinetics-based assessment of bovine serum albumin immobilization on ZnO nanowires // *Journal of materials chemistry C*. ISSN 2050-7526. 2021, vol. 9, iss. 4, p. 1345-1352.

170. Plikusienė, I.; Mačiulis, V.M.; Ramanavičienė, A.; Balevičius, Z.; Buzavaitė-Vertelienė, E.; Čiplys, E.; Slibinskas, R.; Simanavičius, M.; Žvirblienė, A.; Ramanavičius, A. Evaluation of kinetics and thermodynamics of interaction between immobilized SARS-CoV-2 nucleoprotein and specific antibodies by total internal reflection ellipsometry // *Journal of colloid and interface science*. ISSN 0021-9797. 2021, vol. 594, p. 195-203.

171. Plyushch, A.; Macutkevič, J.; Sokal, A.; Lapko, K.; Kudlash, A.; Adamchuk, D.; Ksenevich, V.; Bychanok, D.; Selskis, A.; Kuzhir, P.; Banys, J. The phosphate-based composite materials filled with nano-sized $BaTiO_3$ and $Fe_3O_4$: toward the unfired multiferroic materials // *Materials*. ISSN 1996-1944. 2021, vol. 14, iss. 1, art. no. 133, p. 1-8.

172. Plyushch, A.; Mačiulis, N.; Sokal, A.; Grigalaitis, R.; Macutkevič, J.; Kudlash, A.; Apanasevich, N.; Lapko, K.; Selskis, A.; Maksimenko, S.A.; Kuzhir, P.; Banys, J. 0.7Pb(Mg1/3Nb2/3)O3-0.3PbTiO3 phosphate composites: dielectric and ferroelectric properties // *Materials*. eISSN 1996-1944. 2021, vol. 14, no. 17, art. no. 5065, p. 1-9.

173. Politi, T.; Barisevičiūte, R.; Bartoli, M.; Bonaglia, S.; Cardini, U.; Castaldelli, G.; Kančauskaitė, A.; Marzocchi, U.; Petkuviene, J.; Samuiloviene, A.; Vybernaite-Lubiene, I.; Zaiko, A.; Zilius, M. A bioturbator, a holobiont, and a vector: the multifaceted role of Chironomus plumosus in shaping N-cycling // *Freshwater biology*. ISSN 0046-5070. 2021, vol. 66, no. 6, p. 1036-1048.

174. Qi, L.; Minkevičius, L.; Urbanovič, A.; Švigelj, A.; Grigelionis, I.; Kašalynas, I.; Trontelj, J.; Valušis, G. Antenna-coupled titanium microbolometers: application for precise control of radiation patterns in terahertz time-domain systems // *Sensors*. ISSN 1424-8220. 2021, vol. 21, iss. 10, art. no. 3510, p. 1-11.

175. Račiukaitis, G. Ultra-short pulse lasers for microfabrication: A review // *IEEE journal of selected topics in quantum electronics*. ISSN 1077-260X. 2021, vol. 27, iss. 6, art. no. 1100112, p. 1-12.

176. Ramanavičius, A.; Morkvėnaitė-Vilkončienė, I.; Samukaitė-Bubnienė, U.; Petronienė, J.J.; Barkauskas, J.; Genys, P.; Ratautaitė, V.; Viter, R.; Iatsunskyi, I.; Ramanavičienė, A. Scanning electrochemical microscopy and electrochemical impedance spectroscopy-based characterization of perforated polycarbonate membrane modified by carbon-nanomaterials and glucose oxidase // *Colloids and surfaces: A-physicochemical and engineering aspects*. ISSN 0927-7757. 2021, vol. 624, art. no. 126822, p. 1-8.

177. Ramanavičius, S.; Jagminas, A.; Ramanavičius, A. Advances in molecularly imprinted polymers based affinity sensors (review) // Polymers. ISSN 2073-4360. 2021, vol. 13, iss. 6, no. 974, p. 1-28.

178. Ramanavičius, S.; Bittencourt, C.; Naujokaitis, A.; Pakštas, V.; Jagminas, A. Interfacing perovskite strontium molybdate to molybdenum disulfide nanoplatelts for boosting HER from water // *International journal of hydrogen energy*. ISSN 0360-3199. 2021, vol. 46, p. 14359-14368.

179. Ratas, I.; Pyragas, K.; Tass, P.A. Multistability in a star network of Kuramoto-type oscillators with synaptic plasticity // *Scientific reports*. ISSN 2045-2322. 2021, vol. 11, art.no. 9840, p. 1-15.

180. Ratautaitė, V.; Samukaitė-Bubnienė, U.; Plaušinaitis, D.; Bogužaitė, Ra.; Balčiūnas, D.; Ramanavičienė, A.; Neunert, G.; Ramanavičius, A. Molecular imprinting technology for determination of uric acid // *International journal of molecular sciences*. ISSN 1661-6596. 2021, vol. 22, iss. 9, art. no. 5032, p. 1-18.

181. Raudonytė-Svirbutavičienė, E.; Stakėnienė, R.; Jokšas, K.; Matulaitienė, I.; Mikoliūnaitė, L.; Žarkov, A.; Kareiva, A. Study of microplastic occurrence on the sandy beaches of Šventoji // *Lithuania. Baltica*. ISSN 0067-3064. 2021, vol. 34, no. 1, p. 47-57.

182. Razinkovas, L.; Maciaszek, M.; Reinhard, F.; Doherty, M.W.; Alkauskas, A. Photoionization of negatively charged NV centers in diamond: theory and ab initio calculations // *Physical review B*. ISSN 2469-9950. 2021, vol. 104, iss. 23, no. 235301, p. 1-13.

183. Razinkovas, L.; Doherty, M.W.; Manson, N.B.; Van de Walle, C.G.; Alkauskas, A. Vibrational and vibronic structure of isolated point defects: The nitrogen-vacancy center in diamond // *Physical review B*. ISSN 2469-9950. 2021, vol. 104, iss. 4, art. no. 045303, p. 1-19.

184. Remeikis, V.; Grinevičiūtė, J.; Duškesas, G.; Juodis, L.; Plukienė, R.; Plukis, A. Review of modeling experience during operation and decommissioning of RBMK-1500 reactors. I. Safety improvement studies during operation // *Nuclear engineering and design*. ISSN 0029-5493. 2021, vol. 380, art. no. 110952, p. 1-14.

185. Remeikis, V.; Grinevičiūtė, J.; Duškesas, G.; Juodis, L.; Plukienė, R.; Plukis, A. Review of modeling experience during operation and decommissioning of RBMK-1500 reactors. II. Radioactive waste management // *Nuclear engineering and design*. ISSN 0029-5493. 2021, vol. 380, art. no. 111242, p. 1-28.

186. Rožėnė, J.; Morkvėnaitė-Vilkončienė, I.; Bružaitė, I.; Dzedzickis, A.; Ramanavičius, A. Yeast-based microbial biofuel cell mediated by 9,10-phenantrenequinone // *Electrochimica acta*. ISSN 0013-4686. 2021, vol. 373, art. no. 137918, p. 1-10.

187. Rožėnė, J.; Morkvėnaitė-Vilkončienė, I.; Bružaitė, I.; Zinovičius, A.; Ramanavičius, A. Baker's yeast-based microbial fuel cell mediated by 2-methyl-1,4-naphthoquinone // *Membranes*. ISSN 2077-0375. 2021, vol. 11, iss. 3, art. no. 182, p. 1-10.

188. Rubežienė, V.; Baltušnikaitė-Guzaitienė, J.; Abraitienė, A.; Sankauskaitė, A.; Ragulis, P.; Santos, G.; Pimenta, J. Development and investigation of PEDOT:PSS composition coated fabrics intended for microwave shielding and absorption // *Polymers*. ISSN 2073-4360. 2021, vol. 13, iss. 8, no. 1191, p. 1-21.

189. Samukaitė-Bubnienė, U.; Valiūnienė, A.; Bučinskas, V.; Genys, P.; Ratautaitė, V.; Ramanavičienė, A.; Aksun, E.; Tereshchenko, A.; Zeybek, B.; Ramanavičius, A. Towards supercapacitors: Cyclic voltammetry and fast Fourier transform electrochemical impedance spectroscopy based evaluation of polypyrrole electrochemically deposited on the pencil graphite electrode // *Colloids and surfaces : A-physicochemical and engineering aspects*. ISSN 0927-7757. 2021, vol. 610, art.no. 125750, p. 1-9.

190. Schmidt-Mende, L.; Dyakonov, V.; Olthof, S.; Ünlü, F.; Moritz Trong Lê, K.; Mathu, Sa.; Karabanov, A.D.; Lupascu, D.C.; Herz, L.M.; Hinderhofer, A.; Schreiber, F.; Chernikov, A.; Egger, D.A.; Shargaieva, O.; Cocchi, C.; Unger, E.; Saliba, M.; Malekshahi Byranvand, M.; Kroll, M.; Nehm, F.; Leo, K.; Redinger, A.; Höcker, J.; Kirchartz, T.; Warby, J.; Gutierrez-Partida, E.; Neher, Di.; Stolterfoht, M.; Würfel, U.; Unmüssig, M.; Herterich, J.; Baretzky, C.; Mohanraj, J.; Thelakkat, M.; Maheu, C.; Jaegermann, W.; Mayer, T.; Rieger, J.; Fauster, T.; Niesner, D.; Yang, F.Y.; Albrecht, S.; Riedl, T.; Fakharuddin, A.; Vasilopoulou, M.; Vaynzof, Y.; Moia, D.; Maier, J.; Franckevičius, M; Gulbinas, V.; Kerner, R.A.; Zhao, L.; Rand, B.P.; Glück, N.; Bein, T.; Matteocci, F.; Castriotta, L.A.; Di Carlo, A.; Scheffler, M.; Draxl, C. Roadmap on organic–inorganic hybrid perovskite semiconductors and devices // *APL Materials*. ISSN 2166-532X. 2021, vol. 9, iss. 10, art. no. 109202, p. 1-82.

191. Sereika, R.; Žaltauskas, R.; Bandaru, S.; Liu, F.; Čerškus, A. Two-transition behavior in Bi0.5Sb0.5SeI crystals // *Journal of physics and chemistry of solids*. ISSN 0022-3697. 2021, vol. 154, art. no. 110031, p. 1-5.

192. Sherin, P.S.; Vyšniauskas, A.; López-Duarte, I.; Ogilby, P.R.; Kuimova, M.K. Visualising UV-A light-induced damage to plasma membranes of eye lens // *Journal of photochemistry and photobiology B: biology*. ISSN 1011-1344. 2021, vol. 225, art. no.112346, p. 1-10.

193. Shumakova, V.; Schubert, E.; Balčiūnas, T.; Matthews, M.; Ališauskas, S.; Mongin, D.; Pugžlys, A.; Kasparian, J.; Baltuška, A.; Wolf, J.P. Laser induced aerosol formation mediated by resonant excitation of volatile organic compounds // *Optica*. ISSN 2334-2536. 2021, vol. 8, iss. 10, p. 1256-1261.

194. Siemion, A.; Minkevičius, L.; Jokubauskis, D; Ivaškevičiūtė-Povilauskienė, R; Valušis, G. Terahertz digital holography: Two- and four-step phase shifting technique in two plane image recording // *AIP advances*. ISSN 2158-3226. 2021, vol. 11, no. 10, art. no. 105212, p. 1-12.

195. Siemion, A.; Minkevičius, L.; Qi, L.; Valušis, G. Spatial filtering based terahertz imaging of low absorbing objects // *Optics and lasers in engineering*. ISSN 0143-8166. 2021, vol. 139, art. no. 106476, p. 1-8.

196. Simniškytė, A.; Selskienė, A.; Vaičiūnienė, J.; Pakštas, V. Shallow and ploughed settlement sites in forested environment: Opportunities to multilevel prospection (an example of a prehistoric site in eastern Lithuania) // *Archaeological Prospection*. ISSN 1075-2196. 2021, vol. 28, iss. 4, p. 583-599.

197. Sinkevičius, G.; Baškys, A.; Tamošauskas, G. Active suppression of piezoelectric ringing in pockels cells for laser cavity application // *Symmetry*. ISSN 2073-8994. 2021, vol. 13, iss. 4, art. no. 677, p. 1-10.

198. Sytchkova, A.; Belosludtsev, A; Volosevičienė, L.; Juškėnas, R.; Simniškis, R. Optical, structural and electrical properties of sputtered ultrathin chromium films // *Optical materials*. ISSN 0925-3467. 2021, vol. 121, art. no. 111530, p. 1-9.

199. Skruodienė, M.; Juodvalkytė, R.; Inkrataitė, G.; Pakalniškis, A.; Ramanauskas, R.; Sarakovskis, A.; Skaudžius, R. Sol-gel assisted molten-salt synthesis of novel single phase Y3–2xCa2xTaxAl5–xO12:1%Eu garnet structure phosphors // *Journal of alloys and compounds*. ISSN 0925-8388. 2021, vol. 890, art. no. 161889, p. 1-6.

200. Skurkytė-Papievienė, V.; Abraitienė, A.; Sankauskaitė, A.; Rubežienė, V.; Baltušnikaitė-Guzaitienė, J. Enhancement of the thermal performance of the paraffin-based microcapsules intended for textile applications // *Polymers*. ISSN 2073-4360. 2021, vol. 13, iss. 8, art. no. 1120, p. 1-16.

201. Snarskis, G.; Pilipavičius, J.; Grjaznovs, D.; Mikoliūnaitė, L; Vilčiauskas, L. Peculiarities of phase formation in Mn-based Na superIonic conductor (NaSICon) systems: The Case of Na1+2xMnxTi2-x(PO4)(3) (0.0= x = 1.5) // *Chemistry of materials*. ISSN 0897-4756. 2021, vol. 33, art. no. 21, p. 8394-8403.

202. Sodaitienė, E.; Kaušpėdienė, D.; Gefenienė, A.; Gefenas, V.; Ragauskas, R.; Ramanauskas, R. Utilization of copper plating effluents in the degradation of the dye Sanodure Green in the presence of $H_2O_2$ // *Chemija*. ISSN 0235-7216. 2021, vol. 32, iss. 1, p. 1-8.

203. Stagniūnaitė, R.; Kepenienė, V.; Balčiūnaitė, A; Drabavičius, A.; Pakštas, V.; Jasulaitienė, V.; Tamašauskaitė-Tamašiūnaitė, L.; Norkus, E. An electrocatalytic activity of AuCeO2/carbon catalyst in fuel cell reactions: oxidation of borohydride and reduction of oxygen // *Catalysts*. ISSN 2073-4344. 2021, vol. 11, iss. 3, art. no. 342, p. 1-15.

204. Stankevič, V.; Račiukaitis, G.; Gečys, P. Chemical etching of fused silica after modification with two-pulse bursts of femtosecond laser // *Optics express*. ISSN 1094-4087. 2021, vol. 29, iss. 20, p. 31393-31407.

205. Stankevičius, E.; Ignatjev, I.; Petrikaitė, V.; Selskis, A.; Niaura, G. Gold nanoparticles generated using the nanosecond laser treatment of multilayer films and their use for SERS applications // *ACS Omega*. ISSN 2470-1343. 2021, vol. 6, no. 49, p. 33889-33898.

206. Stankevičius, E.; Vilkevičius, K.; Gedvilas, M.; Bužavaitė-Vertelienė, E.; Selskis, A.; Balevičius, Z. Direct laser writing for the formation of large-scale gold microbumps arrays generating hybrid lattice plasmon polaritons in Vis–NIR range // *Advanced optical materials*. ISSN 2195-1071. 2021, vol. 9, iss. 12, art. no. 2100027, p. 1-10.

207. Stepšys, A.; Mickevičius, S.; Germanas, D.; Kalinauskas, R.K. Calculation of five-particle harmonic-oscillator transformation brackets // *Computer physics communications*. ISSN 0010-4655. 2021, vol. 265, art. no. 108023, p. 1-6.

208. Stygienė, L.; Varnaitė-Žuravliova, S.; Abraitienė, A; Padleckienė, I.; Krauledas, S. Investigation of textile heating element in simulated wearing conditions // *AUTEX research journal*. ISSN 1470-9589. 2021, vol. 21, iss. 3, p. 207-215.

209. Strakšys, A.; Bražinskienė, D.; Mačiulytė, S. Thermal degradation behavior of thin films of fatty acid methyl ester // *Chemical papers*. ISSN 0366-6352. 2021, vol. 75, no. 6, p. 2695-2701.

210. Strakšys, A.; Kochanė, T.; Mačiulytė, S.; Budrienė, S. Porous poly(urethane urea) microparticles for immobilization of maltogenic α amylase from Bacillus stearothermophilus // *Chemija*. ISSN 0235-7216. 2021, vol. 32, no. 3-4, p. 127-136.

211. Strazdaitė, S.; Roeters, S.J.; Sakalauskas, A.; Šneideris, T.; Kirschner, J.; Pedersen, B.; Schiøtt, B.; Jensen, F.; Weidner, T.; Smirnovas, V.; Niaura, G. Interaction of amyloid-β-(1–42) peptide and Its aggregates with lipid/water interfaces probed by vibrational sum-frequency generation spectroscopy // *The journal of physical chemistry B*. ISSN 1520-6106. 2021, vol. 125, iss. 40, p. 11208-11218.

212. Survila, A.; Kanapeckaitė, S.; Girčienė, O.; Gudavičiūtė, L. Impact of pH on the anodic current-voltage characteristics of the alkaline Cu | Cu (II), glycine system // *Journal of the electrochemical society*. ISSN 0013-4651. 2021, vol. 168, iss. 7, art. no. 076507, p. 1-6.

213. Šapolaitė, J.; Ežerinskis, Ž.; Butkus, L.; Garbarienė, I.; Garbaras, A.; Kurila, L.V.; Bučinskas, L.; Pabedinskas, A.; Remeikis, V. Development of an online sulfur trapping system for graphitization of cremated bones with automated graphitization system AGE-3. Nuclear instruments and methods in physics research // *Section B: Beam interactions with materials and atoms*. ISSN 0168-583X. 2021, vol. 505, p. 17-23.

214. Ščajev, P.; Durena, R.; Onufrijevs, P.; Miasojedovas, S.; Malinauskas, T.; Stanionytė, S.; Žarkov, A.; Zukuls, A.; Bite, I.; Smits, K. Morphological and optical property study of Li doped ZnO produced by microwave-assisted solvothermal synthesis // *Materials science in semiconductor processing*. ISSN 1369-8001. 2021, vol. 135, art. no. 106069, p. 1-8.

215. Ščajev, P.; Onufrijevs, P.; Mekys, A.; Malinauskas, T.; Augulis, D.; Subačius, L.; Lee, K.C.; Kaupuzs, J.; Varnagiris, Š.; Medvids, A.; Cheng, H.H. Extension of spectral sensitivity of GeSn IR photodiode after laser annealing // *Applied surface science*. ISSN 0169-4332. 2021, vol. 555, art. no. 149711, p. 1-8.

216. Ščajev, P.; Soriūtė, V.; Kreiza, G.; Nargelas, S.; Dobrovolskas, D.; Malinauskas, T.; Subačius, L.; Onufrijevs, P.; Varnagiris, Š.; Cheng, H.H. Temperature and spatial dependence of carrier lifetime and luminescence intensity in Ge0.95Sn0.05 layer // *Materials science and engineering B*. ISSN 0921-5107. 2021, vol. 270, art. no. 115204, p. 1-12.

217. Šermukšnis, E.; Liberis, J.; Šimukovič, A.; Matulionis, A.; Ding, K.; Avrutin, V.; Özgür, Ü.; Morkoç, H. Self-formation of high-field domain in epitaxial ZnO and its suppression in ZnO/MgZnO heterostructure // *Applied physics letters*. ISSN 0003-6951. 2021, vol. 118, no. 25, art. no. 252102, p. 1-9.

218. Šimoliūnienė, M.; Žukauskienė, E.; Truncaitė, L.; Cui, L.; Hutinet, G.; Kazlauskas, D.; Kaupinis, A.; Skapas, M.; de Crécy-Lagard, V.; Dedon, P.; Valius, M.; Meškys, R.; Šimoliūnas, E. Pantoea bacteriophage vB_PagS_MED16 - a siphovirus containing a 2'-deoxy-7-amido-7-deazaguanosine-modified DNA // *International journal of molecular sciences*. eISSN 1422-0067. 2021, vol. 22, iss. 14, art. no. 7333, p. 1-21.

219. Šimonis, P.; Linkevičiūtė, A.; Stirkė, A. Electroporation assisted improvement of freezing tolerance in yeast cells // *Foods*. ISSN 2304-8158. 2021, vol. 10, iss. 1, art. no. 170, p. 1-9.

220. Švedienė, J.; Novickij, V.; Žalnėravičius, R.; Raudonienė, V.; Markovskaja, S.; Novickij, J.; Paškevičius, A. Antimicrobial activity of L-lysine and poly-L-lysine with pulsed electric fields // *Applied science*. ISSN 2076-3417. 2021, vol. 11, iss. 6, no. 2708, p. 1-12.

221. Talianov, P.M.; Peltek, O.O.; Masharin, M.; Khubezhov, S.; Baranov, M. A.; Drabavičius, A.; Timin, A.S.; Zelenkov, L.E.; Pushkarev, A.P.; Makarov, S.V.; Zyuzin, M.V. Halide perovskite nanocrystals with enhanced water stability for upconversion imaging in a living cell // *Journal of physical chemistry letters*. ISSN 1948-7185. 2021, vol.12, iss.37, p. 8991-8998.

222. Tamašauskaitė-Tamašiūnaitė, L.; Dordi, Y.; Norkus, E.; Stankevičienė, I.; Jagminienė, A.; Naujokaitis, A.; Tumonis, L.; Buzas, V.; Maciulis, L. Electroless platinum deposition using Co3+/Co2+ redox couple as a reducing agent // *Materials*. ISSN 1996-1944. 2021, vol. 14, iss. 8, art. no. 1893, p. 1-11.

223. Tamaševičius, A.V.; Bumelienė, S.; Adomaitienė, E. Using a single deactivated oscillator to stabilize the steady states in an array of coupled FitzHugh–Nagumo cells // *Nonlinear dynamics*. ISSN 0924-090X. 2021, vol. 106, iss. 4, p. 3557-3564.

224. Turiansky, M. E.; Alkauskas, A.; Engel, M.; Kresse, G.; Wickramaratne, D.; Shen, J.X.; Dreyer, C.E.; Van de Walle, C.G. Nonrad: Computing nonradiative capture coefficients from first principles // *Computer physics communications*. ISSN 0010-4655. 2021, vol. 267, art. no. 108056, p. 1-7.

225. Tutkus, M.; Chmeliov, J.; Trinkūnas, G.; Akhtar, P.; Lambrev, P.H.; Valkūnas, L. Aggregation-related quenching of LHCII fluorescence in liposomes revealed by single-molecule spectroscopy // *Journal of photochemistry and photobiology B: Biology*. ISSN 1011-1344. 2021, vol. 218, art. no. 112174, p. 1-7.

226. Tutlienė, S.; Petrulevičienė, M.; Pilipavičius, J.; Žarkov, A.; Selskis, A.; Stanionytė, S.; Juodkazytė, J.; Vilčiauskas, L. Electrochemical performance of sol-gel synthesized NaTi2(PO4)3 - carbon composites as aqueous Na-ion battery anodes // *Journal of the electrochemical society*. ISSN 0013-4651. 2021, vol. 168, iss. 6, art. no. 060545, p. 1-11.

227. Unagar, A.; Hashmi, A.; Tiwari, A.K.; Jawak, S.D.; Desai, B.; Urba, A.; Qureshi, A. Coast of Eastern Antarctica as the source of atmospheric mercury during austral summer // *Atmospheric pollution research*. ISSN 1309-1042. 2021, vol. 12, iss. 12, art. no. 101226, p. 1-14.

228. Valiūnienė, A.; Kavaliauskaitė, G.; Virbickas, P.; Ramanavičius, A. Prussian blue based impedimetric urea biosensor // *Journal of electroanalytical chemistry*. ISSN 1572-6657. 2021, vol. 895, art. no. 115473, p. 1-6.

229. Valušis, G.; Lisauskas, A.; Yuan, H.; Knap, W.; G. Roskos, H. Roadmap of terahertz imaging 2021 // *Sensors*. ISSN 1424-8220. 2021, vol. 21, iss. 12, art. no. 4092, p. 1-52.

230. Van Acker, S.I.; Van den Bogerd, B.; Van Acker, Z.P.; Vailionytė, A.; Haagdorens, M.; Koppen, C.; Ní Dhubhghaill, S.; Dartt, D.A.; Pintelon, I. Characterisation of gel-forming mucins produced in vivo and in ex vivo conjunctival explant cultures // *International journal of molecular sciences*. ISSN 1661-6596. 2021, vol. 22, iss.19, art. no.10528, p. 1-19.

231. Vertelis, V.; Balevičius, S.; Stankevič, V.; Žurauskienė, N.; Schneider, M. The application of a CMR-B-scalar sensor for the investigation of the electromagnetic acceleration of type II superconductors // *Sensors.* ISSN 1424-8220. 2021, vol. 21, iss. 4, art. no. 1293, p. 1-18.

232. Vertelis, V.; Stankevič, T; Balevičius, S.; Stankevič, V.; Žurauskienė, N.; Plaušinaitienė, V.; Tolvaišienė, S.; Schneider, M.; Šimkevičius, Č. Superconducting protector against electromagnetic pulses based on YBCO film prepared on an Al2O3 substrate with a CeO2 sublayer. // *Superconductor science and technology*. eISSN 1361-6668. 2021, vol. 34, no.3, art. no. 035007, p. 1-10.

233. Veselis, L.; Burokas, R.; Ulčinas, O.; Gertus, T.; Michailovas, K.; Michailovas, A. Depolarization compensation with a spatially variable wave plate in a 116 W, 441 fs, 1 MHz Yb:YAG double-pass laser amplifier // *Applied optics.* ISSN 1559-128X. 2021, vol. 60, no. 24, p. 7164-7171.

234. Virbickas, P.; Valiūnienė, A.; Baryševa, D.; Popkirov, G.; Ramanavičius, A. Determination of cyanide concentration by chronoamperometry, cyclic voltammetry and fast Fourier transform electrochemical impedance spectroscopy // *Journal of electroanalytical chemistry*. ISSN 1572-6657. 2021, vol. 895, art. no. 115449, p. 1-7.

235. Vyšniauskas, A.; Cornell, B.; Sherin, P.S.; Maleckaitė, K.; Kubánková, M.; Izquierdo, M.A.; Vu, T.T.; Volkova, Y.A.; Budynina, E.M.; Molteni, C.; Kuimova, M.K. Cyclopropyl substituents transform the viscosity-sensitive BODIPY molecular rotor into a temperature sensor // *ACS sensors*. ISSN 2379-3694. 2021, vol. 6, iss. 6, p. 2158-2167.

236. Voitechovič, E.; Stankevičiūtė, J.; Vektarienė, A.; Vektaris, G.; Jančienė, R.; Kuisienė, N.; Razumienė, J.; Meškys, R. Bioamperometric systems with fructose dehydrogenase from Gluconobacter japonicus for D-tagatose monitoring // *Electroanalysis*. ISSN 1040-0397. 2021, vol. 33, iss. 6, p. 1393-1397.

237. Xia, R.; Xu, Y.; Chen, B.; Kanda, H.; Franckevičius, M.; Gegevičius, R.; Wang, S.; Chen, Y.; Chen, D.; Ding, J.; Yuan, N.; Zhao, Y.; Roldán-Carmona, C.; Zhang, X.; Dyson, P.J.; Nazeeruddin, M.K. Interfacial passivation of wide-bandgap perovskite solar cells and tandem solar cells // *Journal of materials chemistry A*. ISSN 2050-7488. 2021, vol. 9, no. 38, p. 21939-21947.

238. Zhang, Y.; Liang, W.; Esposito, C.; Jin, X.; Sakalas, P.; Schröter, M. LO chain (×12) integrated 190-GHz low-power SiGe receiver with 49-dB conversion gain and 171-mW DC power consumption // *IEEE transactions on microwave theory and techniques*. ISSN 0018-9480. 2021, vol. 69, iss. 3, p. 1943-1954.

239. Zinovičius, A.; Morkvėnaitė-Vilkončienė, I.; Ramanavičienė, A.; Rožėnė, J.; Popov, A.; Ramanavičius, A. Scanning electrochemical impedance microscopy in redox-competition mode for the investigation of antibodies labelled with horseradish peroxidase // *Materials*. ISSN 1996-1944. 2021, vol. 14, iss. 15, art. no. 4301, p. 1-8.

240. Žalnėravičius, R.; Klimas, V.; Paškevičius, A.; Grincienė, G.; Karpicz, R.; Jagminas, A.; Ramanavičius, A. Highly efficient antimicrobial agents based on sulfur-enriched, hydrophilic molybdenum disulfide nano/microparticles and coatings functionnalized with palladium nanoparticles // *Journal of colloid and interface science*. ISSN 0021-9797. 2021, vol. 591, p. 115-128.

241. Žarkov, A.; Kareiva, A.; Tamašauskaitė-Tamašiūnaitė, L. Advances in functional inorganic materials prepared by wet chemical methods // *Crystals*. eISSN 2073-4352. 2021, vol. 11, no. 8, art. no. 943, p. 1-3.

242. Žeimytė, S.; Stončius, S. Chiral bipyridine-annulated bicyclo[3.3.1]nonane N-oxide organocatalysts for stereoselective allylation and hydrosilylation reactions // *Tetrahedron.* ISSN 0040-4020. 2021, vol. 78, art. no. 131831, p. 1-9.

243. Želudevičius, J.; Dubosas, G.; Regelskis, K. Investigation of multipass Yb-doped fiber amplifiers // *Applied optics*. ISSN 1559-128X. 2021, vol. 60, iss. 33, p. 10332-10342.

244. Žemaitis, A.; Gaidys, M.; Gečys, P.; Barkauskas, M.; Gedvilas, M. Femtosecond laser ablation by bibursts in the MHz and GHz pulse repetition rates // *Optics express*. ISSN 1094-4087. 2021, vol. 29, iss. 5, p. 7641-7653.

245. Žukauskienė, E.; Šimoliūnienė, M.; Truncaitė, L.; Skapas, M.; Kaupinis, A.; Valius, M.; Meškys, R.; Šimoliūnas, E. Pantoea bacteriophage vB_PagS_AAS23: A singleton of the genus Sauletekiovirus // *Microorganisms*. eISSN 2076-2607. 2021, vol. 9, iss. 3, art. no. 668, p. 1-15.

246. Žurauskienė, N.; Rudokas, V.; Keršulis, S.; Stankevič, V.; Pavilonis, D.; Plaušinaitienė, V.; Vagner, M.; Balevičius, S. Magnetoresistance and its relaxation of nanostructured La-Sr-Mn-Co-O films: Application for low temperature magnetic sensors // *Journal of magnetism and magnetic materials*. ISSN 0304-8853. 2021, vol. 539, art. no. 168340, p. 1-6.